UNIVERSITÄTSKLINIKUM HAMBURG-EPPENDORF

Klinik für Pädiatrische Hämatologie und Onkologie

Direktor

Prof. Dr. med. Stefan Rutkowski

Deletion Mapping and Phenotype-Genotype Analysis by Multiplex Ligation-dependent Probe Amplification in German Patients with Williams-Beuren-Syndrome

Dissertation

zur Erlangung des Grades eines Doktors der Medizin

an der Medizinischen Fakultät der Universität Hamburg

vorgelegt von:

Katharina Elisabeth Saathoff, geb. Franke

aus Kassel

Hamburg 2020

Angenommen von der

Medizinischen Fakultät der Universität Hamburg am:

24.06.2021

Veröffentlicht mit Genehmigung der

Medizinischen Fakultät der Universität Hamburg.

Prüfungsausschuss, der Vorsitzende:

Prof. Dr. Christian Kubisch

Prüfungsausschuss, zweiter Gutachter:

Prof. Dr. Reinhard Schneppenheim

Table of contents

1 Introduction

1.1 Williams-Beuren-Syndrome

The Williams-Beuren-Syndrome, short WBS or WS (OMIM #194050), which was described for the first time in detail by the two cardiologists Williams and Beuren in 1961 and 1962, is a multisystem disorder caused by a hemizygous de-novo microdeletion of contiguous parts of chromosome 7q11.23. A microdeletion is a submicroscopic deletion which results in the loss of one or more contiguous genes. In a microdeletion only one copy of a gene is preserved (Murken et al. Taschenlehrbuch Humangenetik. P. 197). Rare cases of autosomal dominant transmission of Williams-Beuren-Syndrome have been reported (Pankau et al. 2001, Metcalfe et al. 2005).

The deletion affects the so called "Williams-Beuren-Syndrome chromosome region" (WBSCR) and encompasses genes within a region of approximately 1.54 to 1.85 Mb. The deleted area spans 26 to 28 genes and several pseudogenes. The prevalence is about 1/8000 (Pober 2010, Merla et al. 2010, Schubert 2009, Pankau et al. Das Williams-Beuren-Syndrom, P. 3). Furthermore, several atypical deletions have been reported in the literature (Fusco et al. 2014). The genes of the WBSCR will be presented in this thesis.

Affected individuals often show clinical characteristics. These are cardiac defects, especially supravalvular aortic stenosis (SVAS), craniofacial dysmorphias, mental retardation, impaired visuospatial recognition, but improved abilities in musicality, in name and face memory and a characteristic behavioral pattern with overfriendliness and empathy (Pober 2010).

Due to the unique physical, cognitive and behavioral appearance of WBS patients, several phenotype-genotype studies have already been done (Marshall et al. 2008, Ramocki et al. 2010, Fusco et al. 2013). However, in which way and to what extent the missing genes can affect each other and result in this special phenotype, remains unclear.

1.2 Clinical features of Williams-Beuren-Syndrome

Figure 1.1: Phenotype in typical WBS. The girl on the illustration is called "Josie" and presents some characteristics of the typical WBS phenotype. The illustration was created by the Bundesverband Williams-Beuren-Syndrome e. V. to be presented as a poster in clinics and pediatrics' offices to serve as education about WBS. The content of the speech bubbles was translated from German into English. The illustration was kindly provided by the Bundesverband Williams-Beuren-Syndrome e. V.

1.2.1 Physical appearance

In most cases, individuals with WBS present with a characteristic physical appearance. The manifestations become more apparent as affected individuals get older. Since 1986, the term "elfin facies" is no longer used for the description of these characteristics (Burn 1986). The face in particular is shaped by a full lower face with a small, pointed chin and malar flattening. Furthermore, periorbital fullness, a broad forehead, medial eyebrow flare (synophris), full cheeks and lips with a prominent lower lip, a flat nasal bridge and a wide mouth ("ear-to-ear-smile") can often be found (Burn 1986; figure 1.2). Patients are more frequently affected by strabismus, esotropia and stellate iris pattern than healthy individuals (figure 1.3). Most patients (77%) have blue eye color (Winter et al. 1996). WBS patients show an altered hearing ability with hyperacusis combined with mild hearing loss, contradictory to their affinity to music (Zarchi et al. 2015). Their teeth are typically small and widely spaced, erupt late and appear together with malocclusion (Burn 1986; figure 1.4).

Figure 1.2: Typical WBS phenotype in a male patient. From Pankau et al. Das Williams-Beuren-Syndrom. P. 126.
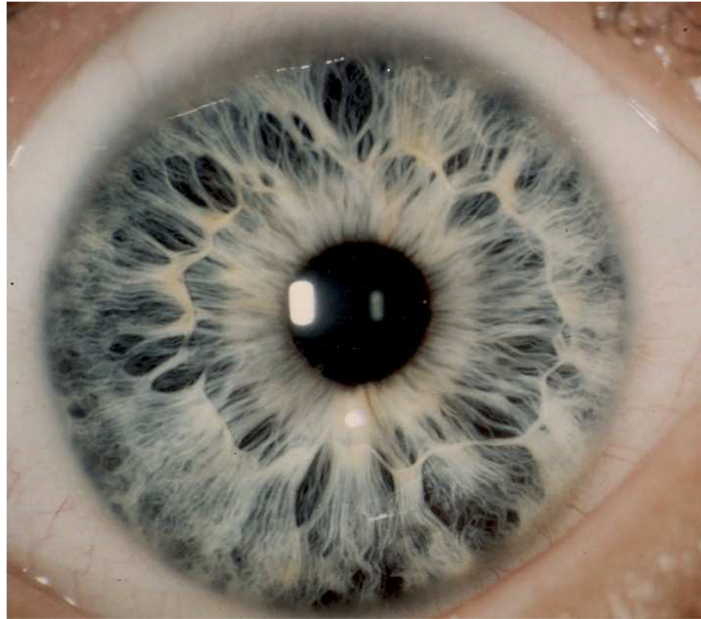
Figure 1.3: Stellate iris pattern in WBS. From Pankau et al. Das Williams-Beuren-Syndrom. P. 126. This pattern results from a hypoplastic and coarsely change of the stroma of the iris (Viana et al., 2015).

Figure 1.4: Teeth anomalies in young WBS patients. From Pankau et al. Das Williams-Beuren-Syndrom. P. 43.

1.2.2 Cardiovascular system

In WBS patients, the most common affected system of the body is the cardiovascular system due to hemizygosity of the elastin locus (*ELN*) (Collins et al. 2010). The occurrence of cardiovascular abnormalities ranges between 75 and 93 %. Most frequent malformations are SVAS with 57 - 64 % and peripheral pulmonary stenosis (PPS) with 45 - 62 % (Collins 2010, Del Pasqua 2009) which often occur combined. Additional manifestations are: valvular and supravalvular pulmonary stenosis (SVPS), aortic hypoplasia, coarctation of the aorta, aberrant subclavian artery, patent ductus arteriosus, disrupted aortic arch, coronary vessel anomalies, aortic stenosis, ventricular and atrial septum defects, tetralogy of Fallot and mitral valve abnormalities (Pankau et al. Das Williams-Beuren-Syndrom. P. 69). Even stenoses of the renal arteries (RAS) have been reported (Pankau et al. Das Williams-Beuren-Syndrom. P. 119, Collins et al. 2010). Most cases of death amongst Williams-Beuren-Syndrome patients occur due to cardiovascular complications (Pober 2010). Surgical repair of SVAS achieves good outcomes (Fricke et al. 2015). An additional common finding in 40 - 45 % of patients is arterial hypertension often combined with renal malformations or RAS (Bouchrieb et al. 2010, Kozel et al. 2014, Del Campo et al. 2006).

Hereditary supravalvular aortic stenosis (OMIM #185500) was first described in 1964 by Eisenberg et al. who reported several cases involving 3 generations of two families. Since the early nineties, a context between *ELN* on chromosome 7 and the occurrence of SVAS was suspected (Ewart et al. 1993a). Larger deletions, including *ELN* but also additional genes were thought to cause Williams Syndrome instead (Ewart et al. 1994). Nowadays, it has been proven that haploinsufficiency and heterozygous point mutations of *ELN* cause hereditary SVAS (Schubert 2009).

1.2.3 Infancy and development

Cases of post-term and pre-term birth with growth and weight deficiencies have been reported. Many children are hospitalized during their first months of life. Most babies suffer from feeding difficulties and therefore failure to thrive with poor weight gain (Morris et al. 1988). In many cases, molecular genetic analysis is performed due to these criteria or due to cardiac murmurs associated with abovementioned heart or vascular malformations. Affected individuals commonly are, even in adulthood, of shorter stature than individuals from a healthy reference group and the commencement of puberty usually occurs earlier (Morris 2013, Pankau et al. Das Williams-Beuren-Syndrom. P. 139, 141). The IQ normally ranges between 40 and 80. In cases of patients with smaller, atypical deletion sizes also normal IQs have been reported (Ferrero et al. 2010).
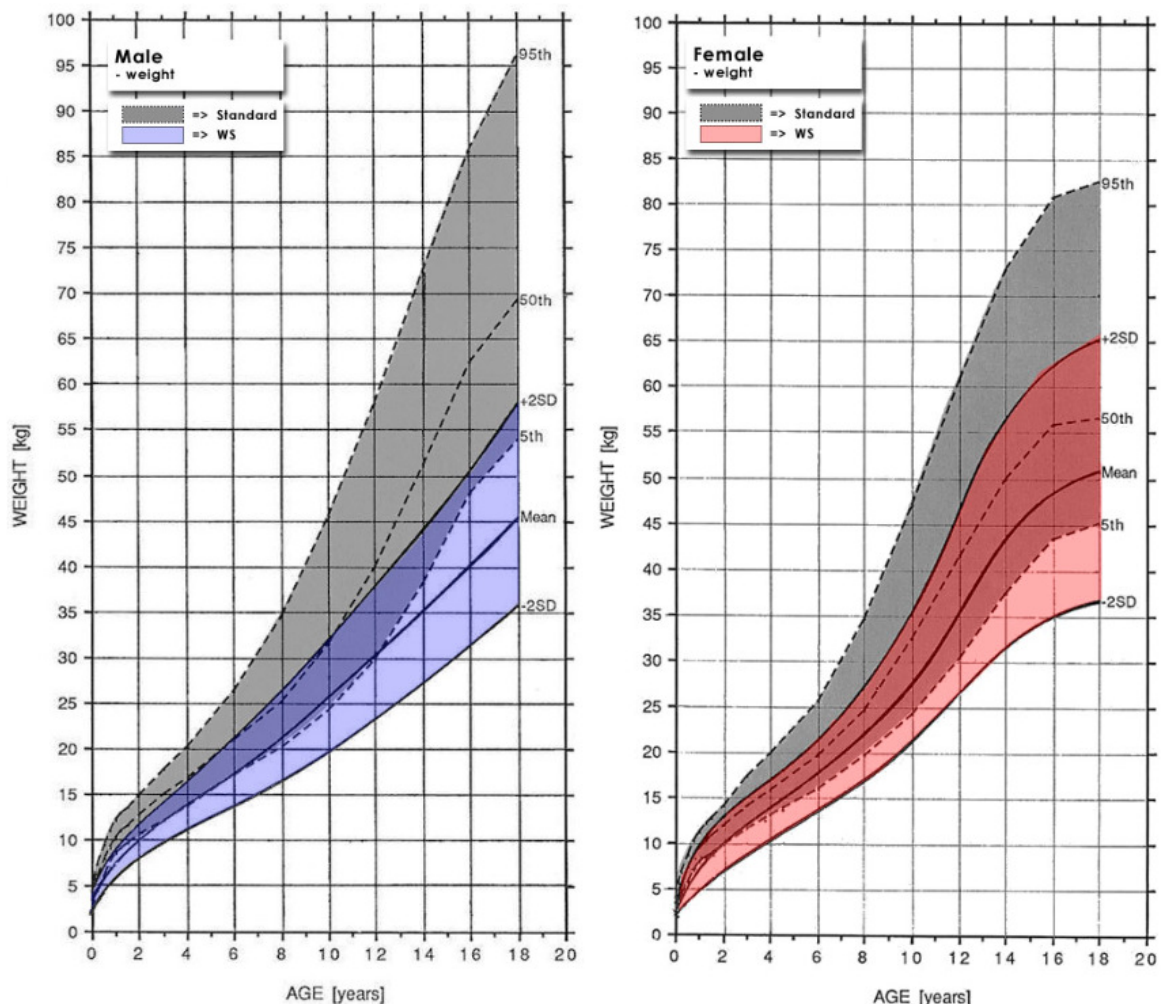
Figure 1.5: Weight growth charts comparing WBS and standard curves.
https://williams-syndrome.org/growth-charts/growth-charts. 13.10.2019. 18:00.
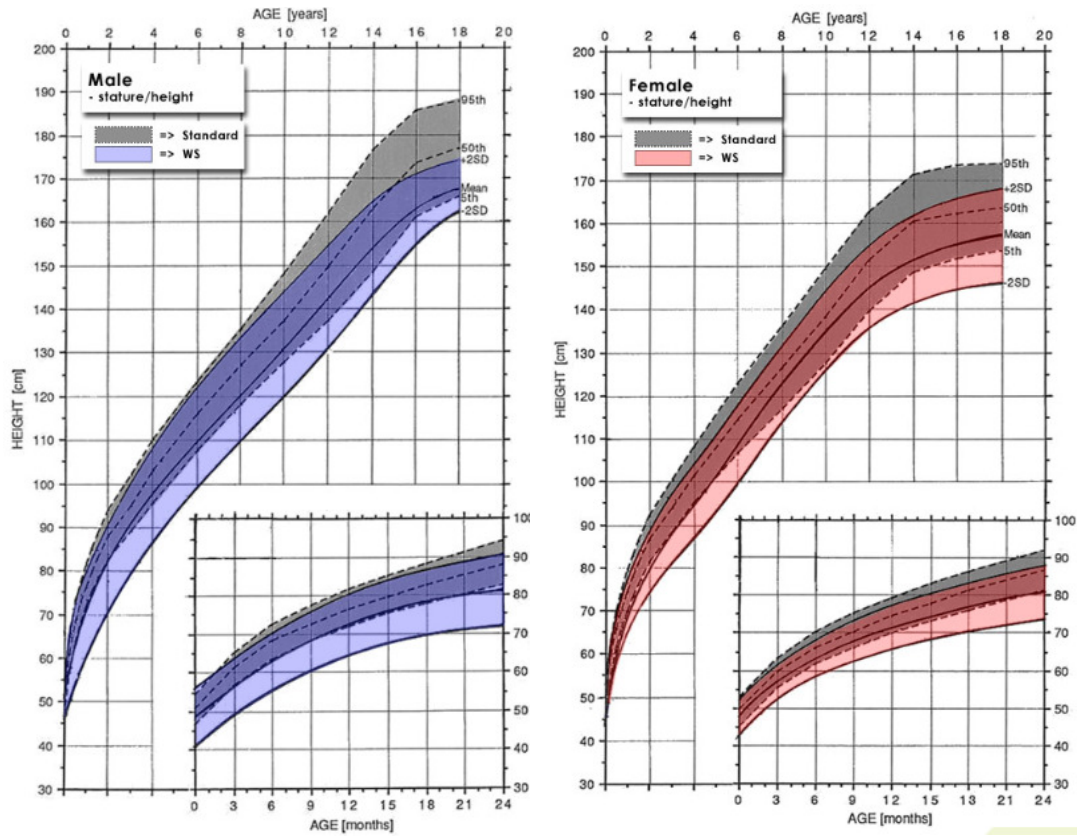
Figure 1.6: Height growth charts comparing WBS and standard curves.
https://williams-syndrome.org/growth-charts/growth-charts. 13.10.2019. 18:00.
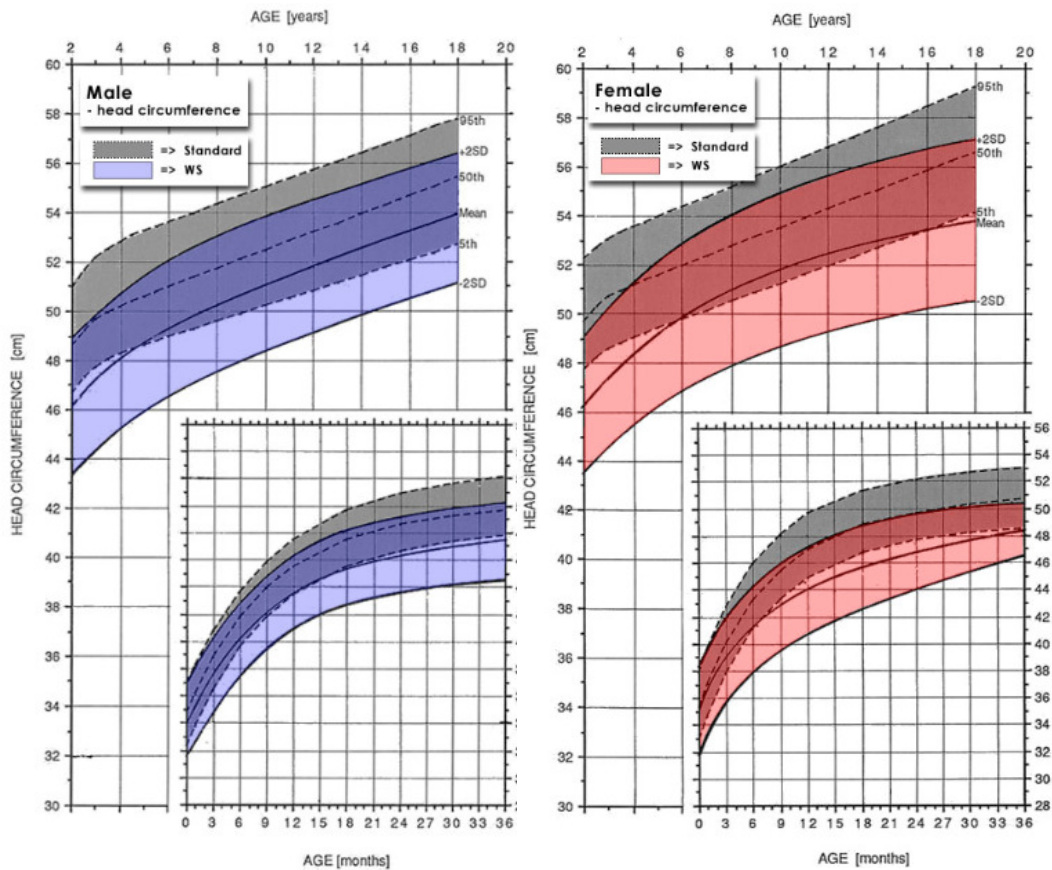
Figure 1.7: Head circumference growth charts comparing WBS and standard curves.
https://williams-syndrome.org/growth-charts/growth-charts. 13.10.2019. 18:00.

1.2.4 Strengths and weaknesses, neurocognitive behavior

Individuals with WBS often present a unique character. They are overfriendly, very empathetic, have a great memory of names, a strength in short-time verbal and auditory memory and decreased skepticism towards strangers (Morris 2010). In contrast, many children have generalized anxiety disorders and special phobias, especially towards loud noises. These anxiety symptoms persist also in adults (Woodruff-Borden et al. 2010). Auditory rote memory ability and language abilities are higher regardless of the lower main IQ level (Morris 2010, Mervis et al. 2000). In contrast, individuals with WBS have severe impairments in visuospatial constructive ability according to their general cognitive ability (Mervis et al. 2000).

Because many of the WBS patients have a great affection to music and are very talented in singing, playing instruments and have a good memory for melodies and song texts, these abilities can be utilized as a resource: music therapy or musical elements could be useful in educational settings to help compensating cognitive deficits or promoting attention (https://williams-syndrome.org/teacher/information-for-teachers. 15.10.2019. 17:00)

1.2.5 Endocrine system

Several endocrine alterations have been reported in WBS patients. They range from several cases with impaired glucose tolerance or diabetes mellitus type 1 or 2 in children (Palacios-Verdú et al. 2015) and adults (Pober et al. 2010) over cases with idiopathic hypercalcemia to those with latent hypothyroidism (Palacios-Verdú et al. 2015). Furthermore, WBS was suggested to be added to genetic syndromes associated with diabetes mellitus type 2 (Stagi et al. 2014). Within a collective of WBS individuals in a study by Pober et al. 75 percent showed diabetes mellitus type 2 or impaired glucose tolerance (Pober et al. 2010). Due to this fact, WBS patients are screened for diabetes mellitus during the second and third decade of life (Palacios-Verdú et al. 2015). Pober et al. presumed *STX1A* which is located in the middle of WBSCR to be the most promising candidate causing diabetes mellitus (Pober et al. 2010). *STX1A* codes for Syntaxin 1A and plays a role in the protein complex that leads to the release of insulin in the pancreatic islets (Daniel et al. 1999).

1.2.6 Gastrointestinal and genitourinary system

Affected children as well as adults might suffer from several different problems affecting the gastrointestinal system, e.g. chronic constipation and abdominal pain or gastro-esophageal reflux (Stagi et al. 2010). Some cases of celiac disease and WBS have been reported. Due to this correlation, further diagnostics such as serological screening is recommended when patients present with corresponding symptoms (Şimşek-Kiper et al. 2014). Sigmoid diverticulitis occurs in WBS more often in adolescents under twenty years of age and younger adults and only in rare cases together with obesity (Stagi et al. 2020). In the latter case, sigmoid diverticulitis seems to require surgical treatment more often due to conservative therapy being less successful (Partsch et al. 2005).

Abnormalities of the genitourinary system are also pervasive in this syndrome. About one third of male children suffer from bilateral undescended testis, nearly every fourth boy presents inguinal hernias and almost half of the girls suffer from umbilical or inguinal hernias (Sammour et al. 2014). Common structural abnormalities of the genitourinary system are hydronephrosis, kidney duplication and unilateral renal agenesis. Nearly half of the patients are diagnosed with bladder diverticula (Sammour et al. 2014). The risk of renal and genitourinary malformations is up to 12 to 36 times higher in comparison to a healthy reference group (Pankau et al. 1996).

1.2.7 Musculoskeletal and nervous system

Several musculoskeletal symptoms have been reported such as joint laxity, joint contractures, scoliosis and radioulnar synostosis (Pober 2010, Schubert 2009) (figure 1.8). Especially joint contractures worsen during growing up of the patients and physiotherapy is often required to prevent further aggravation.

Neurological symptoms are dominated by poor balance and coordination due to altered cerebellar development and size (Pober 2010). The main functions of the cerebellum are coordination and precision of movements, posture and balance. Cerebella of WBS patients show reduced volume. It is assumed that this leads to lack in fine and gross motor skills often found in WBS patients (Osório et al. 2014).

Figure 1.8: X-ray of a radioulnar synostosis as a possible feature of WBS. Radioulnar synostosis is the fusion of radius and ulna. It affects the proximal part of the bones in most cases. Clinically these patients have a restricted elbow movement (https://radiopaedia.org/cases/proximal-radioulnar-synostosis-1 08.05.2020. 11:00).

1.2.8 Overview of common clinical features in WBS

Feature	Manifestations
Cardiovascular system	Supravalvular aortic stenosis, peripheral pulmonary stenosis, arterial hypertension
Face	Broad forehead, periorbital fullness, full cheeks and lips, long smooth philtrum, malar flattening, wide mouth. Facial features become coarser with age.
Eyes	Strabismus, stellate iris pattern in blue eyes
Ears	Hyperacusis, mild hearing loss
Teeth	Small, widely spaced, malocclusion
Infancy and development	Feeding difficulties, failure to thrive, weight and growth deficiencies
Strengths and weaknesses	Overfriendliness, high empathy, great affection to music
Neurocognitive behavior	Impaired visuospatial recognition, lower main IQ
Endocrine system	Short stature, precocious puberty, hypercalcemia, hypothyroidism, impaired glucose tolerance, Diabetes mellitus type 2
Gastrointestinal system	Chronic constipation and abdominal pain, celiac disease, sigmoid diverticulitis
Genitourinary system	Inguinal and umbilical hernias, hydronephrosis, kidney duplication, bladder diverticula, undescended testes
Musculoskeletal system	Radioulnar synostosis, short stature, joint contractures, scoliosis
Neurologic system	Reduced cerebellar volume, muscular hypotonia

Table 1.1: Common phenotypical features in patients with WBS. According to Schubert 2009 and Pober 2010.

1.3   How is Williams-Beuren-Syndrome diagnosed?

Since the early 1990s WBS can be diagnosed confidently by Fluorescence in situ hybridization (FISH) through detecting the hemizygous loss of the *ELN* locus with the help of fluorescent probes. The first publications using FISH emerged in 1993 (Ewart et al. 1993b). Until then, the "Diagnostic Index of Preus" from 1984 was used to confirm the syndrome (Preus 1984). The clinical diagnosis would be possible from the second year of age when typical characteristics were apparent. The recommended consequences ought to be regular pediatric supervision and treatment of syndrome specific problems (Morris et al. 1988).

Until today, FISH is the most common laboratory technique for diagnosing the syndrome which is used besides examining the clinical features (https://williams-syndrome.org/content/diagnosing-williams-syndrome-0. 15.10.2019. 22:00, https://www.w-b-s.de/syndrom/der-fish-test.html. 03.12.2019. 20:00, Merla 2010). Diagnostic markers used for FISH analysis have been extended to *ELN*, *LIMK1* and *GTF2I* (Deutsche Gesellschaft für Humangenetik e. V. Indikationskriterien für die Krankheit: Williams-Beuren-Syndrom. 2009: https://www.gfhev.de/de/leitlinien/Diagnostik_LL/2009_07_16_Indikationskriterien_WBS.pdf. 08.05.2020. 18:00).

Nowadays, *ELN*, *LIMK1* and the marker D7S613 are commonly used diagnostic markers (https://www.klinikum.uni-heidelberg.de/humangenetik/labordiagnostik/molekular-cytogenetisches-labor-fish/methodenspektrum. 15.04.2020. 09:00, http://www.dna-diagnostik.hamburg/analyten/williams-beuren-syndrom/. 15.04.2020. 09:00).

Further methods are real-time quantitative PCR (qPCR) and array comparative genomic hybridization (aCGH) (Merla 2010).

Another method for diagnosing WBS, which gained more and more popularity lately, is to be presented in the further course of this thesis: Multiplex Ligation-dependent Probe Amplification (MLPA). This procedure was first used in laboratories in 2002 (Schouten et al. 2002). The results of the first commercial kit for diagnosing WBS were published in 2007 (Van Hagen et al. 2007a). Van Hagen and colleagues concluded after comparing FISH to MLPA that MLPA was not only faster, but offered a wider range of results as well, concerning atypical deletions (smaller and lager ones) and even duplications.

1.4   Genetic basis of WBS: 7q11.23

1.4.1   Structure of 7q11.23

The clinical features of Williams-Beuren-syndrome are caused by a hemizygous deletion of a contiguous gene region on the long (q-) arm of chromosome 7 at cytoband 11.23. This band is located close to the centromere of chromosome 7. As mentioned above, the phenotype of Williams-Beuren-syndrome is caused by the hemizygous loss of 26 to 28 genes. 22 of these genes are single-copy genes which encompass about approximately 1.2 million base pairs in total (Schubert 2009). Single-copy genes are non-repeated sequences in the genome. They appear as a single copy in the genome (Karp G. Cell and Molecular Biology. P. 399).

The region of single-copy genes is flanked by low copy repeats (LCR) in both, centromeric and telomeric, directions. The LCR are either composed of tandem repeats or of duplications of base pairs from other sites of chromosome 7 (Schubert 2009). These LCR regions are partitioned into three blocks: block A, B and C.

Every block contains a centromeric (cen), a medial (mid) and a telomeric (tel) part (Valero et al. 2000). There are three possibilities: (1) One block comprises one gene and the two other blocks the corresponding pseudogenes (not transcribed or dysfunctional relatives of the ancestral gene). (2) Every block comprises pseudogenes of a gene located somewhere else on the chromosome. (3) Only some blocks harbor single genes that have a coding function (Schubert 2009).

All A blocks (centromeric, medial and telomeric) show a high similarity of nucleotide sequences to each other. The same is seen in Blocks B and C. This makes them vulnerable for mispairing and unequal crossing over (Schubert 2009).

Figure 1.9 gives an overview over the affected chromosomal area 7q11.23 and its genes. The genes of the WBSCR will be addressed in more detail in chapter 1.7.

C cen
POM121
NSUN5P2
TRIM74
FKBP6-like

A cen
STAG3L3P
PMS2P7
SPDYE8P
SPDYE10P

1.85Mb

B cen
GTF2IP4
NCF1BP
GTF2IRD2P1

1.54Mb

C mid
POM121BP
NSUN5
TRIM50
FKBP6

WBSCR
FZD09
BAZ1B
BCL7B
TBL2
MLXIPL
VPS37D
DNAJC30
BUD23   (= WBSCR22)
STX1A
ABHD11
CLDN3
CLDN4
METTL27   (= WBSCR27)
TMEM270   (= WBSCR28)
ELN
LIMK1
EIF4H
LAT2
RFC2
CLIP2
GTF2IRD1*

B mid
GTF2I
NCF1
GTF2IRD2

A mid
STAG3L2P
PMS2P5
SPDYE12P
CASTOR2   (= GATSL2)
RCC1L   (= WBSCR16)

B tel
GTF2IRD2B
NCF1CP
GTF2IP1

A tel
SPDYE13P
SPDYE14P
SPDYE15P
PMS2P2
STAG3L1P

C tel
FKBP6-like
TRIM73
NSUN5P1
POM121C

Figure 1.9: Illustration of chromosome area 7q11.23. The WBSCR is flanked by the highly homologous blocks A, B and C (red, blue, green), each of them with a centromeric, medial and telomeric block (green, red, blue). The two typical WBS deletions are highlighted by grey rectangles. The proximal and distal boundaries of the rectangles only depict the approximate breakpoints in both deletions. Further information about the known breakpoints is given in chapter 1.6. The asterisk next to *GTF2IRD1* stands for the 22th coding gene *WBSCR23*, which is thought to be an intronless gene within *GTF2IRD1*. Not all pseudogenes are depicted. After Schubert 2009, Pober 2010, Bayés 2003.

7q.11.23

Chromosome 7

BOLD = coding
Normal = pseudogene

= Regions in which 1.54Mb and 1.85Mb deletions occur

1.4.2 Evolution of the flanking low copy repeats (LCR)

The theory of the genesis of the highly repetitive flanking LCR is based on the existence of so called Alu repeats which are located directly adjacent to the LCR (Bailey et al. 2003). Alu repeats are Short Interspersed Nuclear Elements (SINE). SINE sequences have an approximated length of 300 base pairs and make up about 13% of the genome. An Alu repeat provides a recognition spot for the restriction enzyme Alu (Murken et al. Taschenlehrbuch Humangenetik. P. 152). The enriched occurrence of Alu repeats predisposes the LCR blocks to genetic mutations, such as deletions or duplications (Schubert 2009).

1.4.3 Block A

Block A comprises three pseudogenes: the ancestral genes are *STAG3* (*STROMALIN 3*), *PMS2* (*PMS1 HOMOLOG 2, MISMATCH REPAIR SYSTEM COMPONENT*) and *SPDYE1* (*SPEEDY/RINGO CELL CYCLE REGULATOR FAMILY, MEMBER E1*) formerly known as *WBSCR19 (WILLIAMS BEUREN SYNDROM CHROMOSOME REGION 19)* (Schubert 2009). Block A has an approximate size of 110 kb (Valero et al. 2000). Additionally, only block A mid harbors a coding gene: *CASTOR2 (CELLULAR ARGININE SENSOR FOR MTORC1 PROTEIN 2)*, formerly known as a pseudogene of *GATS* (Stromalin Antigene 3 Opposite Strand).

The pseudogenes, neither of which have a coding function, are copies of genes that are located on a different spot of chromosome 7. The coding gene *STAG3* for instance is located on 7q22.1 and codes for a protein that acts as a subunit of a cohesion complex during cell division (OMIM *608489, http://www.ncbi.nlm.nih.gov/gene/10734. 20.10.2019. 19:00).

PMS2 is also located on 7q22.1 and encodes for a protein that is amongst others part of a complex, involved in DNA mismatch repair. Mutations in this gene are involved in occurrence of hereditary nonpolyposis colorectal cancer (HNPCC) (OMIM *600259, http://www.ncbi.nlm.nih.gov/gene/5395. 20.102019. 19:05).

Pseudogene variants of *WBSCR19* which is located on 7p13 are not found in block A mid, but appear twice in A cen and four times in A tel (Schubert 2009). The function of *WBSCR19* was not known for a long time. In 2012 it was discovered that *WBSCR19* is in fact a member of cell cycle regulators and was coined *SPDYE1* (Chauhan et al. 2012, OMIM *617623, http://www.ncbi.nlm.nih.gov/gene/285955. 20.10.2019. 20:20).

Until recently, the function of the ancestral gene *GATS* on 7q22 was not known. Its pseudogene variant *GATSL2* is located on A mid (Schubert 2009). In 2016, this pseudogene was termed *CASTOR2*. It codes for products that are involved in the mTORC1 pathway (Chantranupong et al. 2016, OMIM *617033; http://www.ncbi.nlm.nih.gov/gene/352954. 20.10.2019. 20:00).

Attached to the telomeric end of block A mid lays the coding gene *WBSCR16*, also known as *RCC1 like* (*RCC1L*). Its protein may function as a regulator of chromosome condensation (Schubert 2009, http://www.ncbi.nlm.nih.gov/gene/81554. 20.10.2019. 20:30).

1.4.4 Block B

Block B consists of genes with coding functions and their pseudogenes. Each part (cen, mid and tel) contains three different genes or pseudogenes which share an approximate 120 kb continuous sequence homology between each other (Valero et al. 2000).

Block B mid is composed of three coding genes. These are *GTF2I* (*GENERAL TRANSCRIPTION FACTOR II-I*), *NCF1* (*NEUTROPHIL CYTOSOLIC FACTOR 1*) and *GTF2IRD2* (*GTF2I REPEAT DOMAIN CONTAINING PROTEIN 2*)

Block B cen harbors their three pseudogene versions, while B tel hosts one coding gene (*GTF2IRD2B*) and one pseudogene of *GTF2I* and one of *NCF1* (Schubert 2009).

The gene *GTF2I* of block B mid codes for a transcription factor that is part of the transcription factor family TFII-I (Roy 1997, OMIM *601679, https://www.ncbi.nlm.nih.gov/gene/2969. 28.10.2019. 14:00). The copies of *GTF2I* in the blocks B cen and B tel encode for a truncated version of the original protein (Schubert 2009). *GTF2I* works together with *GTF2IRD1* (*GTF2I REPEAT DOMAIN CONTAINING PROTEIN 1*) which is located in the single-copy part (= WBSCR) of 7q11.23 (Schubert 2009).

NCF1 is presumed to be associated with the genesis of vascular stiffness and arterial hypertension. The gene product of *NCF1* (p47^{phox}) is a subunit of the neutrophil NADPH oxidase which generates superoxide anions and reactive free-radicals (OMIM *233700, https://www.ncbi.nlm.nih.gov/gene/653361. 28.10.2019. 14:30). Superoxide anions occur in neutrophils and other phagocytes during oxidative burst in order to eliminate e.g. bacteria and fungi. Reactive free-radicals are tissue-toxic (Rassow et al. Duale Reihe Biochemie. P. 677). In

their study of 96 WBS patients, Del Campo et al. observed that in patients whose deletion spanned *NCF1* hypertension occurred less often (Del Campo et al. 2006). Another study of 99 WBS patients confirmed these results, even for patients under 18 years of age (Kozel et al. 2014). This suggests that reduction of the oxidative burst due to *NCF1* hemizygosity might be a protective factor against hypertension (Del Campo et al. 2006, Kozel et al. 2014).

However, no effect on occurrence of chronic granulomatous disease (CGD) has been observed due to hemizygosity of the *NCF1* gene (Stasia et al. 2013). Homozygous or compound-heterozygous mutations of *NCF1* are causing the most common form of autosomal recessive CGD (Schubert 2009). The most prevalent mutation is a 2bp GT-deletion of *NCF1* which results in a premature stop codon and might also present in the two *NCF1* pseudogenes in the WBS region (Roesler et al. 2000). Compound heterozygosity for the WBS deletion and a *NCF1* gene recombination event with its pseudogenes containing the 2bp deletion are the probable cause for very rare combinations of WBS and autosomal CGD (Stasia et al. 2013, Roesler et al. 2000). Only two genetically confirmed cases with WBS and CGD have been reported in literature (Stasia et al. 2013).

GTF2IRD2 (OMIM *608899 and 608900, https://www.ncbi.nlm.nih.gov/gene/84163. 28.10.2019. 14:45) in block B mid and the telomeric localized gene *GTF2IRD2B* of block B tel code for proteins that are also suspected to be members of the transcription factor family TFII-I (Schubert 2009).

In more than half of the cases with a hemizygous deletion, the breakpoints lay within the *GTF2I* (pseudo-)gene of block B cen and B mid, which results in altered or impaired function of both transcription factor family genes: *GTF2IRD1* (OMIM *604318, https://www.ncbi.nlm.nih.gov/gene/9569. 28.10.2019. 15:00) of the WBSCR and *GTF2I* of block B mid.

GTF2IRD2 is deleted just in some cases. When (1) the breakpoint of a small deletion lays within this gene (16% of the patients of Bayés et al. 2003), (2) in cases with a larger 1.85 Mb deletion or (3) in atypical cases. It is speculated that its function could be the modulation of the effect of the other *GTF2I* genes on the WBS phenotype (Bayés et al. 2003, Merla et al. 2010).

Furthermore, recent studies give evidence that *GTF2IRD1* and *GTF2I* have similar functions in the development of the characteristic cognitive-behavioral profile in WBS. These studies focused on the impairment of visuospatial recognition and hypersociability. In WBS patients'

brain tissue the product of *GTF2I* has been found in reduced levels in neurons of the posterior parietal lobe, which is a part of the visual pathway (Schubert 2009).

By comparing typical WBS patients and typically developing (TD) healthy controls with atypical WBS patients, the relation between *GTF2I* and *GTF2IRD1* and the development of certain parts of the brain was further examined. The region of interest was the intraparietal sulcus (IPS), which is known to be connected to visuospatial cognition. Patients with an atypical deletion excluding *GTF2IRD1* and *GTF2I* had IPS volumes comparable to those of the TD control group. Other patients however, whose deletion included these two genes, showed an altered IPS volume comparable to findings in typical Williams-Beuren-Syndrome cases (Hoeft et al. 2014).

Mouse models showed that *Gtf2i* and *Gtf2ird1* were expressed during embryonic development and that heterozygous or homozygous disruption of *Gtf2ird1* resulted in decreased fear, aggression and anxiety and at the same time increased social behavior. When an unfamiliar mouse, a so-called intruder, was placed in the same area with $Gtf2ird1^{+/-}$ and $Gtf2ird1^{-/-}$ mice, it was contacted more frequent and for longer time periods than normally (Young et al. 2008).

GTF2IRD2 together with *GTF2I* and *GTF2IRD1* form a gene family of transcription factors and are highly expressive in the fetal and adult brain. While the function of *GTF2IRD1* and *GTF2I* in the pathogenesis of WBS has been examined so far, there is lack of information about the role of *GTF2IRD2*. A study with ten patients harboring a larger ~1.85 Mb deletion showed that a loss of *all* (*GTF2I, GTF2IRD1, GTF2IRD2*) members of the transcription factor family results in more severe neurological phenotypes. Affected individuals are more cognitively impaired making them perform poorer in tasks of spatial functioning, social reasoning and cognitive flexibility. Their daily life and psychological well-being were influenced by mood problems, such as depression, greater externalizing problems with obsessions and maladaptive behavior in comparison with individuals with a ~1.54 Mb deletion. The authors hypothesize that the parietal, frontal or cerebellar regions of the brain are more severely affected in these cases than in common WBS cases (Porter et al. 2012).

1.4.5 Block C

Block C comprises four genes and pseudogenes and spans approximately 80 to 100 kb (Valero et al. 2000). The (pseudo-)genes are *POM121* (*TRANSMEMBRANE NUCLEOPORIN*), *NSUN5* (*NOP2/SUN RNA METHYLTRANSFERASE FAMILY, MEMBER 5*), *TRIM50* (*TRIPARTITE MOTIF-CONTAINING PROTEIN 50*) and *FKBP6* (*FK506-BINDING PROTEIN 6*).

Until today, there is no report about consequences of a lack of *POM121* (OMIM *615753, https://www.ncbi.nlm.nih.gov/gene/9883. 30.10.2019. 13:00) which encodes a protein of the nuclear pore complexes (NPCs) which enable transports between the nucleus and the cytoplasm (Mitchell et al. 2010). *POM121* is expressed from C cen (*POM121*) and C tel (*POM121C)* but not from C mid (*POM121BP*) (Schubert 2009).

The definite function of NSUN5 (OMIM *615732, https://www.ncbi.nlm.nih.gov/gene/55695. 30.10.2019. 14:00) to date is still unclear (Schubert 2009). Doll et al. (2001) named *NSUN5 WBSCR20* while Merla et al. (2002) termed it *WBSCR20A*. Therefore, throughout the literature, several names for the same gene locus exist. Hence *NSUN5*, *WBSCR20* and *WBSCR20A* stand for the same gene. The function of *NSUN5* can only be assumed due to its similarity to human p120, which is a nucleolar antigen and is associated with cell cycle regulation and therefore cell proliferation (Doll et al. 2001). The ancestral gene *NSUN5* is located in the block C mid (Schubert 2009) while a truncated copy is located in the block C tel (termed *NSUN5P1* in this thesis) (Doll et al. 2001). The transcripts of both genes are expressed e.g. in skeletal muscle. Thus, Doll and colleagues (2001) assumed that a hemizygous loss of *NSUN5* may lead to the WBS-typical growth retardation and premature aging. Merla and colleagues detected a second truncated copy of *NSUN5*, which they called *WBSCR20C* (termed *NSUN5P2*) and is located in the block C cen (Merla et al. 2002).

TRIM50 (OMIM *612548, https://www.ncbi.nlm.nih.gov/gene/135892. 30.10.2019. 15:00) of block C mid is known to encode for an E3-ubiquitin-ligase (Micale et al. 2008). Two pseudogenes exist, which are the copies *TRIM73* in the block C tel and *TRIM74* in the block C cen. Ubiquitination serves processing and degradation of proteins within the cell (Rassow et al. Duale Reihe Biochemie, P. 374). Therefore, it is suspected that the accumulation of specific *TRIM50* enzyme target substrates could lead to neurodevelopmental disorders. This is supported by the fact that several syndromes like Bardet-Biedl or Opitz syndrome associated with mental impairment are caused by mutations of *TRIM* family E3-ubiquitin-ligases (Micale et al. 2008). For this reason, the authors presume a connection between hemizygosity of

TRIM50 which is located within block C mid and therefore deleted in most of the WBS patients and their (more or less clinically apparent) mental impairment.

The product of *FKBP6* (OMIM *604839, https://www.ncbi.nlm.nih.gov/gene/8468. 12.11.2019. 19:00) of block C mid is involved in the synaptonemal complex required for meiosis and *Fkbp6* knockout mice showed azoospermia (Metcalfe et al. 2005). Although *FKBP6* is exclusively expressed in human testes, the effect on fertility in human male individuals has to be further examined (Metcalfe et al. 2005, Miyamato et al. 2006).

1.5   Mechanism of deletion

The cause of vulnerability towards mutational mechanisms has been extensively reported. The most common explanation is misalignment through crossing over during meiosis, which is facilitated by several factors (Schubert 2009, Valero et al. 2000, Bayés et al. 2003, Pober 2010).

1.5.1   Meiosis and crossing over

Crossing over occurs during the prophase in the first meiotic division. Meiosis provides a reduced, haploid chromosome number in the gametes to ensure a diploid genome after fertilization and at the same time providing the descendant maternal and paternal features (Welsch et Deller. Lehrbuch Histologie. P. 80).

During prophase, pairing of homologous chromosomes -each containing two identical sister chromatids which will be distributed onto two different daughter cells- and crossing over take place. It occurs up to two or three times during each prophase between the corresponding maternal and paternal allele of two homologous chromosomes of a chromosome pair. With the help of spindle fibers that attach to the centromere of the chromosomes, the two homologous two-chromatid chromosomes are fixed at the spindle equator. This ensures that the corresponding alleles of the maternal and paternal chromatid align right next to each other. These chromatids then cross over. This can be observed through a light microscope. Crossing over ultimately aims to enlarge the genomic variability. After the prophase follow meta-, ana- and telophase, which finally result in the division of a pair of homologous chromosomes onto two daughter cells, each containing one chromosome of this pair. Afterwards the second meiotic division takes place. It serves the division of the two chromatids of a chromosome onto two

daughter cells each with one chromatid, ultimately resulting in four haploid gametes (Welsch et Deller. Lehrbuch Histologie. P. 80).

1.5.2 Unequal crossing over events or non-allelic homologous recombination

A special subtype of crossing over is the so-called unequal crossing over or non-allelic homologous recombination (NAHR). Usually, crossing over requires exact sequence homology of two alleles. However, sometimes two sequences show imperfect but very high homology without actually being alleles (Hurles and Lupski 2006). In this case, unequal crossing over can result in one duplicated and one deleted allele which could, if inherited cause diseases or syndromes. Duplications presumably occur as often as deletions, but only in rare cases they result in a clinical phenotype of relevance (Murken et al. Taschenlehrbuch Humangenetik. P. 58-59).

1.5.3 Sequence homology in flanking regions

Most cases of WBS arise as a de-novo deletion (Pober 2010), besides very rare cases of autosomal dominant inheritance (Morris et al. 1993). The WBSCR is thought to be predisposed to get lost during meiotic crossing over, because of the high sequence homology of the flanking gene regions (Pober 2010). Cuscó et al. (2008) presumed that WBS-transmitting parents have a much higher number of LCRs adjacent to the single-copy gene region on chromosome 7q11.23. Therefore, the risk for unequal crossing over and a deletion of the region of interest is 4.6-fold higher than compared to a control group.

All B blocks show contiguous homology over a length of ~120 kb (Valero et al. 2000). B tel and B mid share 99.7% of homology with each other, having ~143 kb of contiguous identical sequence. B cen has ~105 kb identical base pair sequence with both other blocks, thus 99.6% (Bayés et al. 2003). DNA samples of patients harboring the common 1.54 Mb deletion, indicate a recombination between the blocks B cen and B mid. Therefore, unequal crossing over events are thought to happen between centromeric and medial block B copies. This results in loss of the chromosomal part that is in between B cen and B mid, which mainly comprises of the WBSCR (Pérez-Jurado 2003, Bayés et al. 2003). Whether the deletion occurs in the paternal or the maternal allele of chromosome 7 is distributed almost equally between the two genders (Pérez-Jurado 2003). Bayés et al. (2003) analyzed samples of 74 WBS patients: they were able

to determine the origin of the deletion in 67 of the cases. In 45% the deletion was transmitted from the mother and in 55% from the father.

In parallel, with the help of sequence tagged site (STS) marker analysis (Schubert 2009), it was shown that patients carrying the larger 1.85 Mb deletion showed a recombination between block A cen and A mid which have a sequence homology of 98.2% (Bayés et al. 2003). Because of lower homology of A cen with A mid compared to B cen with B mid (98.2 % vs. ~ 99.6%), deletions arise explicitly more frequent between the B blocks than the A blocks. Deletions with a size of 1.54 Mb with breakpoints in B cen and B mid show a frequency of 95%, while those of 1.85 Mb with breakpoints between A cen and A mid arise with a frequency of 5% (Bayés et al. 2003).

Another factor that influences the loss of the WBSCR and its adjacent genes depends on the distance between the centromeric and medial B and A blocks. The shorter deletion of 1.54 Mb is more likely to get lost during meiosis than the larger one with 1.85 Mb. This is supported by the manifestation frequencies of 95% for the shorter deletion compared to 5% of the larger one (Bayés et al. 2003).

An additional premise for the susceptibility for misalignment during crossing over events is assumed to be found in the same orientation (i.e. the direction of transcription: sense or anti-sense) of B cen and B mid, as it is in A cen and A mid (Valero et al. 2000).

1.5.4 Inter- and intrachromosomal NAHR

Unequal crossing over is assumed to take place in two different ways. The first is *interchromosomal* unequal crossing over which is thought to occur in two thirds of WBS cases. The reason most likely lays in the high sequence homology of the B blocks, which leads to misalignment in the spindle equator and crossover of B cen of the one and B mid of the other homologous chromatid (instead of e. g. B cen and B cen, figure 1.10). This results in a duplication of the WBSCR in one and the loss of the WBSCR and some flanking genes in the other chromosome (Bayés et al. 2003, Schubert 2009).
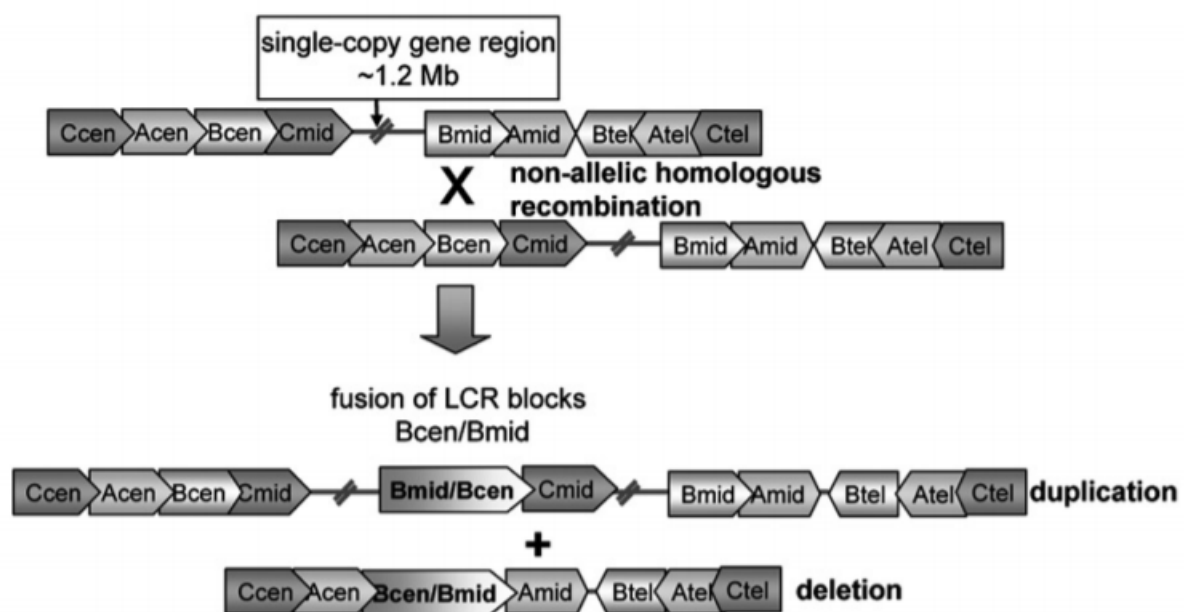
Figure 1.10: Interchromosomal unequal crossing over. Due to the highly homologous sequences of the blocks B mid/B cen, they align next to each other during prophase of meiosis, instead of B cen/B cen and B mid/B mid. This leads to a fusion of the blocks B mid/B cen during crossing over. Normally, the cen or the mid blocks were meant to fuse. The results are a duplication of the WBSCR ("single-copy gene region") in one chromosome and at the same time the loss of the WBSCR in the other chromosome. According to Valero et al. (2000) the susceptibility for misalignment is increased through the same orientation of the blocks B mid/B cen, visualized by the arrow shape of the single blocks. Block B tel shows the opposite orientation. From Schubert 2009.

The second mechanism of unequal crossing over occurs *intrachromosomal* and takes place in one third of WBS cases. Herein, the *intrachromatid* mechanism is more frequent than the *interchromatid* mechanism. Through the formation of a loop in the q-arm of chromosome 7 block B cen and B mid can align next to each other for fusion. The products are a shortened chromatid which has lost its WBSCR and flanking gene regions on one hand and a circular acentric chromosome on the other hand (figure 1.11, Schubert 2009).

Figure 1.11: Intrachromosomal intrachromatid unequal crossing over. Due to the same orientation and high sequence homology of the blocks B cen/B mid, these regions align next to each other and fuse. This results in the deletion of the WBSCR on one hand and the formation of a circular, acentric chromosome part on the other hand. Here unequal crossing over occurs within one chromatid of chromosome 7. From Schubert 2009.
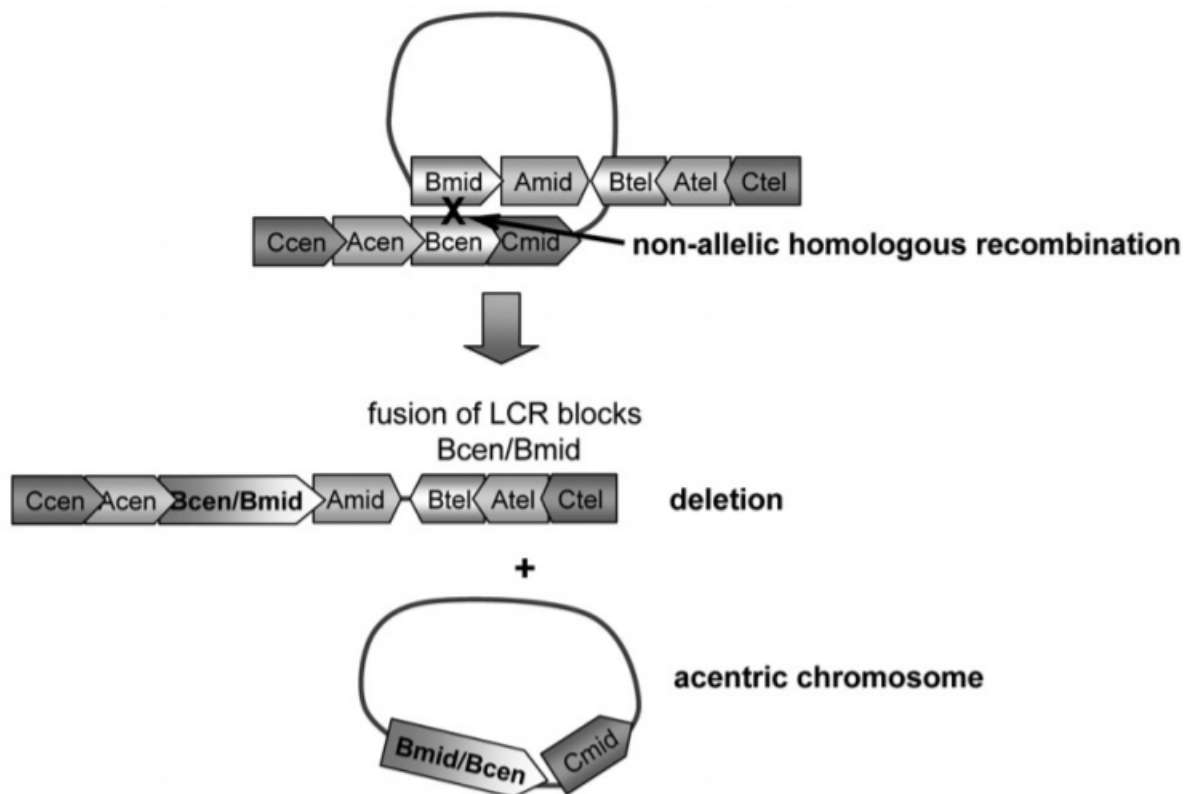
1.5.5 Inversion of WBSCR as predisposing factor

Another factor predisposing 7q11.23 for a deletion is the inversion of the WBSCR and flanking gene regions in transmitting progenitors. This facilitates the misalignment of chromosomes and therefore unequal genomic exchange and loss of affected regions during meiosis (Schubert 2009). Heterozygosity for an inversion of the region of interest on chromosome 7 has been found in approximately 30% of the chromosome-transmitting parents of WBS children compared to 5.8% in the general population (Osborne et al. 2001). Affected individuals in the former cohort show no specific phenotype which fits the assumption of an inversion being a phenotypical benign variant of the carrier (Schubert 2009).

In summary, the probability of occurrence of a deletion of the WBSCR is increased intrinsically due to the high sequence homology and same orientation of the flanking genes of the WBSCR, but is even more increased, if one chromatid carries an inversion (Bayés at al. 2003). A parent who carries an inversion has a 5.4-fold increased chance of having a child with WBS compared to non-inversion carriers (Merla et al. 2012).

Breakpoints leading to an inversion are located external to the WBSCR and no gene function is disrupted (Bayes et al. 2003, Schubert 2009). Inverted gene regions may occur with variable size ranging from 1.8 to 2.9 Mb (Schubert 2009).

1.6 Breakpoints in common WBS deletions

Breakpoints tend to concentrate in the centromeric beginning of block B cen and B mid where they show a higher homology of 99.8% to each other compared to their telomeric ends with 99.4% identity (which makes an overall sequence identity of 99.6%). Bayés et al. (2003) further specified the deletions of 74 WBS patients. In 19 of them a detection of the breakpoints was possible. They were narrowed down to a concentration of breakpoints in a 12 kb region between exon 16 and intron 21 within *GTF2IP1* (in this thesis *GTF2IP4*) (B cen) and within *GTF2I* (B mid). Most of the breakpoints in the larger 1.85 Mb deletion are thought to occur in the blocks A cen and A mid (Bayés et al. 2003).

Centromeric breakpoint	Telomeric breakpoint	Frequency	Deletion size
GTF2IP4 (B cen)	*GTF2I* (B mid)	53-74%	1.54 Mb
GTF2IP4 (B cen) / NCF1BP (B cen) *	*GTF2I* (B mid) / NCF1 (B mid) *		
NCF1BP (B cen)	NCF1 (B mid)	11-31%	1.54 Mb
GTF2IRD2P1 (B cen)	*GTF2IRD2* (B mid)	16%	1.54 Mb

Table 1.2: Breakpoints in WBS patients harboring the small (~ 1.54 Mb) deletion.
*intergenic region. After Bayés et al. 2003. Nomenclature after the Genome Data Viewer.

1.7 Genes of Williams-Beuren-Syndrome Chromosome Region (WBSCR)

Many genes commonly deleted in WBS patients have been explored and reviewed so far (Schubert 2009, Pober 2010) either with the help of genetic and clinical analyses of typical and atypical WBS patients, knock-out mice or peripheral cell lines (Chailangkarn et al. 2019). Therefore, it is possible to match some of the genes of the single-copy region to WBS phenotype characteristics. Most is known about the haploinsufficiency of *ELASTIN* (*ELN*), which causes familial supravalvular aortic stenosis (Curran et al. 1993, Schubert 2009, Pober 2010). In WBS, the phenotype probably appears due to haploinsufficiency and therefore hypoexpression of the hemizygous deleted genes (Pober 2010). Haploinsufficiency means that in a diploid organism the absence of a gene copy on one allele results in a malfunction of the affected gene: one remaining, intact gene copy does not provide enough gene product for an effective gene function (Murken et al. Taschenlehrbuch Humangenetik. P. 83).

Schubert concluded in her 2009 review referring to the other publications about phenotype-genotype correlations that deletions spanning the genes telomeric to *ELN* cause a more severe and impaired phenotype than deletions centromeric to it (Schubert 2009, Fusco et al. 2014). Some of the genes seem to have overlapping functions which is implicated by phenotype-genotype correlations in patients with atypical deletions. To date, it is unknown in which manner deleted and spared genes have an influence on each other.

Patients with atypical shorter deletions sparing *CLIP2* perform better in visuospatial and motor skills than those whose deletion includes *CLIP2*. It is questionable if this phenotype is caused only by *CLIP2*. There are other genes that are attributed to cause this phenotype as well, like *GTF2IRD1* and *GTF2I*. These two genes were also not affected by these atypical shorter deletions (Schubert 2009).

Table 1.3 provides an overview of the function of the coding genes of the WBSCR and the adjacent genes usually deleted in WBS, according to the most common breakpoints located in *GTF2IP1* (here *GTF2IP4*) (B cen) and *GTF2I* (B mid) (Bayes et al. 2003).

Gene	Protein function and (→) putative role in WBS due to haploinsufficiency
NSUN5 (block C mid) *NOP2/SUN RNA METHYLTRANSFERASE FAMILY, MEMBER 5* (alias *WBSCR20, WBSCR20A*) (OMIM *615732)	Cell cycle regulation and cell proliferation.
	→ Putative role in growth retardation, myopathy, premature aging effects (Doll et Grzeschik 2001).
TRIM50 (block C mid) *TRIPARTIFE MOTIF-CONTAINING PROTEIN 50* (OMIM *612548)	Involved in ubiquitination.
	→ Putative role in gastrointestinal pathologies, cognitive profile, mental impairment (Micale et al. 2008).
FKBP6 (block C mid) *FK506-BINDING PROTEIN* (OMIM *604839)	Involved in homologous chromosome pairing during meiosis, *Fkbp6* knockout mice showed azoospermia (Metcalfe et al. 2005).
	→ No known role in WBS.
FZD9 *FRIZZLED CLASS RECEPTOR 9* (OMIM *601766)	A transmembrane receptor for Wnt signaling proteins, involved in early development of the central nervous system (Wang et. al 1997).
	→ Putative role in behavioral characteristics such as overfriendliness, anxiety (Chailangkarn et al. 2016).
BAZ1B *BRODOMAIN ADJACENT TO ZINC FINGER DOMAIN 1B* (alias *WILLIAMS SYNDROME TRANSCRIPTION FACTOR* (*WSTF*), *WBSCR9*) (OMIM *605681)	Involved in DNA transcription and replication (Bozhenok et al. 2002). The possible involvement in vitamin D metabolism and hypercalcemia has been retracted (Kitagawa et al. 2003).
	→ Putative role in neurological findings (e. g. abnormalities in brain volume) and hypersocial features in WBS (Lalli et al. 2016).
BCL7B *B-CELL CLL/LYMPHOMA 7B* (OMIM *605846)	Regulation of the Wnt signaling pathway and apoptosis (C. elegans).
	→ Putative risk of malignancies and interaction with other tumor-related genes (e. g. in WBS) (Uehara et al. 2015).
TBL2	A Beta-transducing protein (Pérez-Jurado et al. 1999).

TRANSDUCIN-BETA LIKE 2 (alias *WBSCR13*) (OMIM *605842)	→ No known role in WBS.
MLXIPL MLX INTERACTING PROTEIN-LIKE (alias *WBSCR14*)	Glucose-responsive transcription factor, involved in regulation of hepatic glycolysis, lipogenesis, gluconeogenesis.
(OMIM *605678)	→ Putative involvement in hypotriglyceridemia in WBS (Palacios-Verdú et al. 2015).
VPS37D *VACUOLAR PROTEIN SORTING 37* (alias *WBSCR24*) (OMIM *610039)	Product is homologous to proteins of the endosomal sorting complex (Micale et al. 2008).
	→ No known role in WBS.
DNAJC30 *DNAJ/HSP40 HOMOLOG, SUBFAMILY C, MEMBER 30* (alias *WBSCR18*) (OMIM *618202)	Interaction with mitochondrial ATP synthase in human neocortical neurons. *Dnajc30*-knockout-mice showed some WBS characteristics.
	→ Putative reason for smaller corpus callosum, hypersociability, anxiety, lower brain and body weight. Also, putative role of mitochondrial dysfunction in WBS pathogenesis (Tebbenkamp et al. 2018).
BUD23 *rRNA METHYLTRANSFERASE AND RIBOSOME MATURATION FACTOR BUD23* (alias *WBSCR22*) (OMIM *615733)	Putative methyltransferase activity (Doll et Grzeschik 2001). Regulation of glucocorticoid receptors and loss of glucocorticoid sensitivity in inflammation (Jangani et al. 2014).
	→ Putative role in premature aging effects (Doll et Grzeschik 2001).
STX1A SYNTAXIN 1A (OMIM *186590)	Membrane vesicle fusion and pancreatic exocytosis of insulin (Bennett et al. 1992). Either excess or deficiency of STX1A leads to an impaired glucose release (Lam et al. 2005).
	→ Putative prime candidate for impaired glucose metabolism in WBS (Pober et al. 2010).
ABHD11 *ABHYDROLASE DOMAIN CONTAINING 11* (alias *WBSCR21*) (https://www.ncbi.nlm.nih.gov/gene/83451/. 01.12.2019. 12:00)	Hydrolase activity.
	→ No known role in WBS (Schubert 2009).

CLDN3* and *CLDN4 *CLAUDIN 3* and *4* (OMIM *602910 and *602909)	Part of tight junctions in various tissues (Morita et al. 1999).
	→ No known role in WBS.
WBSCR27 *WILLIAMS-BEUREN-SYNDROME CHROMOSOME REGION 27* (OMIM *612546)	Assumed function as SAM-dependent methyltransferase, unknown exact cellular function (Mariasina et al. 2018).
	→ No known role in WBS.
WBSCR28 *WILLIAMS-BEUREN-SYNDROME CHROMOSOME REGION 28* (OMIM *612547)	Function unknown (Schubert 2009).
	→ No known role in WBS.
ELN *ELASTIN* (OMIM *130160)	Component of elastic fibers in the extracellular matrix of connective tissue. Provides elasticity for e.g. blood vessels, lung, cardiac valves and skin (Rassow et al. Duale Reihe Biochemie. P. 391).
	→ Best explored gene of the WBSCR. *Proven* role in WBS: SVAS, arteriopathy with vascular stenoses and hypertension. Putative role in hernias, premature aging of skin, joint laxity, joint contractures, hoarse voice, bladder and colon diverticulosis, dysmorphic facial features (Ewart et al. 1993b, Pober 2010). Haploinsufficiency and heterozygous point mutations cause isolated SVAS (OMIM #185500) (Schubert 2009).
LIMK1 *LIM KINASE 1* (OMIM *601329)	Protein kinase involved in actin cytoskeleton reorganization and synapse formation in the central nervous system (Scott et Olson 2007).
	→ Putative role in hyperacusis and progressive hearing loss (Matsumoto et al. 2011), in long term memory and learning (Todorovski et al. 2015) and in impaired spatial cognition (Morris et al. 2003). Putative effect of *LIMK1* hemizygosity on weakness in spatial cognition (Gray et al. 2006, Smith et al. 2009).
	Involved in translation initiation (Richter et al. 1999).

EIF4H *EUKARYOTIC TRANSLATION INITIATION FACTOR 4H* (alias *WBSCR1*) (OMIM *603431)	→ *Eifh4* null mice show growth deficits, brain abnormalities with hippocampal impairment (learning, memory) (Capossela et al. 2012).
LAT2 *LINKER FOR ACTIVATION OF T CELLS FAMILY, MEMBER 2* (alias *WBSCR5*) (OMIM *605719)	Activation of T-cells and putative activation of mast cells (Iwaki et al. 2007).
	→ No known role in WBS (Schubert 2009).
RFC2 *REPLICATION FACTOR C, SUBUNIT 2* (OMIM *600404)	DNA replication, cell cycle checkpoints, DNA damage response (Noskov et al. 1998).
	→ Putative role in microcephaly and growth retardation (Kerzendorfer et O`Driscoll 2009).
CLIP2 *CAP-GLY DOMAIN CONTAINING LINKER PROTEIN 2* (alias *CYLN2*, *WBSCR4*) (OMIM *603432)	Linker between organelles and microtubules, expressed in the brain (Hoogenraad et al. 1998).
	→ Putative main candidate for motor and cognitive impairments in WBS (Van Hagen et al. 2007b). Probably only combined with haploinsufficiency of *GTF2IRD1* and *GTF2I* (Vandeweyer et al. 2012).
GTF2IRD1 (alias *WBSCR11*) **GTF2I (both block B mid)** *GENERAL TRANSCRIPTION FACTOR II-I FAMILY* (together with *GTF2IRD2*) (OMIM *604318 and 601679)	Transcription factors, involved in tissue development and differentiation (Thompson et al. 2007).
	→ Putative role of <u>*GTF2I*</u> in visual-spatial and cognitive aspects (Vandeweyer et al. 2012) and of <u>*GTF2I*</u> and <u>*GTF2IRD1*</u> in reduced fear and aggression as well as increased social abilities (Young 2008, Martin et al. 2017).
	→ Putative role of <u>*GTF2IRD1*</u> in sensorineural hearing loss (Canales et al. 2015) and in tooth abnormalities (Ohazama et Sharpe 2007).

Table 1.3: Coding genes of the WBSCR and coding flanking genes absent in a 1.54 or 1.85 Mb deletion and their putative role in WBS. The genes ordered from centromeric to telomeric location on 7q11.23. Genes examined by MLPA are colored blue.

1.8   Research objective

Williams-Beuren-Syndrome is a de-novo hemizygous microdeletion syndrome in which the patients typically have a distinct clinical appearance. This phenotype however can vary and WBS is associated with a variety of other pathologies in all other organ systems like the cardiovascular, endocrine or genitourinary system. Even some of the most common symptoms like the supravalvular aortic stenosis often require close monitoring and surgical treatment. Hence, an early diagnosis helps to screen the patients for the known symptoms. WBS patients also have a different set of social skills with overfriendliness, advanced musical abilities, but also a low general IQ and reduced scepticism towards strangers. This makes them a group of patients whose individual abilities need to be addressed during development but also in adulthood. As in other syndromes, atypical clinical and molecular genetic cases have been described.

This thesis includes previously gathered clinical and molecular genetic information focussing on the physical and mental development of WBS patients provided by Prof. Dr. Rainer Pankau (paediatrician and one of the authors of the book "Das Williams-Beuren-Syndrom: Genetik-Medizin-Psychologie"), Dr. Elke Reutershahn (Chief resident of the Department of Paediatrics at the Helios Clinic Duisburg, specialized in Williams-Beuren-Syndrome), Dr. Stephanie Demuth (human geneticist, Erfurt), Dr. Verena Gravenhorst (children's cardiologist, University of Göttingen) and by Harry Nuss, a medical student at the University of Kiel who worked on his doctoral thesis about WBS (under supervision of PD Dr. Hiltrud Muhle, neuropediatrician, University of Kiel) at the same time as the experiments for this thesis were carried out. Part of the FISH analyses of patients with WBS were performed by Dr. Manfred Schneider, a former medical student at the Department of Human Genetics at the Christian-Albrechts University Kiel. The cohort of patients in this thesis was collected over three decades and hence documentation and samples suffered from relocation of the DNA and change in documentation methods.

The intention of this thesis is to confirm the patients' former FISH results by MLPA and to detect divergences in the results of the two methods. Fragment analysis is used to further specify the sizes of the deletions detected by MLPA, their breakpoints and to differentiate between a maternal and paternal inheritance. The results will be compared to the available clinical data to establish a possible phenotype-genotype correlation, especially by the help of atypical patients. The expected clinical affection and the associated prognosis which is addressed in genetic counselling is of utmost importance for the patients and their parents.

2 Patients, methods and materials

2.1 Patients, materials and storage

Since the early 1990s over 300 individuals from Germany were diagnosed with Williams-Beuren-Syndrome through a collaboration of the Departments of Human Genetics of the University Medical Centre Hamburg-Eppendorf (UKE) and the Christian-Albrechts University of Kiel (Prof. Reiner Siebert). The most commonly performed diagnostic method was FISH analysis. In addition, in many cases the parents' or sometimes the siblings' DNA were extracted as well. With informed consent of the patients themselves and/or of their parents the DNA samples were stored at -20°C until today in the Department of Human Genetics of the UKE. These samples represent the largest collection of DNA samples of WBS patients in Europe.

Because initially consent of every patient (and/or the parents) was sought, a reconfirmation of the informed consent (German "Ethikvotum") was not necessary. There was no conflict of interest.

There were several different lists, almost exclusively in paper form, which often provided different information on the patients, their relatives and the final result of molecular diagnostics. Usually name, date of birth, suspected diagnosis and referring paediatrician were known. Some lists contained information about FISH analysis and its results and sometimes a comment about other clinical features than WBS (e.g. short stature or tetralogy of Fallot). Some patients even had various numbers of DNA samples that were collected over the years. In several cases, there were considerable differences regarding the information on the patients and their relatives. Sometimes the names or dates of births differed and could only be identified with the help of the WBS specialists mentioned in chapter 1.8 who additionally provided first-hand clinical information, especially about the clinically atypical cases.

Among the stored DNA collective were several DNA samples of patients which were not included in the WBS-lists of the UKE or the University of Kiel. Most of these samples were also analysed. Totally, a number of 341 presumed patients and 260 relatives were identified. 179 of the patients were male, 155 were female and in 7 case the sex could not be determined.

The collective comprised three pairs of twins, one dizygotic and two monozygotic pairs. The parents of two pairs (one di-, one monozygotic) were reported healthy. Of the other monozygotic pair, neither clinical information nor parental DNA were available. Furthermore, two mother-daughter pairs and one mother-son pair, all of them with WBS, could be identified.

In cases of atypical molecular genetic results, additional efforts were made to collect more information.

2.2 DNA extraction

2.2.1 Phenol-chloroform extraction (not part of this thesis)

This method was used for the older, long-term stored DNA samples of WBS patients and their parents or siblings and was not performed as part of this thesis.

Phenol-chloroform extraction of DNA is a method for partitioning DNA, RNA and proteins applied in biochemical sciences. It is used for the isolation of DNA or RNA out of small amounts of tissue or cells to perform additional molecular genetic studies. The procedure was developed by Chomczynski and Sacchi in 1987. It is a method based on the different solubilities of several compounds (in this case DNA, RNA and proteins) in two different immiscible phases (water and phenol-chloroform) (Chomczynski et Sacchi 1987 and 2006). In the end, after centrifugation, RNA can be found in the lighter and therefore upper, polar, aqueous phase and DNA in the heavier and therefore lower, non-polar, organic, phenol-chloroform phase. The proteins will remain in the interphase (Sambrook et Russell 2006).

The upper phase (water with RNA) is pipetted off and the whole procedure is performed several times to increase the purity of the DNA.

2.2.2 QIAmp® DNA Blood Mini Kit

2.2.2.1 Required equipment

For DNA extraction out of EDTA blood samples the QIAamp® DNA Blood Mini Kit (QIAGEN Hilden, Germany) was used. Content of the kit:

1. QIAamp® spin columns
2. Collection tubes (2ml)
3. Buffer AL
4. Buffer AW1
5. Buffer AW2
6. Buffer AE
7. QIAGEN Protease
8. Protease solvent

2.2.2.2 Procedure

The procedure was performed after the *Blood and Body Fluid Spin Protocol 09/2001* but modified in some single aspects.

In the beginning, 20 µl Protease were added to 1.5 ml microcentrifuge tubes, followed by 200 µl EDTA blood and lastly 200 µl Buffer AL. It is important not to mix Protease and Buffer AL directly. The ingredients were mixed by pulse-vortexing for 15s and afterwards incubated in the thermoblock at 56 °C for 10 minutes. Centrifugation for 1 minute at 6000 x g (8000 rpm) was required before adding 200 µl ethanol (96-100%) followed by pulse-vortexing for 15s and short centrifugation. The total volume of 620 µl was added to the QIAamp® spin column positioned in a 2 ml collection tube and centrifugation for 1 minute at 6000 x g was performed. Then, the 2 ml collection tube was exchanged with a clean tube. The filtrate was discarded. 500 µl Buffer AW1 were added to the sample, centrifugation for 1 minute at 6000 x g was performed and the 2 ml collection tube again replaced by a clean one. 500 µl Buffer AW2 were added to the spin column followed by centrifugation for 1 minute at 20.000 x g. The collection tube was emptied and the sample was again centrifuged for 3 minutes at 20.000 x g. The QIAamp® spin column was placed in a new 1.5 ml microcentrifuge tube and 60 µl Buffer AE were added. This mixture was incubated at room temperature for 5 minutes and afterwards centrifuged for 1 minute at 6000 x g. The filtrate was pipetted to the column again, incubated at room temperature for 5 minutes followed by centrifugation for 1 minute at 6000 x g. The final amount of the filtrate matched the amount of the Buffer AE with nearly 60 µl.

2.3 DNA concentration measurement

Qubit® Fluorometer and the dsDNA BR Assay Kit were used to measure the concentration of the extracted DNA.

2.3.1 Function principle

With the help of a fluorescence dye it is possible to measure just the concentration of double-strand DNA (dsDNA) while excluding RNA, proteins and impurities. The DNA concentration measurement with Qubit® 2.0 Fluorometer is a very sensitive method.

2.3.2 Required equipment

1. Qubit® 2.0 Fluorometer
2. Qubit® dsDNA BR Assay Kit (Invitrogen™ by life technologies, Carlsbad, CA, USA)
   a. Qubit® dsDNA BR Reagent
   b. Qubit® dsDNA BR Buffer
   c. Qubit® dsDNA BR Standard #1
   d. Qubit® dsDNA BR Standard #2
3. Qubit® Assay tubes (500 µl)
4. Plastic container for working solution

2.3.3 Performance

For the preparation of the working solution, per sample 199 µl of Qubit® dsDNA BR Buffer and 1 µl of Qubit® dsDNA BR Reagent were added to a plastic tube and mixed properly by thorough vortexing. After labelling the Qubit® Assay tubes, 198 µl of this working solution were added to each tube for the DNA measurement. To two tubes, 190 µl were added to serve as the pre-diluted DNA standards.

To the former ones 2 µl of the DNA sample in question and to the latter ones 10 µl of Qubit® dsDNA BR Standard #1 and #2 were added respectively. All tubes were mixed by vortexing and subsequently incubated for 2 minutes at room temperature. After calibrating the Qubit® 2.0 Fluorometer with help of the two standards the DNA samples were measured.

2.4 Dilution of the DNA

According to the preferred DNA concentration range between 50 and 100 ng/µl recommended by MRC Holland for the MLPA procedure, the DNA samples were diluted with Invitrogen™ TE Buffer. Further information about MLPA (material and procedure) will follow below.

2.5 Polymerase chain reaction (PCR)

2.5.1 Function principle

The following procedure of PCR is based on the Standard Operating Procedure (SOP) of the laboratory of the Clinic and polyclinic of Hematology and Oncology University Clinic Hamburg Eppendorf "Polymerasekettenreaktion (PCR)" 2.11.6 Version 03.

The PCR was first described by Mullis et al. in 1986. It is the amplification of a certain DNA sequence of interest in an exponentially growing number to do further tests or analyses. The procedure is a succession of three steps: DNA denaturation, annealing and DNA synthesis that are repeated in 20 to 40 cycles. Each step requires a different temperature which is generated by a thermocycler.

Initially, the DNA samples have to be incubated for 5 minutes at 95 °C for denaturation of the DNA. The DNA of interest is called template and contains the region that is to be amplified. 95 °C is the required temperature to release the hydrogen bridge bonds between the nucleotides for separation of the double-strand into two single DNA strands.

During the next step, which is called annealing, the primers, synthetic oligonucleotides, hybridize with their complementary nucleotide sequence on the DNA single-strands. The ideal annealing temperature for this step varies within the different primers and ranges from 40 to 70 °C. The temperature needs to be accurate to ensure an exact complementary binding of the primer (15 to 30 nucleotides) with the target template. The primer provides the 3'-end for the polymerase, which binds to the primer-marked template.

The third step is called DNA synthesis or elongation. It is usually performed at 72°C to match the optimal activity temperature of the Taq polymerase. The Taq polymerase originated from the thermophile bacteria Thermus aquaticus and has the advantage of not being inactivated at high temperatures. The polymerase elongates the primers from 5' to 3' direction by linking single nucleotides (dNTPs), which hybridize complementary to the template single-strand. The PCR is limited by an insufficient Taq polymerase or the lack of substrates.

These three steps are repeated in a certain number, so called cycles. After the predetermined number of cycles are completed, there is a final elongation at 72 °C to ensure that every single-strand has been amplified completely. The terminating temperature of 15 °C serves at optimal temperature for short-time storage (Rassow et al. Duale Reihe Biochemie. Page 482ff., Murken et al. Taschenlehrbuch Humangenetik. P. 105f.).

A PC-reaction as part of this thesis is required for MLPA as well as for fragment analysis.

2.5.2 Required ingredients

1. dH$_2$O
2. Taq DNA Polymerase Recombinant Kit
   a. Taq DNA Polymerase
   b. 10x PCR Buffer
   c. MgCl$_2$
3. Primer Sn
4. Primer Asn
5. dNTP-Mix (Thermo Scientific, Waltham, MA, USA, #0192)

2.6 Multiplex Ligation-dependent Probe Amplification (MLPA)

Multiplex Ligation-dependent Probe Amplification (MLPA) was first described in 2002. This technique was initially developed to detect deletions or duplications in the *BRCA1*, *MSH1* and *MLH1* genes (Schouten et al. 2002). Furthermore, it was used in the detection of trisomies and the characterization of the chromosomal constitution in tumor and peripheral blood samples (Schouten et al. 2002). The application of MLPA as a reliable method for detecting copy number variations (CNV) in the *BRCA1* gene was confirmed in 2003. MLPA of *BRCA1* showed advantages in diagnosing hereditary breast and ovarian cancer compared to PCR alone (Hogervorst et al. 2003).

Although MLPA is a very sensitive method, it still is limited in some aspects: copy number neutral inversions will not be detected as well as translocations (MRC Holland, MLPA General Protocol 2019).

The following descriptions are based on:

- MRC Holland. Designing synthetic MLPA probes. Version 14. Last update 19-12-2014.
- MRC Holland. General MLPA protocol for the detection and quantification of nucleic acid sequences. MLPA DNA protocol version MDP-005, last revised on 22 September 2014.
- SALSA MLPA probemix P029-B1 Williams-Beuren-Syndrome. Description version 11. 05-05-2014.

- SOP of the Clinic and Polyclinic of Pediatric Hematology and Oncology "Multiplex Ligation-dependent Probe Amplification (MLPA)" 2.11.13 Version 01.

2.6.1 Intended use

MLPA is a semi-quantitative method to detect abnormal CNVs e. g. deletions or duplications in defined chromosomal areas. A semi-quantitative test does not provide the absolute number of products (quantitative test) but the number of products relative to another, in this case the reference sample of a healthy control. The DNA sample of interest is put into a relation to one or more samples which are known to have no CNV. The relative copy number of up to 60 different DNA sequences can be determined in just one single PCR-based reaction.

2.6.2 Function Principle

2.6.2.1 Overview

MRC Holland provides a large variety of probemixes to detect copy number variants in different syndromes and diseases that are caused by chromosomal aberrations. Each probemix contains probes that detect alterations in copy numbers by hybridizing with the probe target, a defined part of the sample DNA. In case of a deletion, the number of hybridizing probes is reduced compared to the reference sample. In case of a duplication it is increased.

In the beginning of the MLPA procedure, the probes of the probemix are separate and comprise of two different parts: the left and the right probe oligonucleotide (LPO and RPO). The components of LPO and RPO are: *LPO* and *RPO hybridizing sequence* (LHS and RHS), stuffer sequence (which can be part of the LPO and/or RPO) and primer sequence (forward and reverse, figure 2.1). Stuffer and primer sequences flank the LHS and RHS (figure 2.1). The minimum length of the LHS and RHS is 21 nt each. The stuffer sequence provides a variability of length of the LPO and RPO, because the LHS and the RHS are almost of the same length for every exon. LPO and RPO can hybridize with the exons within the gene of interest next to each other but are not connected (figure 2.1).
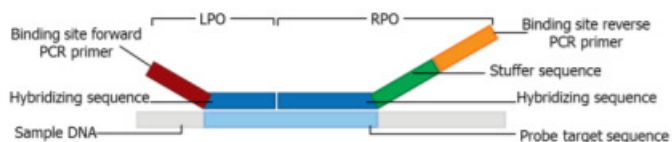
Figure 2.1: Model of sample DNA and probe oligonucleotides. From MRC Holland MLPA. Designing synthetic MLPA probes and probemixes. Version 04. Nov 2018.

The LPO provides the 5´-end for the sense primer (forward primer), the RPO provides the 3`-end for the antisense primer (reverse primer). The 5´-end of the RPO has to be phosphorylated to enable the ligase enzyme to join the two adjacent oligonucleotides into one complete probe.

The hybridization sequences are held as short as possible still ensuring that the base pairing is exact in every single nucleotide. Combined, oligonucleotides, stuffer sequences and primer sequences form the complete probes with a total length ranging between 130 and 500 nt. The minimum total length difference between the single probes has to be 4 nt to ensure an adequate separation during the following capillary electrophoresis.

The probemix also contains some reference probes. They do not hybridize with the examined DNA locus, but with various other chromosomal loci in the genome. The reference probes are relevant for later capillary electrophoresis and analysis and allow so called *intrasample normalization* which will be elucidated below.

A SALSA MLPA Kit contains:

Reagent kit component	Ingredients
Application-specific MLPA probemix	Contains reference probes, MLPA control fragments, synthetic probes can be added
SALSA MLPA Buffer	KCl, Tris-HCl, EDTA, PEG-6000, oligonucleotide
SALSA Ligase-65	Glycerol, EDTA, Beta-Mercaptoethanol, KCl, Tris-HCl, non-ionic detergent, Ligase-65 enzyme (bacterial origin)
Ligase Buffer A	Coenzyme NAD (bacterial origin)
Ligase Buffer B	Tris-HCl, $MgCl_2$, non-ionic detergent
SALSA PCR Primer Mix	Synthetic oligonucleotides with fluorescent dye, dNTPs, Tris-HCl, KCl, EDTA, non-ionic detergent
SALSA Polymerase	Glycerol, non-ionic detergents, EDTA, DTT, KCl, Tris-HCl, Polymerase enzyme (bacterial origin)

Table 2.1: Content of a MLPA kit.

With the help of the following polymerase chain reaction, hybridized and ligated probes are amplified and then separated by capillary electrophoresis. The MLPA only needs one pair of sense and antisense-primer, one of them is marked with a fluorescence dye (dye FAM).

The primer binding sequence of the oligonucleotides standardly have the following nucleotide sequence: GGGTTCCCTAAGGGTTGGA (LPO) and TCTAGATTGGATCTTGCTGGCAC (RPO).

Only a complete probe provides two primer sequences for the forward and the reverse primer that are necessary for the following PCR. The advantage of using the same primer binding sequences for every single probe is that only one primer pair is necessary for simultaneously amplification (Schouten et al. 2002). The fluorescent signal of the amplified products subsequently detected by the ABI sequencer can be set into relation to the standardized signals depicted by another fluorescing dye, the LIZ standard. Incomplete probes are not amplified in a sufficient quantity and therefore they do not provide a measurable lightning signal.

Every single amplification product will be depicted either as a peak or as a column depending on the way of representation in the following computer analysis. The interpretation of the data will be explained below.

2.6.2.2   MLPA Procedure

2.6.2.2.1   Denaturation and hybridization reaction (day 1):

The MLPA general protocol recommends 5 µl of DNA with a preferred concentration between 50 and 100 ng within a possible range of 50 to 250 ng. If required, the DNA was diluted with TE buffer. Samples of interest and reference/control samples are chosen, added to tubes and denaturized in a thermocycler for 5 minutes at 98 °C to separate double-stranded into single-stranded DNA. Afterwards, the samples are cooled down to 25 °C and removed from the thermocycler.

In the next step a hybridization master mix with two components is prepared: 1.5 µl MLPA probemix that contains the probes, LPO and RPO (They are still separate. The quantity-fragments (Q fragments) are complete probes from the start.) and 1.5 µl MLPA buffer per sample. 3 µl of this master mix are added to each sample and mixed well by pipetting up and down. The thermocycler program continues with incubation at 95 °C for 1 minute and then at

60 °C for 16-20 hours. During this period, LPOs and RPOs and the Q fragments hybridize with the single-stranded DNA.

2.6.2.2.2 Ligation and PCR (day 2):

The ligase-65 master mix is prepared containing 25 µl dH$_2$O, 3 µl of ligase Buffer A, 3 µl ligase Buffer B and 1 µl Ligase-65 enzyme per sample. The ligase enzyme has to be stored at -22 °C before and immediately after use. When the thermocycler is paused at 54 °C, 32 µl of the master mix are added to each sample. The thermocycler program is continued for 15 minutes at 54 °C for the ligation of the LPOs and RPOs by the ligase to form a complete probe. Then heating for 5 minutes at 98°C ensures the heat inactivation of the ligase. Afterwards, the cycler is cooled down to 20 °C and the samples can be removed for further usage.

Finally, the polymerase master mix is prepared with 7.5 µl dH$_2$O, 2 µl SALSA PCR primer mix and 0.5 µl SALSA Polymerase for each reaction. The PCR primer mix has to be stored protected from light and the Polymerase has to be stored at -22 °C before and after use. 10 µl of the master mix are given to each sample and mixed well before putting them back to the thermocycler for the final part of the MLPA program, the PCR.

PCR program requires 35 cycles of:

> 30 seconds at 95°C
> 30 seconds at 60°C
> 60 seconds at 72°C

The PCR ends with 20 minutes of incubation at 72°C and pauses at 15°C.

2.6.2.2.3 Fragment separation by capillary electrophoresis

To prepare the samples for the ABI capillary electrophoresis, a master mix containing 17.75 µl formamide and 0.25 µl LIZ standard for each sample is mixed and 18 µl are placed to each tube. Afterwards, the samples are heated at 86 °C for 3 minutes and cooled at 4 °C for 2 minutes. Formamide prevents the single-stranded DNA hybridizing again after denaturation. LIZ functions as a standard for fragment sizes.

2.6.3   Interpretation

2.6.3.1   MLPA Quality Control Fragments

Each probemix contains one 92 nt benchmark probe, four Q-fragments (= quantity), two D-fragments (= denaturation) and one X- and Y-fragment.

Four Q-fragments at lengths of 64, 70, 76 and 82 nt respectively serve as indicators for insufficient DNA quantity and are compared to the 92 nt control fragment peak. If all four Q fragments reach at least one third of the height of the 92 nt control fragment, the amount of DNA is too small or the ligation has failed. The Q-fragments are complete probes that do neither need to be ligated nor need to hybridize to DNA template to get amplified during PCR. The higher the amount of DNA in the sample, the lower the quantity fragments.

The kit contains two D-fragments at 88 and 96 nt, which are also evaluated in comparison to the 92 nt benchmark. If the D-fragment peaks are at least 40% shorter than the 92 nt control fragment it is a sign of insufficient DNA denaturation. The D-fragments detect chromosomal areas that lay within CpG islands. D-fragments operate as a reliable indicator for proper denaturation because CpG islands are difficult to denature due to their triple hydrogen bridge bonds. If denaturation has failed, the fragments are not able to hybridize with the CpG islands and for that reason there is no amplification of them during the following PCR.

The kit also encompasses two gender control fragments. The X-fragment has a length of 100 nt and the Y-fragment a length of 105 nt and marks the according gender.

2.6.3.2   Principles of MLPA Data Analysis

To be able to analyze DNA copy number variations the samples have to be standardized. This is possible because of at least eight reference probes which are contained in the probemix. First, there is an intrasample normalization with the help of each probe's measured fluorescence and then an intersample normalization through comparison with a group of samples. The intrasample normalization compares each probe peak to the reference probe peaks. The reference probes are located on various chromosomes and are expected to have a normal copy number. Therefore, relative probe peaks are yielded instead of absolute ones. Intersample normalization compares the relative probe peaks in the DNA sample to all reference samples. Samples with no expected variation in copy numbers are chosen as reference DNA.

With the help of the software SequencePilot (SeqPilot) for MLPA data analysis the visualization via computer is possible. The reference samples including the standard deviation are shown as a blue column next to a green column, which symbolizes the DNA sample of interest. In figure 2.2, the percentages are plotted on the y-axis ranging from zero to 200 percent. The exons are arranged corresponding to the chromosomal order from centromeric on the left to telomeric on the right side of the diagram and not according to their nucleotide number. Samples without any copy number variant will show green columns as high as the light blue column of the reference sample and the diagram beneath will show no bar. In this case the DNA sample of interest and the average reference samples have the same copy numbers, therefore 100%.
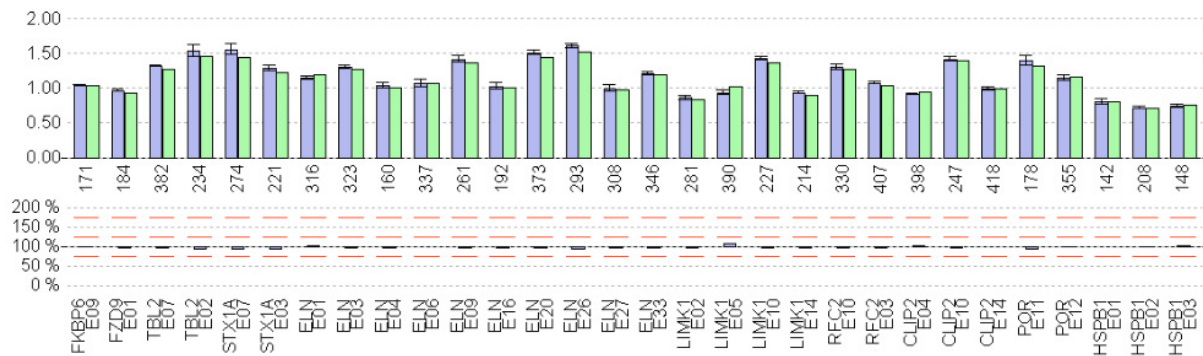
Figure 2.2: WBS-MLPA analysis of a DNA sample with a normal gene dose/normal genotype.

If a deletion or a duplication of single or several exons is detected, a column of dark blue color appears: if the column is at zero percent, the analyzed sample DNA shows a homozygous deletion for the exons of interest. If the column is at least 35-50% lower than those of the reference samples, it represents a hemizygous deletion as it appears in case of WBS (figure 2.3). If the column is above 100 % a duplication was detected. The hemizygous deleted chromosomal region in a typical WBS patient ranging from exon 9 of *FKBP6* to exon 14 of *CLIP2* approximately measures ~1.05 Mb.

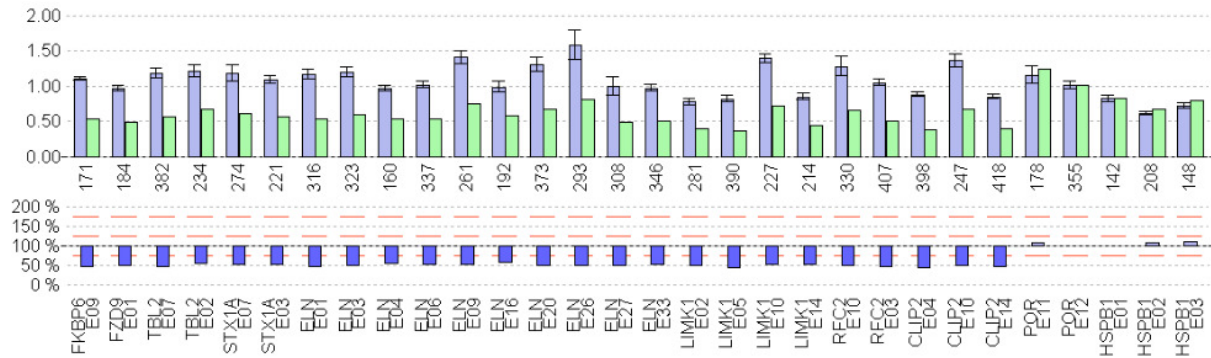**Figure 2.3: MLPA analysis of a DNA sample with a hemizygous deletion in a patient with WBS.** The green columns measure only half the height of the light blue columns. Accordingly, the dark blue columns below indicate only 50% of the gene dose compared to the reference sample. The diagram fits the findings in a typical WBS patient.

2.6.4 WBS probemix

The SALSA MLPA probemix P029-B1 for Williams-Beuren-Syndrome contains 10 exons within the *ELN* gene, 15 exons of adjacent genes that are deleted in most of the typical WBS patients and 5 exons of genes, which are located telomeric on chromosome 7 and are typically not deleted. Altogether, the kit comprises of 39 probes that result in amplification products between 132 and 427 nt. In addition, it contains nine control fragments with amplification products smaller than 120 nt.

2.6.4.1 The P029-B1 probemix

Length (nt)	SALSA MLPA probe	Chromosomal position
64-70-76-82	Q-fragments	-
88-92-96	D-fragments	-
100	X-fragment	-
105	Y-fragment	-
132	Reference probe	5q31
154	Reference probe	6q22
166	Reference probe	2p16
197	Reference probe	20q13
202	Reference probe	8q21
254	Reference probe	9q21
287	Reference probe	15q21

364	Reference probe	1p13
427	Reference probe	3p22

Table 2.2: Components of the commercial WBS-MLPA kit P029-B1. Q- and D-fragments are control fragments. Q-fragment: Sufficient quantity of the DNA sample of interest. D-fragment: Sufficient denaturation of the DNA sample of interest. The reference probes are listed as well. On the left side the length of each fragment and reference probe is given.

2.6.4.2 7q11 region probes arranged according to their chromosomal location

Length (nt)	Gene Exon
171	*FKBP6* exon 9
184	*FZD9* exon 9
382	*TBL2* exon 7
234	*TBL2* exon 2
274	*STX1A* exon 7
221	*STX1A* exon 3
316	*ELN* exon 1
323	*ELN* exon 3
160	*ELN* exon 4
337	*ELN* exon 6
261	*ELN* exon 9
192	*ELN* exon 16
373	*ELN* exon 20
293	*ELN* exon 26
308	*ELN* exon 27
346	*ELN* exon 33
281	*LIMK1* exon 2
390	*LIMK1* exon 5
227	*LIMK1* exon 10
214	*LIMK1* exon 14
330	*RFC2* exon 10
407	*RFC2* exon 3
398	*CLIP2* exon 4

247	*CLIP2* exon 10
418	*CLIP2* exon 14
178	*POR* exon 11
355	*POR* exon 12
142	*HSPB1* exon 1
208	*HSPB1* exon 2
148	*HSPB1* exon 3

Table 2.3: Components of the commercial WBS-MLPA kit P029-B1. The comprised exons are listed from centromeric to telomeric localization. On the left side the length of each exon is shown.

2.7 Fragment analysis

2.7.1 Intended use and overview

With the help of fragment analysis, it is possible to examine certain alleles in the genome by the use of special fluorescence dye labeled markers. Fragment analysis does not aim to detect the correct sequence of genes or base pairs in a certain chromosomal area, e. g. 7q11.23 in the case of WBS. It does however allow conclusions about CNVs (deletions and duplications) as well as the determination of the origin of inherited alleles, if DNA of the parents is available.

STS markers have determined positions in the genome and comprise of primer sequences that hybridize with certain parts of alleles of interest. Finally, in this thesis one allele is represented by one marker (Dutra et al. 2011 and 2012). The primer pair flanks so-called microsatellites on both sides. These are built of up to five nucleotides which repeat 8 to 25 times and in most cases lie within the non-coding parts of the genome. Microsatellites are a certain class of polymorphism and make up to 0.5 % of the human genome. They are also called short tandem repeats (STRs). The length of the repetitive sequence of nucleotides is variable from one genome to another and can therefore be used as a genetic marker (Murken et al. Taschenlehrbuch Humangenetik. P. 12, 379).

The microsatellites which are amplified with the help of PCR have different lengths enabling a distinction from one another. They are analyzed by capillary electrophoresis and with the help of different fluorescence-dye labeled primers to distinguish between the different alleles. Depending on the different number of nucleotides, two amplified products of different lengths indicate heterozygosity for the allele, while products of the same length indicate homozygosity.

The fluorescence dye labeled PCR products are compared to a size standard "ladder" provided by a fluorescence dye, the LIZ standard. Even a small difference of two nucleotides in the total length of the amplicons, the amplified product of a PCR, can be detected. The microsatellites are represented by peaks during the subsequent computer analysis.

Summarizing, in a DNA sample in which no copy number variant is expected, for instance a healthy parent, only *one* length of microsatellite is found in case of homozygosity for the allele of interest. Heterozygous individuals have *two* different lengths of microsatellites.

2.7.2   Fragment Analysis in Williams-Beuren-Syndrome

It is known that about 5% of the patients show a deletion spanning ~1.85 Mb, but the common size of deletion in 95% of the patients is ~1.54 Mb. The intention of performing fragment analysis in Williams-Beuren-Syndrome was to approximate the size of the hemizygous 7q11.23 deletions previously detected by MLPA. It is important to notice that with the help of microsatellite markers it is not possible to detect the exact but only the approximated size of the deletion (Schubert 2009). The used primer pair only marks one certain spot within the whole genome. Deletions up- or downstream this spot therefore remain undetected. In this thesis, WBS fragment analysis is used supplementary to MLPA analysis.

Besides the approximate size of deletion, in this thesis the aim was to detect, whether the deletion was inherited from the maternal or the parental side. Several previous studies used genetic marker analysis in Williams-Beuren-Syndrome (Dutra et al. 2011 and 2012).

2.7.3   Analyzed collective

Only the DNA of those patients with an MLPA-confirmed deletion in region 7q11.23 and therefore definitive WBS patients were chosen as samples for further fragment analysis. If available the corresponding parental DNA were also examined.

2.7.4 Primers

Several fluorescence dye labeled primer pairs (= markers) were used to designate certain alleles in the DNA sample of interest. A PCR with four primer pairs was performed to amplify the targeted microsatellites. The reverse primer of every pair was fluorescence-dye labeled.

The four applied genomic markers were **D7S2476, D7S613, D7S1870 and D7S489-A** (Metabion International AG, Planegg, Germany), each of them consisting of a forward and a reverse primer.

STS marker (DYE, color)	Length (nt)	Forward primer sequence	Reverse primer sequence	Gene locus (GRCh 37)	(Pseudo-) Gene
D7S2476 (ROX, red)	~ 148	GGGCAACATAG CACGATT	CAGGAGTCAGTT AGATAAGGTCAC	73,015,454-73,015,601	*MLXIPL*
D7S613 (CY3, black)	~ 110	CAGCCTGGGTA ACAAAAGC	CCTCCCTCCCTAA TCCATG	73,572,082-73,572,188	*LIMK1/ EIF4H*
D7S1870 (FAM, blue)	~ 120	TTCACTCAGGA AGTGGC	TGGTGATGTGCTT TACTACG	74,126,782-74,126,899	*GTF2I* (B mid)
D7S489-A (YAK, green)	~ 426	GCACCTATGATC ACAGCTTCTC	ATGACATGAAGG TACTGGCCTT	74,298,089-74,298,514	*STAG3L2P* (A mid)

Table 2.4: The four markers used in this thesis for fragment analysis. Markers are ordered from centromeric to telomeric. In the left column the name of the marker, and the name of its dye is given as well as the color used for the depictions of fragment analysis. The right column shows the position of the marker on 7q11.23. The first, third and fourth marker are located within a gene, while the second marker (D7S613) is located in an intergenic region.

2.7.5 PCR in fragment analysis

Initially, a primer master mix is prepared. It contains an equal amount of each sense and antisense primer and dH$_2$O to achieve a 1:10 dilution. Directly before and after use the markers have to be stored under light protected conditions because of the fluorescence dye.

1. D7S2476   sense primer 1µl   D7S2476   antisense primer 1µl
2. D7S613   sense primer 1µl   D7S613   antisense primer 1µl
3. D7S1870   sense primer 1µl   D7S1870   antisense primer 1µl

4. D7S489-A sense primer 1µl   D7S489-A antisense primer 1µl
5. 72µl dH$_2$O

Two different compositions were used. One includes all four markers at once and the other one includes just one marker. In both cases the primer concentration has to be diluted in a ratio of 1:10 at first.

Ingredients	Required volume: 4 markers	Required volume: 1 marker
dH2O	14.5 µl	18 µl
10x Buffer	2.5 µl	2.5 µl
MgCl2	1.3 µl	1.3 µl
dNTPs	1 µl	0.5 µl
Primer mix	4 µl	1 µl
Taq polymerase	0.2 µl	0.2 µl

Table 2.5: Composition of the different mixes used for PCR for fragment analysis.

After adding 1.5 µl of the DNA sample of interest to a 0.2 ml tube, 23.5 µl of the mixtures from table 2.5 are pipetted to each tube to obtain a total volume of 25 µl. The tubes are placed into a thermocycler and PCR is performed with the following settings:

```
5 min       95°C
30 s        95°C  ┐
30 s        60°C  │ x 25-27
30 s        72°C  ┘
10 min      72°C
Pause       15°C
```

To prepare the samples for the following ABI capillary electrophoresis, a master mix containing 17.75 µl formamide and 0.25 µl LIZ standard per sample is mixed, and 18 µl are added to each tube. Afterwards, the samples are heated at 86°C for 3 minutes and cooled at 4°C for 2 minutes. Formamide prevents the single-stranded DNA from re-hybridization after denaturation. LIZ standard functions as a standard for fragment sizes and provides a standard ladder as a reference.

2.7.6 Analysis and interpretation

The separation of the amplified products which is required for further analyses takes place in the sequencer ABI3130GA via capillary electrophoresis according to the SOP "Sequenzierer AB3130GA", 2.11.8., Version 02. Clinic and Polyclinic for pediatric Hematology and Oncology. Capillary electrophoresis uses the negative charge of the PCR products which migrate after voltage is applied. The amplicons separate according to their size respectively (Applied biosystems by life technologies. DNA Fragment Analysis by Capillary Electrophoresis. Publication number 4474504. Version B. Page 18).

A sufficient conclusion of fragment analysis is only possible in cases: (1) If the parents are heterozygous in an examined allele (two peaks, figures 2.4 and 2.5), (2) if they are homozygous in an allele (one peak) but have STRs with different lengths (figure 2.6) or (3) if one parent is heterozygous and the other one homozygous (figure 2.7).

The herein examined collective is comprised of patients that were detected and confirmed by MLPA and one or both parents, if available. Because the four markers are all located in the chromosomal area of 7q11.23, together with the MLPA findings approximations of the length of the deleted chromosomal site are possible.
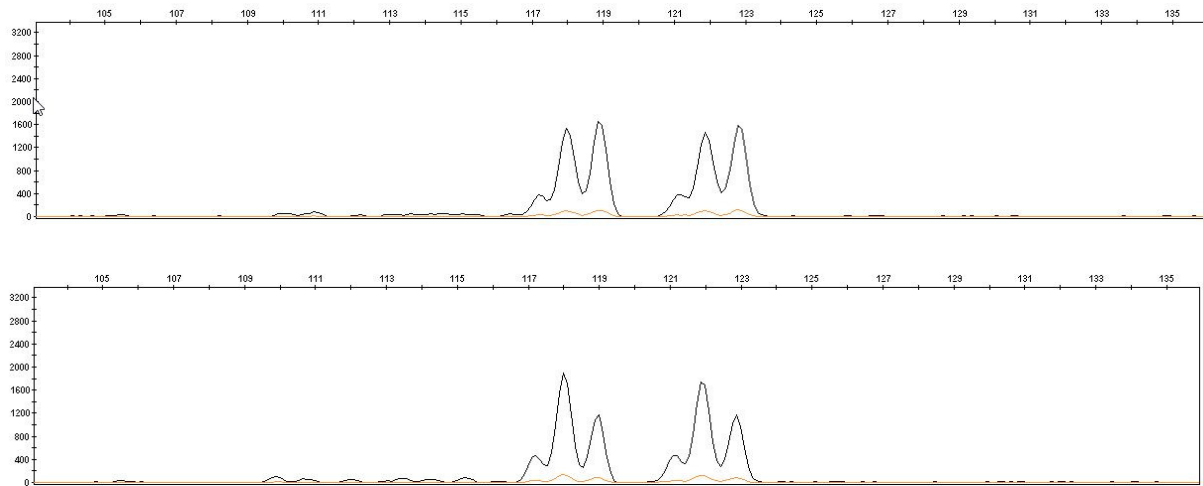
Figure 2.4: Illustration of the results of fragment analysis. The x-axis depicts the number of base pairs (nt), the y-axis the relative fluorescence. The height of the peaks does not allow a sufficient conclusion, because the DNA concentration of the single samples was neglected. Only the highest peak serves for interpretation, smaller peaks occur due to impurity of the DNA samples. Maternal DNA is above, paternal DNA below. In this example, both parents show fragments (= microsatellites or STRs) of different numbers of base pairs (= sizes) in the same gene locus on two homolog chromosomes. Maternal DNA: 119 nt, 123 nt. Paternal DNA: 118 nt, 122 nt. Therefore, the parents are both heterozygous for the chromosomal site (= STR) of interest that is depicted by the marker D7S613 (black dye CY3) and is located in the intergenic region between *LIMK1* and *EIF4H* on 7q11.23.
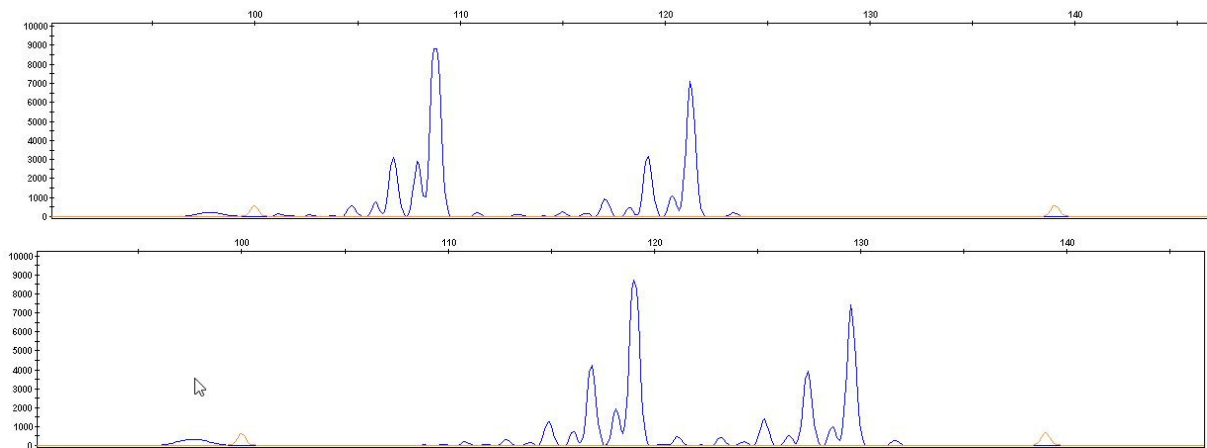

Figure 2.5: Fragment analysis of heterozygous parents of a WBS patient. Parents show different peaks in the marker D7S1870 (blue dye FAM). Therefore, both are heterozygous for the chromosomal site of interest. Both have STRs of different lengths. Mother above, father below.
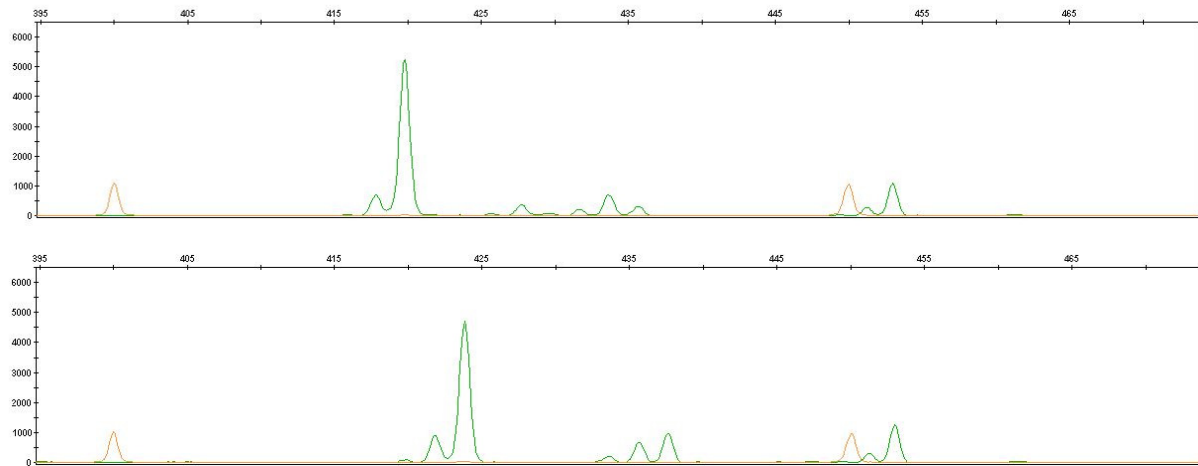
Figure 2.6: Fragment analysis of homozygous parents of a WBS patient. Each parent shows one different peak in the marker D7S489-A (green dye YAK). Therefore, they are both homozygous for the chromosomal site of interest, but show different STRs. Mother above, father below.
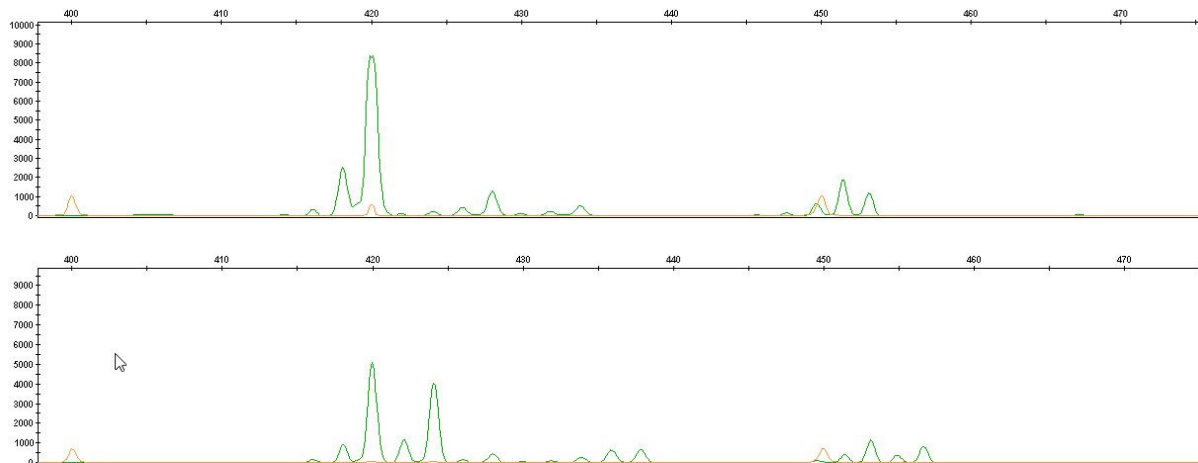

Figure 2.7: Fragment analysis of a hetero- and a homozygous parent of a WBS patient. The mother (above) shows one peak and therefore is homozygous for the STR depicted by the marker D7S489-A. The father (below) shows two peaks and therefore is heterozygous.

Three of the applied genetic markers are located in the chromosomal area which is commonly deleted in WBS patients (table 2.4). D7S2476, labeled with the fluorescence dye ROX, lays within the gene *MLXIPL*, which is a gene of the WBSCR. D7S613 is labeled with CY3 and is located in between two genes of the WBSCR that are telomeric to *MLXIPL*, between *LIMK1* and *EIF4H*. The marker D7S1870 is labeled with FAM and lays within the gene *GTF2I*, which is the first gene of the block B mid and flanks the WBSCR at its telomeric end. Most of the telomeric breakpoints of the common 1.54 Mb deletion lay within block B mid (see chapter 1.6, Bayés et al. 2003).

The fourth marker D7S489-A is YAK-labeled and is the only marker used in this thesis that lays outside the usually deleted 1.54 Mb region within the pseudogene *STAG3L2P*, which is

the most centromeric pseudogene of the block A mid. Breakpoints in cases with the larger 1.85 Mb deletion have not been specified to date, but it is assumed that they are variably located in the blocks A cen and A mid (Bayés et al. 2003, Li et al. 2016).

DNA samples with MLPA-confirmed deletions show only one peak of each of the three markers D7S2476 (ROX), D7S613 (CY3) and D7S1870 (FAM) because of hemizygosity in this area. A healthy heterozygous subject would present two peaks of all three markers or one peak if homozygous. The most telomeric gene of the WBSCR detected by MLPA is *CLIP2*, which is located telomeric to the positions of D7S2476 and D7S613. The position of D7S1870 is not represented by the examined exons of the regular WBS-MLPA kit. However, the breakpoints of the common 1.54 Mb deletion have already been researched and it was shown that WBS patients are hemizygous for *GTF2I*, which is the location of the marker D7S1870 (figure 2.8). Therefore, it is presumed that patients with the common 1.54 Mb deletion are also hemizygous for D7S1870 (Bayés et al. 2003).
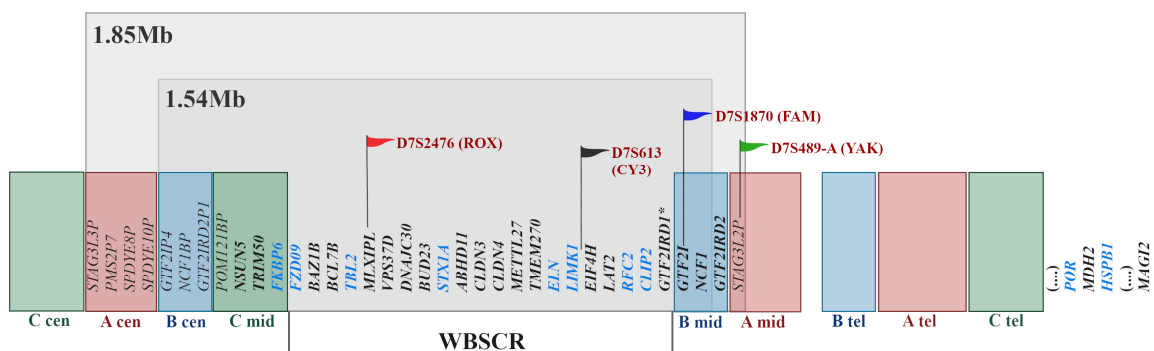

Figure 2.8: Locations of the markers for fragment analysis to distinguish small and large deletions in WBS. The marker D7S489-A helps to differentiate between a 1.54 Mb and a larger deletion. It is located outside the chromosomal region that is absent in a 1.54 Mb deletion and is only affected by a larger deletion. Genes depicted in blue are genes examined by the WBS MLPA analysis.

Performing fragment analysis in addition to MLPA intends to further specify the length of the deletion which was previously detected by MLPA. As mentioned above, the two markers D7S1870 (*GTF2I*) and D7S489-A (*STAG3L2P*) are located on a chromosomal site, which is not covered by the common MLPA kit. These two markers lay between *CLIP2* and *POR* (figure 2.8) which are covered by MLPA as 'adjacent' genes but actually have a distance of ~1.7 Mb and therefore several coding and non-coding genes between each other. By the use of MLPA alone, a conclusion about the actual deletion size is not possible and can only be determined approximately. Performing fragment analysis with the additional marker D7S489-A (YAK)

extends the information given by MLPA and was used to distinguish between the common and a larger deletion.

2.7.7 Size of the deletion

2.7.7.1 1.54 Mb deletion

As stated above, the marker D7S489-A allows the distinction between the 1.54 Mb and the 1.85 Mb deletion. In case D7S489-A shows two peaks in the fragment analysis, the patient is heterozygous in the corresponding allele, thus has no deletion in this gene locus and therefore the small deletion of ~1.54 Mb (figure 2.9). If the patient is homozygous in this allele (one peak), unfortunately no sufficient conclusion can be made.
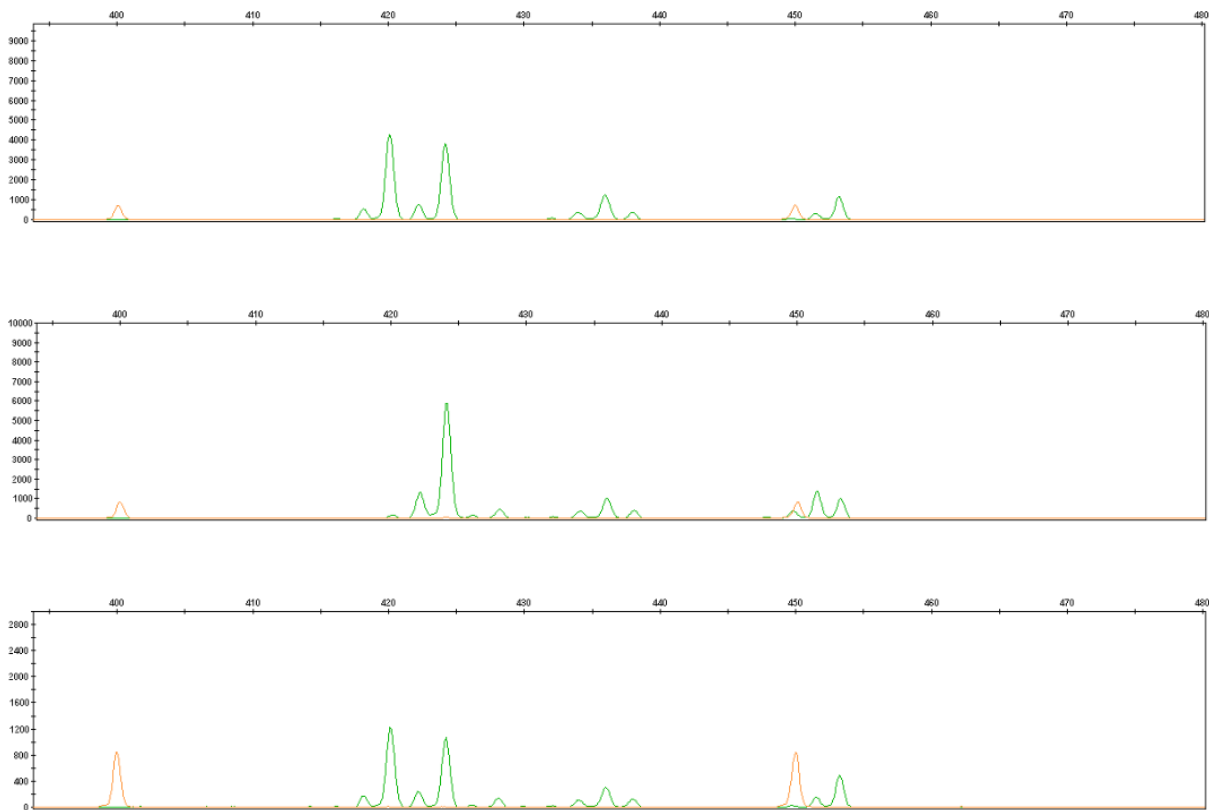
Figure 2.9: Fragment analysis of marker D7S489-A. Peaks of the D7S489-A marker in maternal, paternal and patient DNA (from top to bottom). The mother is heterozygous (two peaks), the father is homozygous (one peak). The patient is heterozygous in the allele of interest and therefore shows two peaks. He inherited the allele with the shorter STR from the mother and the longer STR from the father. Conclusion: Small 1.54 Mb deletion**.**

2.7.7.2   1.85 Mb or larger deletion

If there was only one D7S489-A (YAK) peak detectable in the patient's DNA, assumptions about the deletion size could only be established, if one or both parents' DNA were also available. There are three possible constellations of the D7S489-A peaks.

(1) Both parents are homozygous for the allele of interest represented by D7S489-A and show only one peak but with a different oligonucleotide size, which therefore makes them distinguishable from each other. The patient shows only one peak corresponding to either the mother's or the father's peak. In this case, it is possible to conclude that the patient has a larger deletion. None of the patients examined in this thesis had this constellation.

(2) One parent is heterozygous (two peaks) while the other parent is homozygous (one peak) in the allele of interest. The patient's peak matches only one peak of the parents. As a consequence, the patient carries only one of the two parental alleles and shows a larger deletion (figure 2.10). In case the single peak of the patient and one of the parents' match the STR length of one of the other parents' peaks, no differentiation is possible.
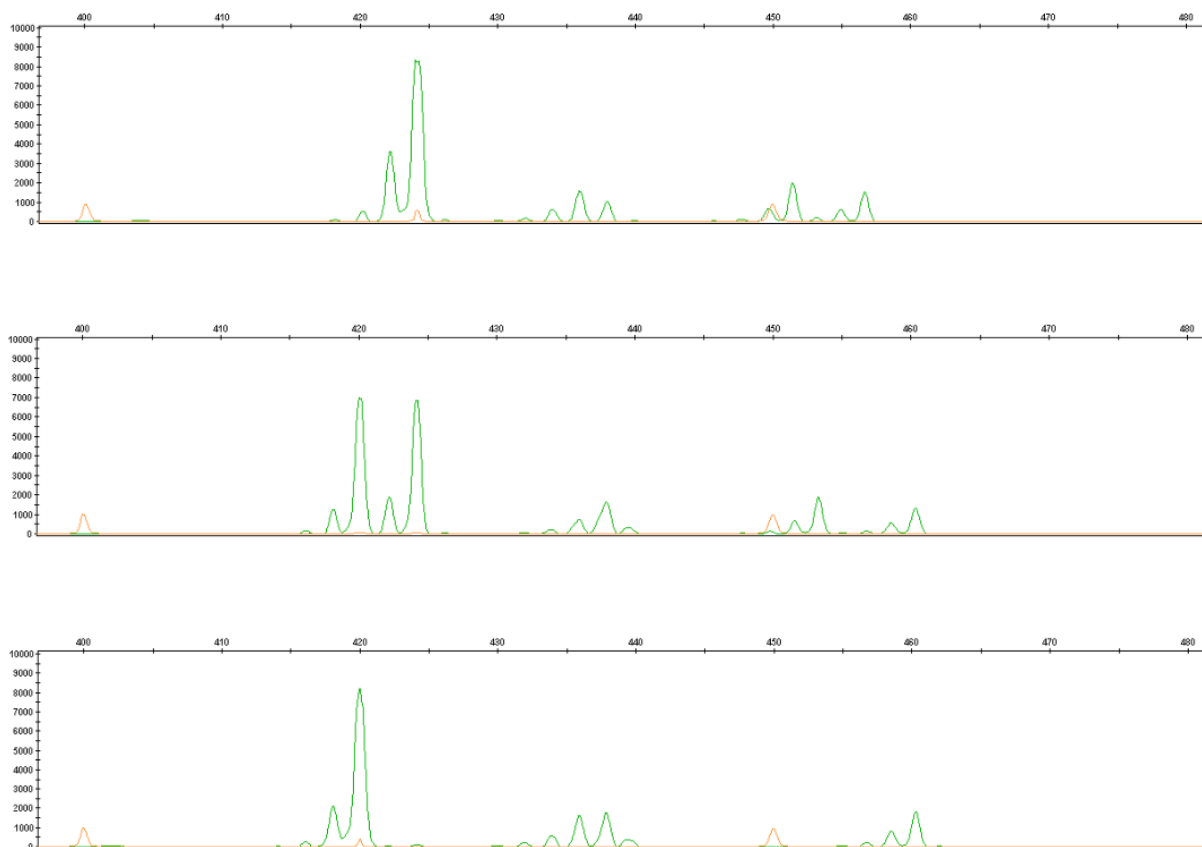

Figure 2.10: Fragment analysis of D7S489-A showing a maternal deletion. Peaks of the D7S489-A marker in maternal, paternal and patient DNA (from top to bottom). The patient shows only one peak, which is the peak at 420nt. This peak corresponds to one of the father's. Conclusion: The paternal allele was inherited. The maternal allele is deleted. The deletion is larger than 1.54 Mb.

(3) Only genomic material of one parent is available. This parent can be heterozygous (two peaks) or homozygous (one peak) in the allele of interest represented by D7S489-A. The patient shows only one peak with a different oligonucleotide size than any of the peaks of the examined parent (figure 2.11). In this case the patient is also carrier of a larger hemizygous deletion, because the allele of the available parent has not been inherited to the child.
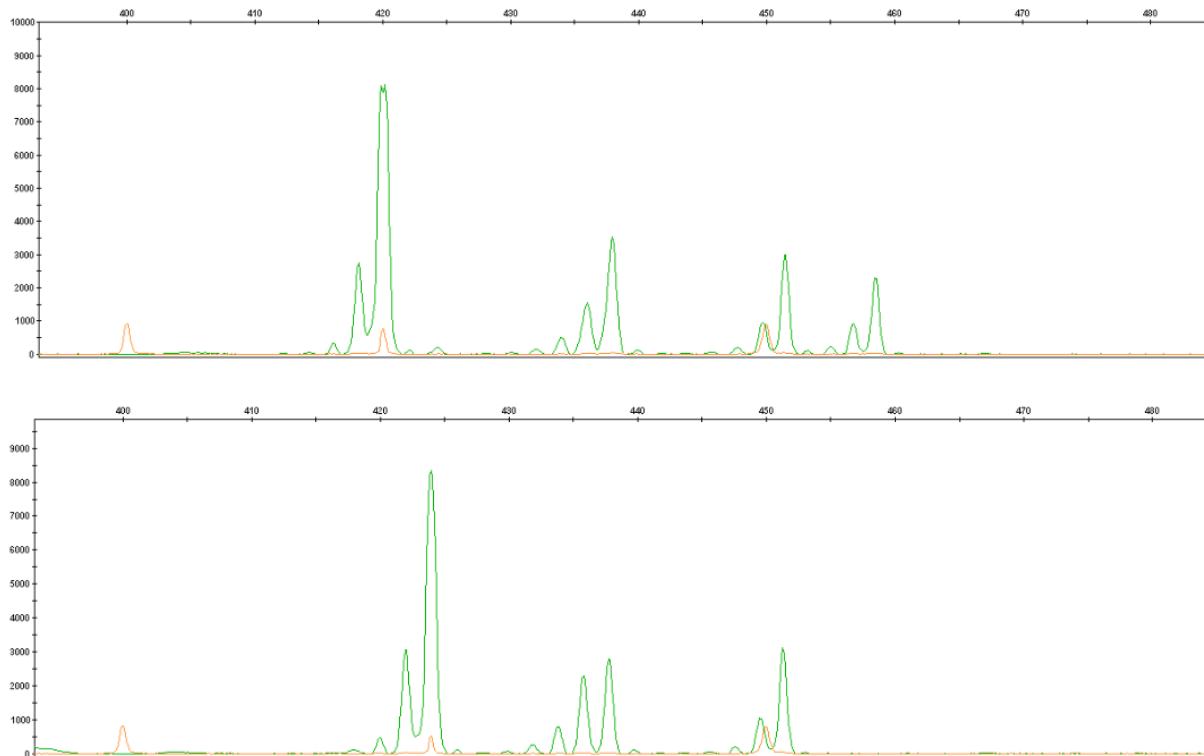

Figure 2.11: Fragment analysis of D7S489-A with only one parent available. Peaks of the D7S489-A marker in maternal and patient DNA (from top to bottom). Note that only the high peaks on the left represent the actual position of the marker. The numerous small peaks to the right are artifacts due to impurity of the DNA sample. The relevant peaks differ from each other in the oligonucleotide size. Conclusion: the maternal allele was not inherited. The deletion is larger than 1.54 Mb.

2.7.7.3   Origin of the deleted allele: maternal or paternal?

In some cases, it was possible to conclude if the parental origin of the deletion was maternal or paternal. For example, in figures 2.10 and 2.11 the origin of the deletion was maternal, because the patient's and the mother's STRs differ from each other. Dutra et al. (2011) published in their study of 84 WBS patients that the deletion in 52 % of cases was of maternal and in 48 % of cases of paternal origin. Bayés et al. (2003) performed fragment analysis in 74 WBS patients: In 45 % the deletion was of maternal and in 55 % of paternal origin.

2.8 Microarray analysis (not part of this thesis)

Different arrays were performed by the Institute of Human genetics of the Christian-Albrechts University of Kiel, Germany.

2.8.1 Array-CGH (Comparative genomic hybridization)

This method relies on the principle of hybridization of complementary DNA and helps diagnosing deletions or duplications of submicroscopic size as well as breakpoints (https://www.medizinische-genetik.de/index.php?id=array-cgh. 04.01.2020. 19:00, Lindgren et al. 2011). In an array CGH the whole genome is covered and represented by short non-polymorphic oligonucleotides which are fixated on a matrix on a chip. The fluorescently marked DNA of interest and reference DNA hybridize with the oligonucleotides competitively. The hybridization product is analyzed by special software programs (https://www.medizinische-genetik.de/index.php?id=array-cgh. 04.01.2020. 19:00). This procedure was performed only on one patient.

2.8.2 SNP (Single Nucleotide Polymorphism) Array

SNP array analysis is based on the existence of Single Nucleotide Polymorphisms (SNPs). In most cases SNPs arise through reading errors during replication and result in the exchange of a single nucleotide in the DNA of an individual. This provides genetic variability and more than 5 million common SNPs have been detected to date. If SNPs are located in the coding sequences of a genome, they form alleles. If an individual shows two different SNPs in the two alleles of its diploid chromosome number, heterozygosity occurs. If the two SNPs are equal, the individual is homozygous for these two alleles. The occurrence of SNPs provides variability within the genome (Murken et al. Taschenlehrbuch Humangenetik. P. 13f).

A SNP array works, like array CGH, with the help of several oligonucleotides representing the entire genome. The diagnostic value is increased compared to the array CGH by using polymorphic oligonucleotides (https://www.medizinische-genetik.de/index.php?id=array-cgh. 04.01.2020. 19:00). Not only copy number aberrations can be detected but also copy-neutral events, such as loss of heterozygosity (LOH) (Lindgren et al. 2011). The DNA of interest and the reference DNA are fluorescence-dye-labelled and hybridize with the oligonucleotides.

Afterwards the fluorescence signals are measured and compared by a laser (https://www.medizinische-genetik.de/index.php?id=array-cgh. 04.01.2020. 19:00).

In this thesis, SNP-microarray analysis was used to further examine the results obtained by MLPA. In total, four atypical deletions detected by MLPA were confirmed and refined by microarray analysis. By this technique it was possible to analyze a region on chromosome 7 that was much larger than the one covered by MLPA and even to detect the approximate breakpoints.

3 Results

3.1 MLPA results

Altogether, **341** presumed WBS patients were gathered. Of those, there was a fallout of **33** samples which were documented on the numerous above-mentioned lists but no DNA material was available. On the remaining **308** DNA samples MLPA was performed.

The comparison of the current MLPA to the previous FISH findings resulted in **208** patients who had been formerly diagnosed with the help of FISH and whose diagnosis could be confirmed by MLPA (figure 3.1). While FISH analysis in WBS only detects the hemizygous deletion of *ELN*, and in some cases *LIMK1* (see chapter 1.3), the commercial MLPA kit P029-B1 by MRC Holland comprises of exons of the genes *FKBP6*, *FZD9*, *TBL2*, *STX1A*, *ELN*, *LIMK1*, *RFC2* and *CLIP2* that are all deleted in a typical WBS patient.

10 additional patients whose DNA was among the stored collective but without any information about prior molecular genetic investigations were shown to have a deletion in the region of interest by MLPA. In total, **218** patients had WBS-specific deletions. According to the Genome Data Viewer the depiction of a typical 1.54 Mb deletion by the exons of the commercial WBS MLPA kit encompasses approximate 1.05 Mb (https://www.ncbi.nlm.nih.gov/genome/gdv/browser/genome/?id=GCF_000001405.25. 17.04.2020. 13:00).

70 DNA samples showed no deletion by MLPA. Of those, in **57** cases previous results seemed to be unreliable, mostly due to contradictory documentation. For example, the person of interest was listed as a "patient" but no FISH analysis result was documented, sometimes with a comment of insufficient DNA material. In other cases, the diagnosis "WBS" of a patient was given but without any specification of the diagnostic procedure (FISH analysis or clinical diagnosis). The causation of the discrepancy in these 57 cases remains unclear. How many of these individuals actually once showed a deletion in FISH analysis, how they became part of the stored DNA collection or if they showed any special clinical features was not possible to determine retrospectively.

13 patients showed neither a deletion in FISH nor MLPA in the region of interest although they were among the presumed patient collective.

53 presumed WBS patients appeared on the lists or were among the stored DNA collective without any information about previous FISH-testing. However, the diagnosis of WBS could neither be verified nor excluded. Of these individuals, in **33** cases the DNA samples were not available, while in **20** cases DNA material was insufficient.
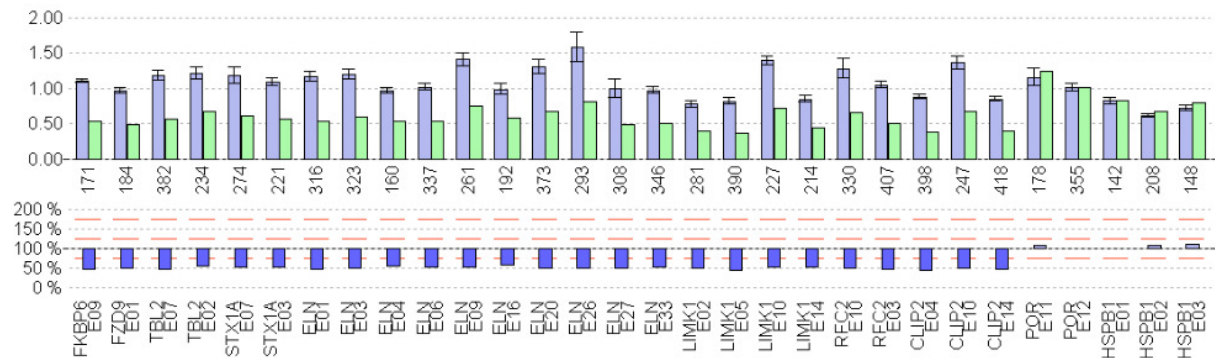
Figure 3.1: WBS-MLPA analysis of a DNA sample with a hemizygous deletion. The picture represents the findings in a typical WBS patient.

Patient subgroups

There were three pairs of twins among the analysed collective. Two pairs of monozygotic and a pair of dizygotic twins. In all six cases, the MLPA confirmed the previous FISH results. The MLPA showed a typical deletion (as in figure 3.1).

Furthermore, in three cases information about one parent was available: there were two mother-daughter pairs and one mother-son pair among the collective. All six of them had been diagnosed by FISH before and were confirmed by MLPA to have a typical deletion.

3.1.1 Atypical MLPA results

3.1.1.1 Cases 1, 2 and 3

Three patients with an atypical, extremely long deletion were detected by MLPA. Interestingly, all of them showed the same pattern of deletion (figure 3.2). The results showed a hemizygous deletion in all available exons of the WBS kit P029-B1. The distance from the first to the last exon is ~ 3.2 Mb according to the Genome Data Viewer.

Figure 3.2: MLPA showing a deletion from exon 9 of *FKBP6* to exon 3 of *HSPB1*. This deletion was found in cases 1 – 3 and is larger than the typical WBS deletion (~ 3.2 Mb).

3.1.1.2 Case 4

This patient showed an atypical, extremely short deletion and atypical clinical features as well, although being among the WBS collective. The detected deletion by MLPA starts at exon 1 of *ELN* and ends with exon 4 of *CLIP2* (figure 3.3). The clinical features will be addressed in chapter 3.4. The length between these exons according to the Genome Data Viewer is ~ 320 kb.

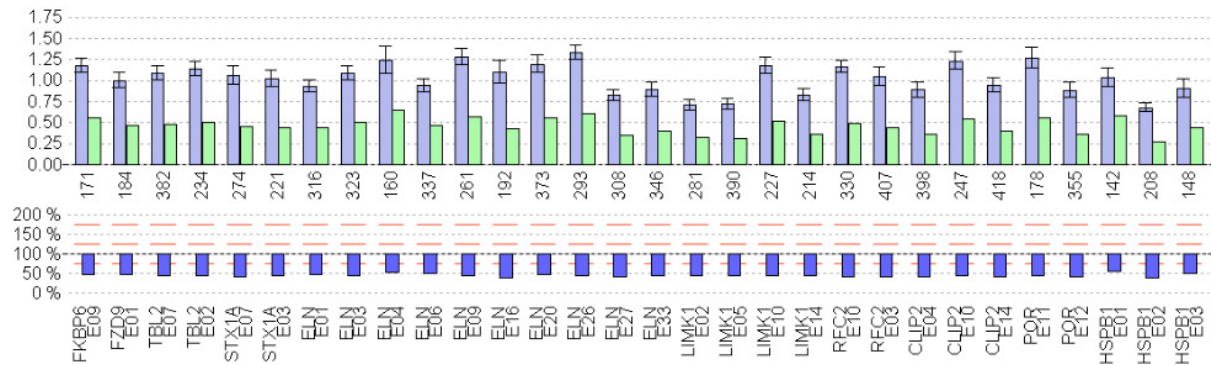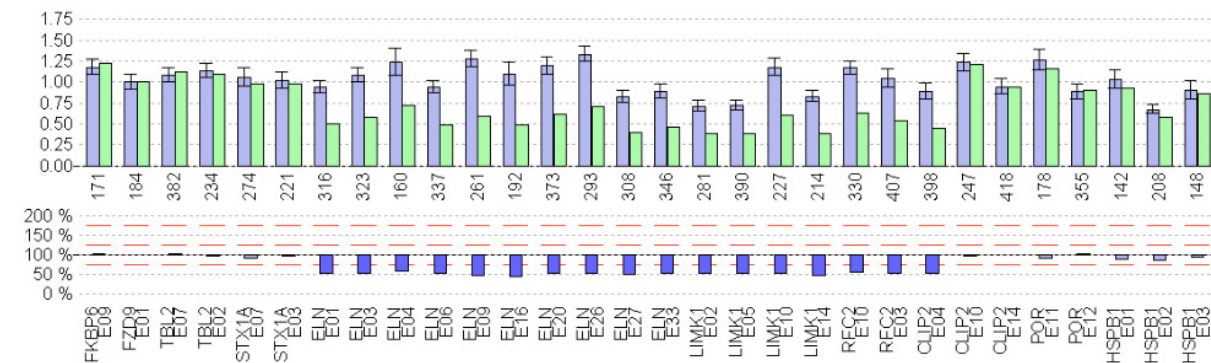**Figure 3.3: MLPA showing a deletion from exon 1 of *ELN* to exon 4 of *CLIP2*.** This deletion was found in case 4 and is shorter than the typical WBS deletion.

3.2   Results of fragment analysis

Out of the total amount of presumed WBS patients 218 had a hemizygous deletion in MLPA analysis.

Fragment analysis was performed to gather more information about the origin of the deletion, to identify if the maternal or paternal allele was missing in the patients. The additional tests were only possible in cases of sufficient amounts of parental DNA.

In total, **379** DNA samples were processed via fragment analysis. The total amount of processed samples (MLPA and fragment analysis) was over 700.

3.2.1   WBS patients

The precondition for performing fragment analysis was a deletion detected by MLPA. By analysing just the patient's DNA, in some cases it was possible to conclude, if the deletion was either common (i.e. 1.54 Mb) or larger. This was only possible, when a patient showed heterozygosity (two peaks) in the pseudogene *STAG3L2P* located in the block A mid. *STAG3L2P* is the most proximal located pseudogene in block A mid. All of the common 1.54 Mb deletions have their telomeric breakpoints within block B mid according to Bayés (2003). As a consequence, an individual with the common deletion shows no hemizygosity in *STAG3L2P*, but two peaks in fragment analysis if heterozygous for this allele.
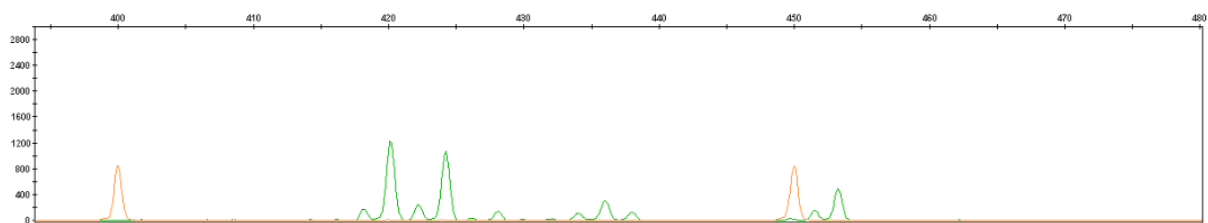
Figure 3.4: Fragment analysis in a WBS-patient with marker D7S489-A in pseudogene *STAG3L2P* showing a state of heterozygosity. This patient is heterozygous for the genomic marker D7S489-A and therefore shows two peaks at 420 and 425 nt. Conclusion: Common, 1.54 Mb deletion. The patient has two different alleles. Note: orange peaks caused by fluorescence dye LIZ.

If a patient is homozygous for *STAG3L2P* no further conclusion about the size of deletion can be made without the parental DNA.

In **115** patients, fragment analysis was done exclusively with the marker D7S489-A which is located in *STAG3L2P* (table 2.4). In these cases, parental DNA was not available. **42** patients showed a hemizygous deletion spanning 1.54 Mb (figure 3.4). In **73** cases no useful result was obtained due to homozygosity (one peak).

3.2.2 Family analysis: both parents available

With the availability of one or both parental DNA, it was further possible to draw conclusions about the estimated size of the deletions and additionally if the maternal or the paternal allele was deleted.

The entire collection of WBS DNA samples stored in the laboratory comprised a lot more samples than the number of potential patients which were gathered from the WBS lists. According to the information collected from these lists or through documentation on the tubes, several parents of some of the patients could be identified.

In **76** cases the patient's and *both* parental DNA samples were available. Of those 76 families two had twins. All parents were reported healthy and hence showed no deletions. All four genetic markers were applied. In **five** cases the smaller deletion was detected in the WBS patients, while the fact whose allele was deleted remained unclear. In **six** cases neither the size of the deletion, nor the origin of the missing allele could be specified (see chapter 2.7.6).

In **37** cases the maternal allele was deleted. Of those, in **eleven** cases a small and in **three** a large deletion was identified. In **30** cases the paternal allele was deleted. Of those, in **seven** cases a small deletion was detected.

3.2.3 Family analysis: one parent available

An additional opportunity was given by the available DNA of *one* parent which could be assigned to a single WBS patient:

Out of a collective of **23** patient-parent-pairs, in **six** cases no further information could be obtained. In **five** cases, a small deletion was detected, while the origin of the deleted allele remained unclear. In **ten** cases, the loss of the maternal allele was verified. **Two** of those cases showed a small and **two** a larger deletion.

One of the cases, in which the loss of the maternal allele was proven, was that of an affected mother and her affected daughter. In both, the diagnosis was confirmed by FISH and MLPA. All four genetic markers were applied. The daughter showed a peak which was not found in the analysis of the mother and therefore the according allele had been inherited from the father. The mother transmitted the haploid set of chromosomes with the deleted allele to her daughter. This follows the known pattern of an autosomal-dominant inheritance with a 50% probability of inheritance from one affected parent to the offspring.

In **two** further cases, the paternal allele was absent, while the size of deletion remained unclear.

3.2.4 Conclusion

The final result of **72** patients (~ 94%) with a small, 1.54 Mb deletion, and **five** patients (~ 6%) with a larger, at least 1.85 Mb deletion, fits the data published by Bayés and colleagues (2003) with a distribution of 95 and 5% respectively (table 3.1). Additionally, they performed fragment analyses in 74 WBS patients. In 67 cases the parental DNA was available so that a detection of the parental origin of the deletion was possible: in 45% of the patients the deletion was of maternal origin and in 55% of paternal origin.

The results in this thesis however, differ slightly from these results. In **79** patients a statement about the origin of the deletion was possible: in **47** cases (~ 59%) the deletion was of maternal origin and in **32** cases (~ 41%) of paternal origin.

If the origin of the deletion or the size of the deletion have an effect on the clinical manifestation of the Williams-Beuren-Syndrome, still needs to be answered. Some aspects will be addressed in later chapters.

Fragment analysis in this thesis closes a gap between the single exons of some genes contained in the MLPA kit. The widest gap is located between *CLIP2* and *POR* and measures about 1.7 Mb. Applying the genomic marker D7S489-A which is located within *STAG3L2P* of the block A mid, enlightens a small part of this huge gap. It provides a possibility for the distinction of a 1.54 Mb and a larger -in most cases a 1.85 Mb- deletion which cannot be obtained by MLPA alone.

Deletion	German Patients in this thesis		Spanish Patients of Bayés, 2003	
	Patients (n)	Rate	Patients (n)	Rate
Small (1.54 Mb) del.	72 (77)	94 %	70 (74)	95 %
Large (≥1.85 Mb) del.	5 (77)	6 %	4 (74)	5 %
Maternal del.	47 (79)	59 %	30 (67)	45 %
Paternal del.	32 (79)	41 %	37 (67)	55 %

Table 3.1: Overview of the results regarding the size and origin of deletions analyzed in the German WBS collective. Comparison with the analyzed collective of Spanish patients by Bayés (2003).

3.3 SNP array results

The MLPA results have been kindly complemented in the Laboratory for Human Genetics of the Christian-Albrechts University in Kiel, Germany by performing SNP array analyses on the four samples harboring atypical deletions. In all of the four cases, the results gained through MLPA were confirmed by SNP array analysis. To further narrow down the approximated breakpoints according to the SNP array results the "Genome Data Viewer" of the National Center for Biotechnology Information (NCBI) was used (https://www.ncbi.nlm.nih.gov/genome/gdv/. 15.01.2020. 12:00). A prediction of the *exact* breakpoints is not possible by this procedure.

3.3.1 Atypical cases

Case 1

The deletion size in this case measured ~3.64 Mb. The centromeric breakpoint was located in the block B cen, within the pseudogene *GTF2IRD2P1*. This is the region in which some of the breakpoints described by Bayés et al. (2003) were located. The approximated telomeric breakpoint was located downstream of the gene *POMZP3*. This atypical deletion ends ~ 2.15 Mb downstream to the most frequent detected telomeric breakpoint in the block B mid, which lies within *GTF2I* or downstream of it (Bayés et al. 2003).

Figure 3.5: Illustration of the SNP array analysis of case 1. The deletion measures ~ 3.64 Mb and encompasses a genomic region from *GTF2IRD2P1* to *POMZP3*.

Case 2

This patient harbors a deletion with a size of ~4.04 Mb. The centromeric breakpoint lies within the first gene of the flanking block C cen, in *POM121*. It is located much more upstream than the common breakpoints (Bayés et al. 2003). The telomeric breakpoint is located distal to *POMZP3* as well, hence encompassing the whole gene.

Figure 3.6: Illustration of the SNP array analysis of case 2. The deletion measures ~ 4.04 Mb and encompasses a genomic region from *POM121* to *POMZP3*.

Case 3

This case presents by far the largest hemizygous deletion with ~ 6.29 Mb. The proximal breakpoint lays within the gene *CALN1*, at least 0.8 Mb upstream the common breakpoints. The distal breakpoint lays within the gene *MAGI2*, nearly 4 Mb downstream the common breakpoints.

Figure 3.7: Illustration of the SNP array analysis of case 3. The deletion measures ~ 6.29 Mb and encompasses a genomic region from *CALN1* to *MAGI2*. This is the largest atypical deletion identified by this work.

Case 4

As presented in chapter 3.1.1.2, this patient harbors the smallest hemizygous deletion encompassing ~ 0.39 Mb. The centromeric breakpoint was located upstream of *ELN* without affecting the next gene. The telomeric breakpoint was located within *CLIP2*. According to the MLPA results, at least the first four exons of *CLIP2* were missing which makes up a total deletion of ~ 320 kb. Both breakpoints are within the WBSCR and the whole deletion measures one quarter of the usual deletion.
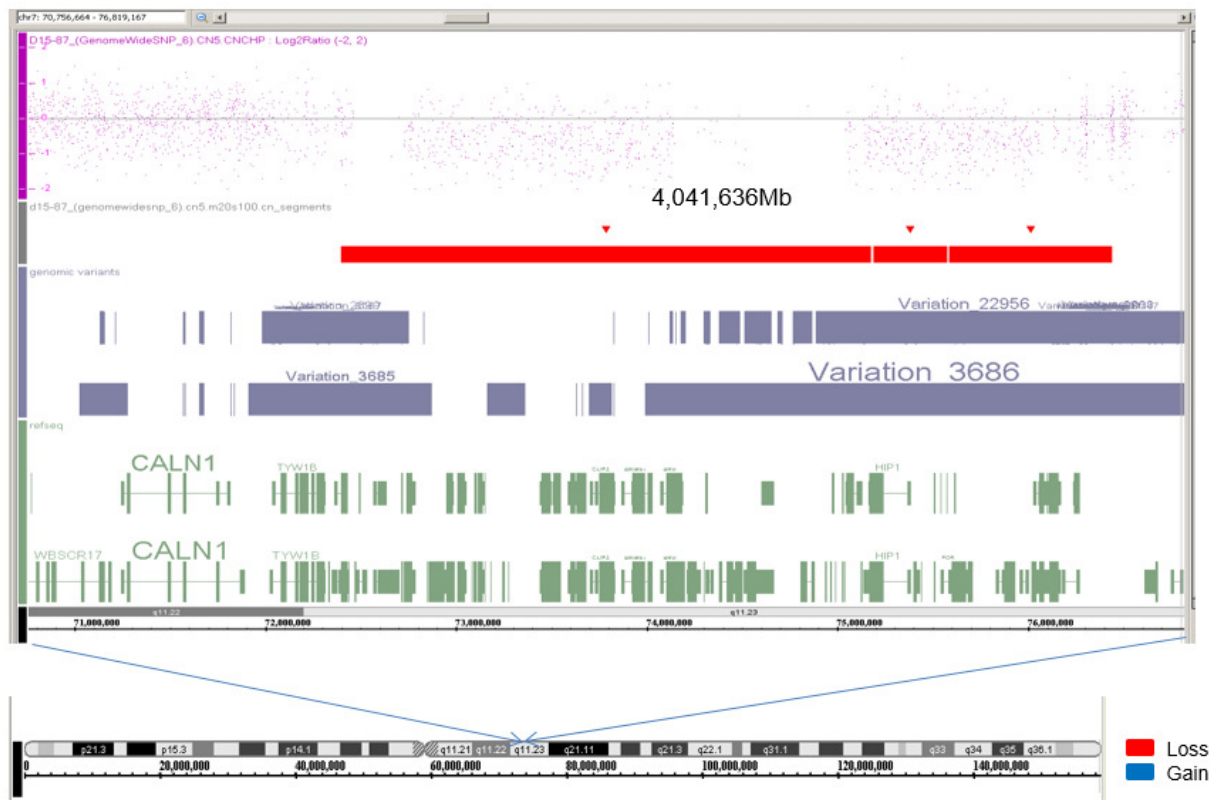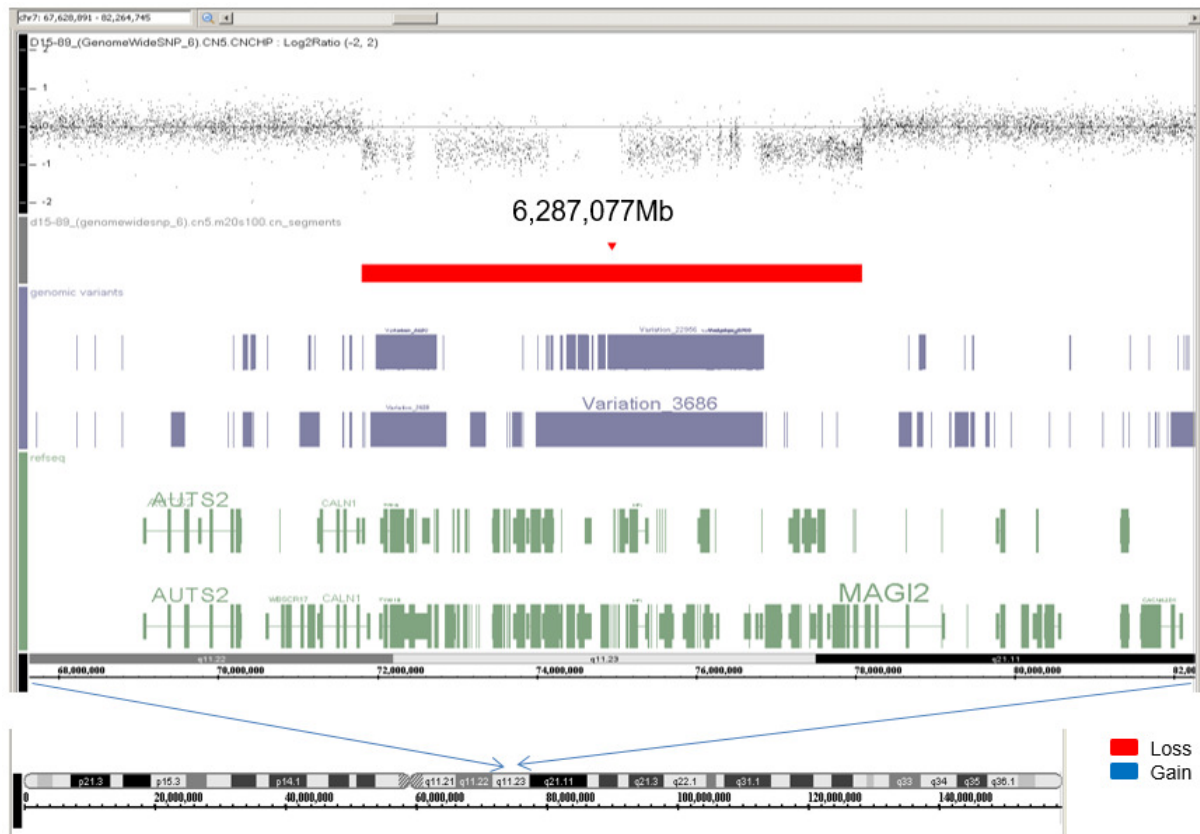

Figure 3.8: Illustration of the SNP Array analysis of case 4. The deletion measures ~390 kb and encompasses a genomic region from *ELN* to *CLIP2*, including the entire gene locus of *ELN* and large parts of *CLIP2*. However, upstream of *ELN*, no additional gene is deleted.

3.3.2 Comparison between MLPA and SNP array results

Case	MLPA result	Position (bp) (GRCh37)	Size		SNP array result	Position (bp) (GRCh37)	Size
Typical deletion	*FKBP6* (Ex.9) – *CLIP2* (Ex. 14)	72,742,164 – 73,820,265	1.05 Mb		-	-	-
1	*FKBP6* (Ex.9) - *HSPB1* (Ex.3)	72,772,000 - 75,933,300	**3.16 Mb**		*GTF2IRD2P1-POMZP3*	72,659,595-76,300,635	**3.64 Mb**
2	*FKBP6* (Ex.9) - *HSPB1* (Ex.3)	72,772,000 - 75,933,300	**3.16 Mb**		*POM121-POMZP3*	72,399,447-76,441,083	**4.04 Mb**
3	*FKBP6* (Ex.9) - *HSPB1* (Ex.3)	72,772,000 - 75,933,300	**3.16 Mb**		*CALN1-MAGI2*	71,803,280-78,090,357	**6.29 Mb**
4	*ELN - CLIP2* (Ex.4)	73,442,119 - 73,768,150	**326 kb**		*ELN-CLIP2*	73,390,431-73,781,468	**391 kb**

Table 3.2: Comparison between MLPA and SNP array results in a typical deletion and cases 1 – 4. The positions (bp) in the genome were approximated with the Genome Data Viewer.

In smaller deletions (as in case 4), MLPA gives a useful hint regarding the size of the deletion. In contrast, the larger the deletion, the larger the difference between the detected deletion sizes in MLPA vs. SNP array analysis (e. g. 3.16 vs. 6.29 Mb in case 3). The visualization of a typical deletion (1.54 Mb) in MLPA spans approximate 1.05 Mb. The widest gap between the exons of the MLPA kit is located between *CLIP2* and *POR*. The distance measures ~ 1.7 Mb and therefore is vulnerable for deletions which are not detected by MLPA (not analyzed in this thesis).

3.4 Clinical data

The clinical data of the four atypical cases were provided by Prof. Dr. Rainer Pankau, Dr. Elke Reutershahn, Dr. Stephanie Demuth and Dr. Verena Gravenhorst (see chapter 1.8). The available data regarding height, weight and head circumference of these atypical deleted patients are shown in detail in chapter 8.1. The height measurements were plotted on the WBS specific percentile curves provided by Pankau et al. (Das Williams-Beuren-Syndrom. P. 146, 147. Figures 3.9 and 3.10 below).

3.4.1 Case reports

Case 1

The boy was delivered by caesarian section after an uneventful pregnancy in the 43rd week with 2740 g and 47 cm. Caesarian section was performed due to insufficient uterine contractions and exhaustion of the mother.

As a newborn, the patient showed feeding difficulties, failure to thrive and vomiting. From the age of five months he constantly had a short stature. As he was 4 weeks old, he was diagnosed with pyloric stenosis, which was treated surgically by pyloromyotomy. Furthermore, a mild SVAS and peripheral pulmonary stenosis were found. Cardiologic examination at the age of 5 months revealed an additional mild coarctation of the aorta. Because of the mild manifestation there was no need of surgery but surveillance was recommended.

During his first year of life the patient showed an increased susceptibility to infections and was hospitalized due to pneumonia and rotavirus infection.

Early reports described conspicuous phenotypically features at the age of ten weeks. He showed some craniofacial features fitting to those of WBS, such as a prominent forehead, a long philtrum, a flat nasal bridge and full lips.

At the age of eight months, the patient underwent neuropaediatric examination due to muscular hypotonia. He showed poor motor development skills for his age. The report states that he was at the developmental status of a four-month-old child.

According to the information given by the parents, during his first eight months the boy cried a lot, showed sleeping problems and a lack in facial expression and poor motor activity. He was

described as a very uneasy child, which showed positive and calming reaction mostly to music. During this period, he received physiotherapy (Vojta, Bobath) constantly.

At the age of 13 months, when the boy was not yet able to sit on his own, Williams-Beuren-Syndrome was diagnosed by FISH analysis. Molecular genetic diagnostics were initialized by the children's cardiologist. Cardiological and vascular findings at this time were at a steady state without any hemodynamic relevance.

Case 2

This patient and his parents consulted a human geneticist for the first time at the age of 12 months. The boy was born by vaginal delivery after an uneventful pregnancy with normal weight (3190g) and length (48cm) during the 42nd gestation week. He presented frequent vomiting during the first year of life, occasional diarrhea and poor weight gain. Two inguinal hernias required surgical therapy. Besides, he suffered from congenital facial nerve paralysis, increased susceptibility to infections and general developmental delay.

At the age of 12 months, he had a height of 70 cm and weighted 7400g while presenting a motor and mental development status of a six-month-old child. Impaired hearing was suspected as well. Some of his craniofacial features fitted those of WBS with a flat nasal bridge, a long philtrum, a wide mouth and a stellate iris pattern. He was sensitive to noise, but enjoyed listening to music. Later he presented a typical tooth morphology as well. He showed muscular hypotonia.

With 12 months of age, Williams-Beuren-Syndrome was diagnosed by FISH analysis. Further diagnoses were a mild to moderate supravalvular aortic stenosis (Vmax. 2.8 m/s and pressure gradient 30 mmHg), a mild supravalvular and peripheral pulmonary stenosis and a mild coarctation of the aorta. The blood pressure was elevated during sporadic measurements and further controls were recommended. Fortunately, cardiac and vascular findings were at a steady state during further controls during the following years.

Finally, the boy was able to sit on his own at the age of 1.5 years. At the same time, he started speaking his first words. Later, the boy caught up in developing motor and language skills and visited an integrative kindergarten and later a special needs school. Constant logopedics, physio- and music therapy were recommended.

At the age of 14, a progress of the SVAS was detected by coronary angiography and the boy was hospitalized for resection of the SVAS by Doty technique. At that time, he presented a bilateral inhibition of supination of his forearms (caused by radioulnar synostosis). While he was hospitalized for heart surgery an EEG was performed as part of the surgery preparation. EEG findings showed an increased susceptibility for seizures without any known patient history for seizures. Further information about the neurological status was not available in the following reports.

Case 3

This male patient was delivered at gestation week 40 by caesarian section. He weighed 2655 g and measured 49 cm at birth. A cardiac murmur was diagnosed directly after birth and the boy was provided with home monitoring, because his older sibling died from sudden infant death syndrome (SIDS). The first hospitalization of this patient occurred at the age of three months due to failure to thrive. He presented typical craniofacial stigmata of the Williams-Beuren-Syndrome and muscular hypotonia. A mild SVAS (Vmax 3 m/s), mild supravalvular and peripheral pulmonary stenosis and a mild coarctation of the aorta were diagnosed. Further echocardiographic and blood pressure controls were recommended, as well as physiotherapy. Following reports documented a steady state regarding the cardiovascular findings.

This patient was diagnosed with WBS by FISH at the age of 5 months. In addition, he suffered from infantile spasms (Blitz-Nick-Salaam (BNS) seizures). The available reports stayed vague regarding the exact time of manifestation. Except one unremarkable electroencephalography at the age of 3 4/12 years, no further reports about this neurologic aspect were available. Three follow-up examinations described a significant progress in thriving, motor and social development. At the age of 3.5 years, the boy entered a special needs kindergarten. He was given physiotherapy and swimming therapy regularly.

The patient's younger brother who was born with hypoplastic left heart syndrome and was also suspected to have WBS showed normal results by FISH analysis.
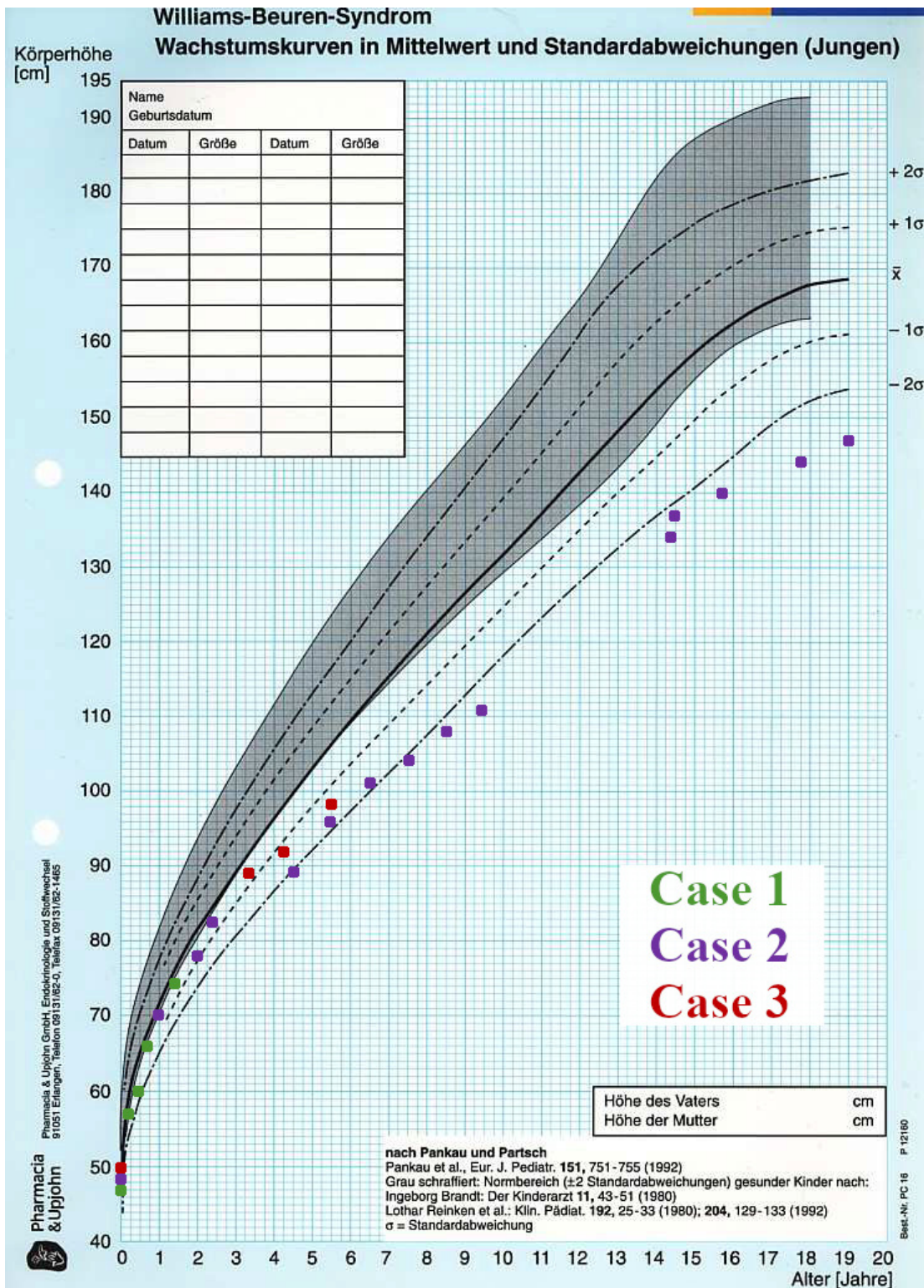
Figure 3.9: Height growth charts with average values and standard deviations in boys with WBS after Pankau and Partsch. The grey shade depicts the normal range ± 2 standard deviations in healthy boys. Measurements of case 1 are green, of case 2 violet and of case 3 red (Pankau et al. Das Williams-Beuren-Syndrom. P. 147).

Case 4

The girl was delivered spontaneously in the 39th gestation week after an uneventful pregnancy as the parents' first child. During a routine examination in the first week of life a cardiac murmur was noticed. An echocardiography showed a moderate to severe supravalvular aortic stenosis (pressure gradient 45 mmHg) and a bilateral peripheral pulmonary stenosis (pressure gradient 75 mmHg). Interestingly, the girl's mother had a history of an aortic stenosis of unknown localization.

According to the reports from the clinic of pediatric cardiology during the first ten months of the girl's life, Williams-Beuren-Syndrome must have been ruled out, but no further information about the diagnostic procedure is mentioned. None of the available reports described any craniofacial conspicuities. At the age of 10 ½ months the diagnosis of a hereditary supravalvular aortic stenosis was made. A progress of the aortic stenosis could not be excluded by echocardiography and further controls were recommended. Meanwhile both ventricles showed signs of hypertrophy.

At 1 year of age, a further progress of the supravalvular aortic stenosis was diagnosed and surgery a few months ahead was planned. The mother underwent a surgery of her own supravalvular aortic stenosis in the same year. The girl's peripheral pulmonary stenosis showed a steady state at that point. Additional reports to enlighten the post-interventional outcome or further development of the child were not available. To this point the thriving of the girl showed a normal progress.

Regarding the girl's height and weight development, it becomes clear that contrary to the other three patients (cases 1 - 3, discussed below) this patient ranges in much higher percentiles. The measurements are all above the average level of a female WBS patient. Interestingly, according to the percentile curves of normal developing girls (figure 1.6), the patient from case 4 ranges between the 5th and 50th percentile, except at birth, where she ranges at the 50th percentile. Maybe her fragile, feathery stature was due to her congenital heart defect (Hereditary SVAS), because she did not suffer from Williams-Beuren-Syndrome. Because the patient and her DNA sample were among the collective with a WBS diagnosis, the sample was processed within this thesis as the other presumed WBS patients.
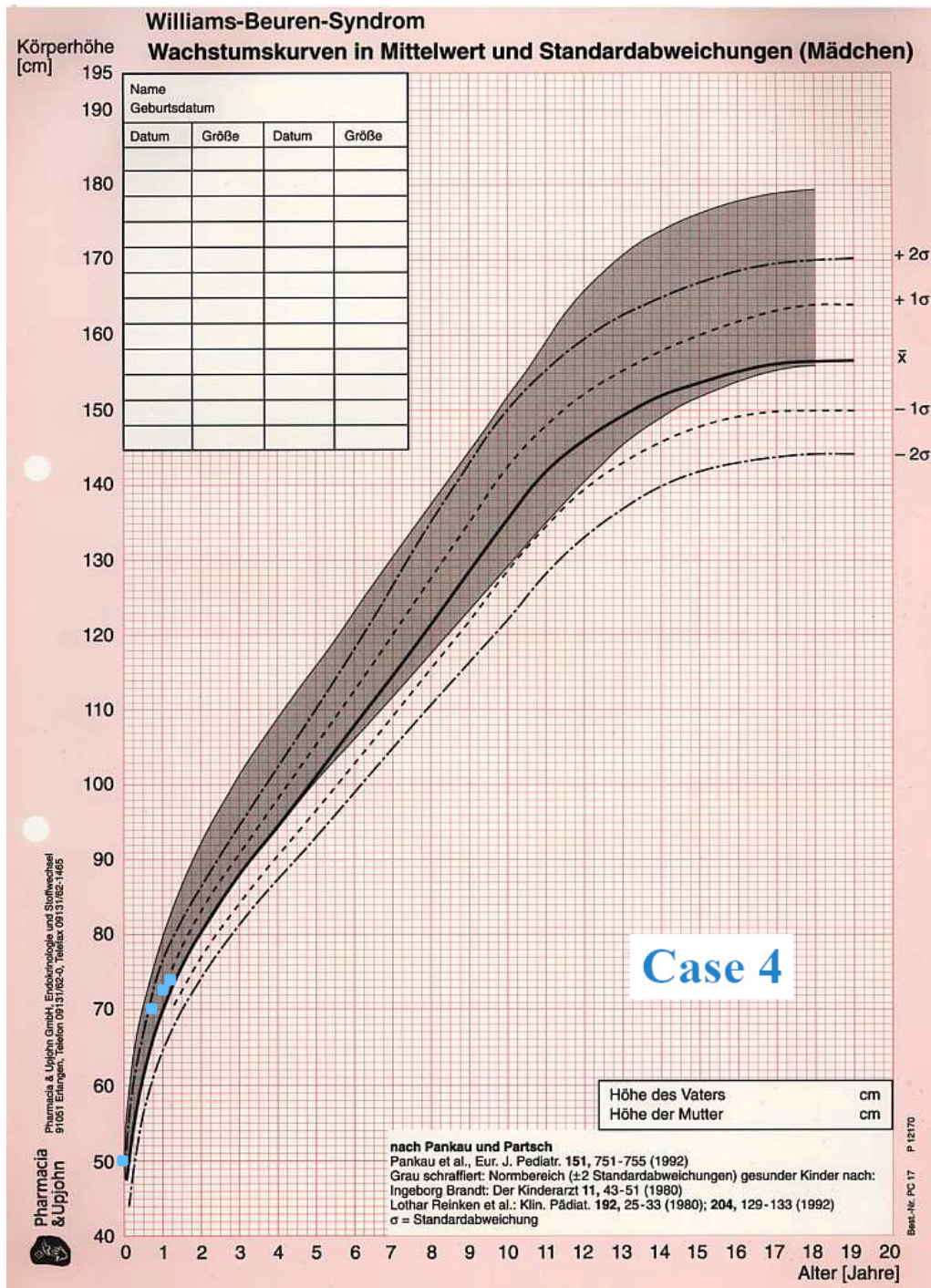
Figure 3.10: Height growth charts with average values and standard deviations in girls with WBS after Pankau and Partsch. The grey shade depicts the normal range ± 2 standard deviations in healthy girls. Measurements of case 4 are blue (Pankau et al. Das Williams-Beuren-Syndrom. P. 146).

3.5   Genes affected in patients with atypical deletions

This chapter will give an overview of the affected region on chromosome 7 and its genes. The illustration below (figure 3.11) shows chromosome 7 with an enlargement of region 7q11.22 to 7q21.11 with the WBSCR, its single-copy genes and the flanking gene regions encompassing coding and non-coding genes. The four atypical deletions are depicted including the approximate breakpoints obtained through SNP array analysis. Additionally, four STS markers (D7S2476, D7S613, D7S1870, D7S489-A) which were used in the further course, are depicted. The gene map mainly refers to the genetic overviews of Schubert (2009), Pober (2010) and Bayés (2003) and was generated with the help of "Genome Data Viewer".
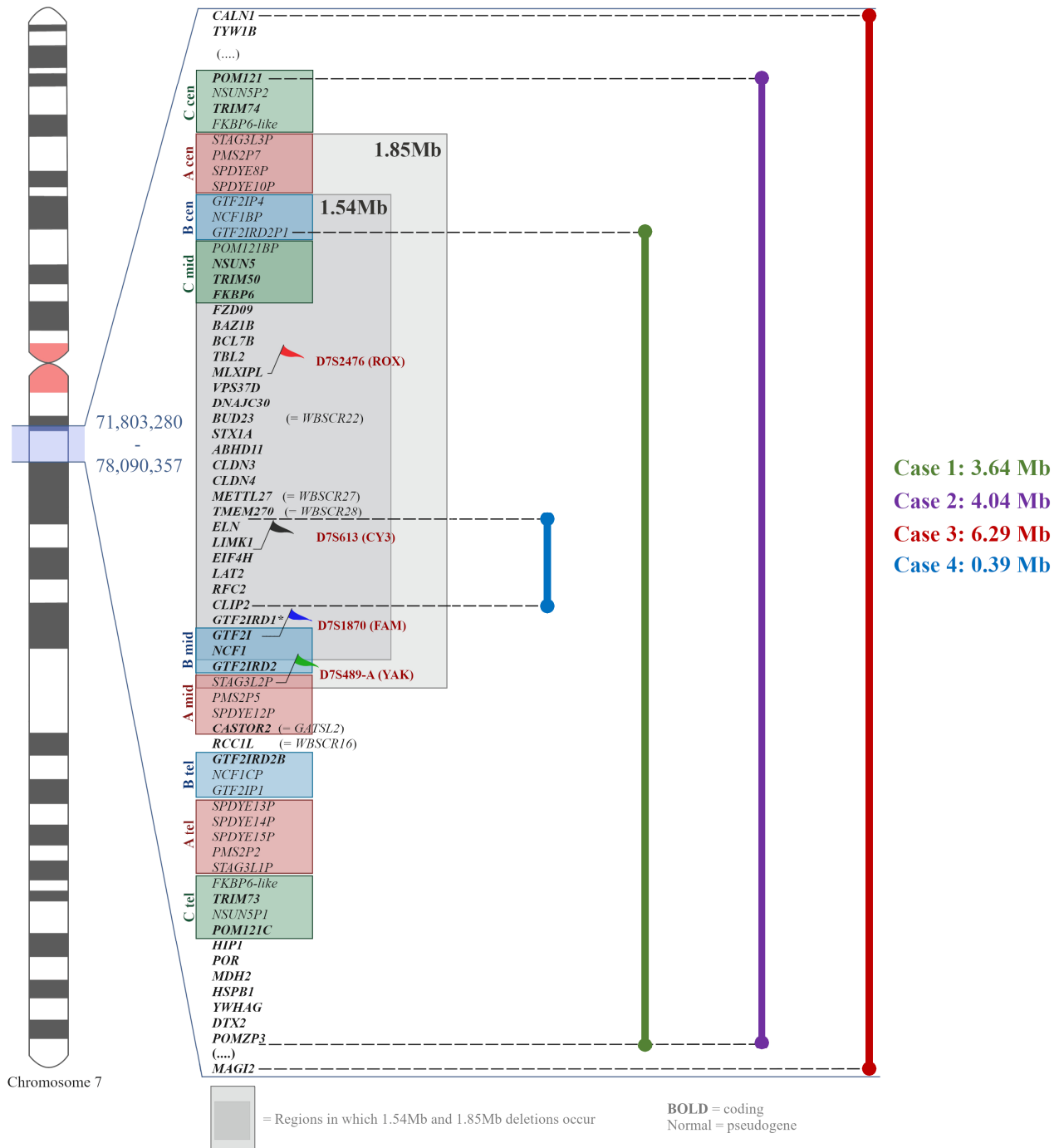
Figure 3.11: Genomic map of 7q11.22 to 7q21.11. The enlargement of this part of chromosome 7 encompasses the WBSCR, the flanking A, B and C blocks (red, blue and green blocks) with their centromeric, middle and telomeric sections and further adjacent genes in centromeric and telomeric direction with a putative relevance for the atypical cases presented in this thesis. The base pair numbers on the left side of the illustration refer to the GrCh37 nomenclature. If genes have an alternative name, it is bracketed on the right-hand side of the gene name. The asterisk next to *GTF2IRD1* stands for the 22th coding gene *WBSCR23*, which is thought to be an intronless gene *within GTF2IRD1*. The approximate sizes of both typical deletions spanning either 1.54 or 1.84 Mb are marked by grey blocks. The proximal and distal extensions of those blocks only depict the approximate breakpoints. Further information about the known breakpoints is given in chapter 1.6. The four applied STS markers are highlighted by little flags. The colors of the flags correspond to the fluorescence dye of the markers. The dye's names are bracketed. In the middle and on the right-hand side of the illustration the four atypical deletions of this thesis are depicted (cases 1 – 4). The sizes of the deletions were determined by SNP array analysis. The approximate breakpoints are shown by dashed lines. After Schubert 2009, Pober 2010, Bayés 2003.

The provided SNP array results revealed some additional hemizygous deleted genes adjacent to the typical WBS deletion, some in centromeric, others in telomeric direction. Some of them having a potential clinical relevance for WBS are presented in table 3.3 ordered from centromeric to telomeric position.

Gene	Potential gene function	Potential clinical effect
CALN1 (*CALNEURON 1*) OMIM *607176	*CALN1* encodes for a neuron-specific protein which is thought to play a role in normal cognitive development, learning and memory signal transduction (Wu. et al. 2001).	Memory and learning (Wu et al. 2001). Infantile spasms (Komoike et al. 2010).
POM121 (*POM121 TRANSMEMBRANE NUCLEOPORIN*) (Block C cen) OMIM *615753	POM121 acts a protein of nuclear pore complexes (NPC) which interacts with other NPC units and stabilizes the NPC (Mitchell et al. 2010).	Unknown.
TRIM74 (Block C cen) OMIM *612550 *TRIM50* (Block C mid) OMIM *612548 *TRIM73* (Block C tel) OMIM *612549 (*TRIPARTIFE MOTIF-CONTAINING PROTEIN 50, 73 and 74*)	*TRIM73* and *TRIM74* have a similar function as *TRIM50*, which encodes for an E3-ubiquitin-ligase (~ 96% identity). TRIM50 is expressed in stomach, intestine, liver and brain (Micale et al. 2008).	Mental impairment: Several syndromes associated with mental impairment are caused by mutations of TRIM family E3-ubiquitin-ligases (Opitz syndrome, Bardet-Biedl syndrome, limb-girdle muscular dystrophy) (Micale et al. 2008). Gastrointestinal symptoms: Specific expression of TRIM50 in

		stomach, intestine and liver (Micale et al. 2008).
NSUN5P2 **(Block C cen)** *NSUN5* **(alias *WBSCR20*, *WBSCR20A*)** **(Block C mid)** **OMIM *612548** *NSUN5P1* **(alias *WBSCR20B*)** **(Block C tel)** (*NOP2/SUN RNA METHYLTRANSFERASE FAMILY, MEMBER 5*)	*WBSCR20B* might be related to *WBSCR20*, which is thought to encode for a protein involved in cell cycle regulation and cell proliferation in skeletal muscle cells (Doll et Grzeschik 2001).	Growth retardation, myopathy, premature aging effects (Doll et Grzeschik 2001).
GTF2IRD2 (*GTF2 REPEAT DOMAIN CONTAINING 2*) **(Block B mid)** **OMIM *608899**	Member of transcription factor family TFII-I. Encodes for transcription factors required for synapse development (Serrano-Juarez et al. 2018).	Increased impairment in daily life / psychological well-being (e. g. depression, greater externalizing problems, including obsession and maladaptive behaviour) (Porter et al. 2012). Increased impairment in visuospatial abilities (Serrano-Juarez et al. 2018).
NCF1 (*NEUTROPHIL CYTOSOLIC FACTOR 1*) **(alias p47-PHOX)** **(Block B mid)**	Encodes an NADPH oxidase subunit (Del Campo et al. 2006).	Hemizygosity in *NCF1* prevents risk of arterial hypertension in WBS (Del Campo et al. 2006).

OMIM *608512		Simultaneous occurrence of WBS and CGD possible, 2 cases in literature (Roesler et al. 2000).
CASTOR2 (**_CELLULAR ARGININE SENSOR FOR MTORC1 PROTEIN 2_**) (**alias** _GATSL2_) (**Block A mid**) **OMIM *617033**	CASTOR2 participates in the negative regulation of mTORC1, a growth regulator (Chantranupong et al. 2016).	Unknown.
POM121C (**_POM121 TRANSMEMBRANE NUCLEOPORIN C_**) (**Block C tel**) **OMIM *615754**	POM121C is, like POM121, a protein of the NPC. Knockdown of both reduced assembly of the NPCs and them clustering (Funakoshi et al. 2007).	Unknown.
HIP1 (**_HUNTINGTIN INTERACTING PROTEIN_ 1**) **OMIM *601767**	_HIP1_ encodes Huntingtin interacting protein 1, which together with other proteins acts during AMPA receptor endocytosis in the CNS (Metzler et al. 2003).	_HIP1$^{-/-}$_ mice showed wasting, tremor and gait ataxia besides a thoracolumbar kyphosis (Metzler et al. 2003). In contrast, other studies found no connection to cerebral or neurological abnormalities (_hip1_ knockdown in zebrafish) (Komoike et al. 2010). _HIP1_ haploinsufficiency is a candidate for epilepsy and/or cognitive

		dysfunction (Ramocki et al. 2010).
POR (***CYTOCHROME P450 OXIDOREDUCTASE***) **OMIM *124015**	*POR* encodes for an electron donor for several CYP enzymes. Homozygous or compound-heterozygous mutations lead to POR deficiency (PORD) (Fukami et Ogata 2014).	PORD leads to one form of congenital adrenal hyperplasia and/or skeletal malformations (Antley-Bixler syndrome) (Fukami et Ogata 2014).
MDH2 (***MALATE DEHYDROGENASE, MITOCHONDRIAL***) **OMIM *154100**	Encodes for the Krebs cycle enzyme mitochondrial malate dehydrogenase. The consequence of reduced enzymatic activity is the accumulation of MDH2 substrates (Ait-El-Mkadem et al. 2017).	In 2017, *early infantile epileptic encephalopathy-51* in 3 patients with bi-allelic mutations in *MDH2* was described for the first time (OMIM #617339). Patients presented epileptic seizures besides hypo-tonia and failure to thrive (Ait-El-Mkadem et al. 2017).
HSPB1 (***HEAT-SHOCK 27kD PROTEIN 1***) (**alias** *HSP27*) **OMIM *602195**	Heat-shock proteins play a role in aggregation, transport and folding of proteins. The transcriptional rate increases due to heat or metabolic stress. HSP27 regulates actin-polymerization (Stock et al. 2003).	Lower mean IQ of 44 (Kaufman-Brief-Intelligence-Test) in comparison to mean IQ of 71 by WBS patients with common length of deletion (Stock et al. 2003).
YWHAG (***TYROSINE 3-MONOOXYGENASE/***	Protein for signal transduction in mitosis and cellular proliferation (Gardino et Yaffe 2011).	Neurological and neuropsychological deficits (e. g. inattention, hyperactivity,

TRYPTOPHAN 5-MONOOXYGENASE ACTIVATION PROTEIN, GAMMA ISOFORM) **OMIM *605356**		impulsivity, aggression), epilepsy, autistic traits (Fusco et al. 2014). Reduced brain size and infantile spasms, enlargement of the heart tube (*ywhag* knockdown in zebrafish) (Komoike et al. 2010). *YWHAG* haploinsufficiency is considered a candidate for epilepsy and/or cognitive dysfunction (Ramocki et al. 2010).
POMZP3 (***POMZ3 FUSION PROTEIN***) **OMIM *600587**	Unknown.	Unknown.
DTX2 (***DELTEX E3 UBIQUITIN LIGASE 2***) **OMIM *613141**	E3-Ubiquitin-ligase (Takeyama et al. 2003).	Unknown.
MAGI2 (***MEMBRANE-ASSOCIATED GUANYLATE KINASE, WW and PDZ DOMAINS-CONTAINING, 2***) **OMIM *606382**	MAGI2 serves as a structure for synaptic protein complexes and is essential for development and maintenance of synapses (Marshall et al 2008).	Infantile spasms (Marshall et al 2008). Röthlisberger B. et al. (2009) reported a patient with infantile spasms and a long chromosome 7 deletion excluding *MAGI2*.

Table 3.3: Overview of the genes affected by the atypical deletions in WBS patients in this thesis.

4   Discussion and phenotype-genotype correlation

4.1   Overview

218 patients with WBS could be identified with the help of MLPA, most of them well known to several WBS specialists all over Germany. Four particular deletions, differing in size, were detected. Three of them were much larger while one of them was notably smaller than a typical deletion.

All of the atypical deletions were further analysed by SNP array to determine the approximate size and breakpoints. This also allowed identification of additional hemizygously deleted genes which were not detectable by MLPA.

Several publications focus on potential phenotype-genotype correlations in Williams-Beuren-Syndrome (Marshall et al. 2008, Ramocki et al. 2010, Fusco et al. 2013). The effect of a disruption of the *ELASTIN* gene could be connected to arterial stenosis and cardiovascular abnormalities, especially the supravalvular aortic stenosis in WBS (Pober 2010, Schubert 2008). This congenital heart defect has a severe impact on affected families because they have to attend regular cardiologic check-ups with their children, some of them requiring heart surgery.

This thesis tries to further establish a potential correlation between genes that are disrupted or deleted in the abovementioned atypical WBS cases (cases 1 - 3) and the possible phenotypic deviations. All of these cases harbour some additional deleted genes adjacent to the WBSCR, either in centromeric or telomeric direction. Case 4 is omitted from this analysis, because this patient suffers from familial supravalvular aortic stenosis (OMIM #185500) which is caused by heterozygous variants in or deletions of *ELN* resulting in a functional hemizygosity of this gene (Metcalfe et al. 2000).

4.2   Atypical cases

Case 1

The affected genes -amongst others- were *GTF2IRD2B* (B tel), *TRIM73* (C tel), *NSUN5P1* (C tel), *POM121C* (C tel), *HIP1*, *POR*, *MDH2*, *HSPB1*, *YWHAG*, *DTX2* and *POMZP3* (from centromeric to telomeric direction). Most of them are located telomeric to the common WBS deletion region. The approximate centromeric breakpoint of case 1 is located in the B cen region within *GFT2IRD2P1*.

Clinical data of case 1 were available at six points in time (table 8.1). The latest measurement is only at 17 months of age. The height measurements are below the mean height of the respective points but within two standard deviations of the German WBS cohort (figure 3.10). The same is true for the first two weight measurements (weight references are based on American WBS cohort https://williams-syndrome.org/growth-charts/growth-charts. 13.10.2019. 18:00). However, from approximately 6 months of age the weight approaches the mean in WBS.

Summarizing, case 1 ranges slightly below the percentile curve of the healthy control group but within the lower range of WBS reference heights.

Other data provided by the clinical reports seem to be characteristic for WBS itself and do not differ from other individuals who carry a common deletion measuring ~ 1.54 Mb.

The reference data quoted above were collected by Pankau and colleagues and is based on an analysis of a collective of 90 male German WBS patients with respect to their age-related height. Pankau et al. concluded that in general the length of a mature German newborn with WBS ranges within the lower normal percentile region compared to healthy German newborns. This is seen in case 1 as well. The difference between both groups increases within the first six months of life. Between the age of six months and eleven years, the mean height of a WBS patient is around the third percentile of a standard population. After puberty, starting one year earlier than normal, the average and even the final height of German WBS patients is below the third percentile of the normal range (Pankau R. et al. Das Williams-Beuren-Syndrom. P. 141).

However, worth highlighting in the context of growth retardation might be the putative gene *NSUN5P1* (alias *WBSCR20B*) in the block C tel. Only little information can be found in the literature about *NSUN5P1* and *NSUN5* (alias *WBSCR20*) to which the former one is closely related, because they differ only in one exon (Doll et Grzeschik 2001). According to recent data

from the Genome Data Viewer, *NSUN5P1* is a pseudogene and therefore should not be transcribed and translated into a functioning protein (https://www.ncbi.nlm.nih.gov/genome/gdv/browser/genome/?id=GCF_000001405.25. 27.01.2020. 14:00) while Doll and Grzeschik (2001) mention *NSUN5P1* as a *putative* gene with a potential involvement in growth retardation of WBS patients.

NSUN5 stands for *NOP2/SUN RNA METHLYTRANSFERASE FAMILY, MEMBER 5*. Doll and his colleague Grzeschik (2001) reported a similarity between the transcribed product of *NSUN5*, which is expressed in skeletal muscle and the human protein p120. P120 is a proliferation-associated nucleolar antigen with a putative role in cell-cycle regulation and cell proliferation in mammals. Due to this similarity, *NSUN5* itself might also play a role in the control of the cell cycle. During their experiments, another gene very similar to *NSUN5* was detected: *NSUN5P1* (alias *WBSCR20B*). Because of the distribution of its gene product in skeletal muscle, the authors assumed that a hemizygous deletion of *NSUN5*, which is located in the commonly deleted region of WBS, as well as the hemizygous disruption of *NSUN5P1*, might result in growth retardation and premature aging in WBS patients (Doll et Grzeschik 2001).

Case 2

The hemizygous deletion of this patient is ~ 0.4 Mb larger than in case 1. The narrowed telomeric breakpoint of both cases is nearly the same, but the estimated centromeric breakpoint of case 2 lies at the very edge of block C cen, and therefore much more centromeric than in case 1. There are only two additional coding genes affected compared to case 1: *TRIM74* and *POM121*.

Besides WBS-typical features (craniofacial features, SVAS, noise sensitivity, music affinity), this boy showed conspicuously low values in height and weight. Height measurements of case 2 are presented and compared to the figures of WBS patients of Pankau et al. in table 4.1 (Pankau et al. Das Williams-Beuren-Syndrom. P. 139).

While data at the first three points in time of case 2 show no suspicious deviation compared to the WBS figures, the height measurements between four and six years of age range at a lower level but within two standard deviations of the WBS cohort. With increasing age (> 6 years) the measurements range progressively below minus two standard deviations which is illustrated in figure 3.10.

Case 2			Pankau et al.	
Age	**Height**		**Mean height**	**Age (n)**
Birth	**48 cm**		**49 cm**	Birth (65)
12 months	**70 cm**		**72.3 cm**	12 months (39)
23 months	**78 cm**		**81.5 cm**	2 years (38)
4 5/12 years	**89.5 cm**		**97.6 cm**	4 years (35)
5.5 years	**96 cm**		**105.2 cm**	5 years (23)
6.5 years	**101 cm**		**110.5 cm**	6 years (23)
7 5/12 years	**104 cm**		**116.3 cm**	7 years (22)
8 5/12 years	**108 cm**		**125.3 cm**	8 years (22)
9 5/12 years	**111 cm**		**127.2 cm**	9 years (24)
14 5/12 years	**134 cm**		**155.2 cm**	14 years (14)
15 8/12 years	**140 cm**		**159.2 cm**	16 years (7)
17 10/12 years	**144.6 cm**		**167.1 cm**	18 years (15)
19 years	**147.6 cm**		**168.2 cm**	>18 years (27)

Table 4.1: **Comparison of the measurements of case 2 to the cohort from Pankau et al.** (Pankau et al. Das Williams-Beuren-Syndrom. P. 139).

Summarizing, the data from cases 1 and 2 fit the assumption that a hemizygous deletion of *NSUN5P1* might lead to noticeable lower results in height. Only a few phenotype-genotype correlations concerning the growth development of individuals with WBS have been established so far. It is not clear if *NSUN5P1* operates as a valid gene with a coding function at all. In WBS, a hemizygous deletion of *NSUN5P1* is always associated with a hemizygous deletion of *NSUN5*, which is located in the block C mid, and is itself a putative candidate for growth retardation. In this thesis, like other studies, mediating effects of single haploinsufficient genes, resulting from a larger than usual contiguous deletion, on each other cannot be ruled out.

Pankau et al. discussed their growth data assembly in comparison to growth data from Morris et al. from the year 1988. While Morris et al. suggested that growth retardation occurs due to low caloric intake and high caloric turnover, Pankau and his colleagues suggested that the typical growth retardation is due to the syndrome itself. In their opinion, *additional* growth retardation only becomes clinical apparent in very severe cases of malnutrition and maldigestion. Furthermore, they saw no connection between congenital heart diseases and growth retardation. Neither did Morris et al. observe WBS patients catch up in growth and development after heart surgery, nor did they observe a difference in growth of children with WBS with and without congenital heart diseases at all (Pankau et al. Das Williams-Beuren-Syndrom. P. 144). On the other hand, Morris et al. consider WBS typical skeletal morphologies as further factor negatively affecting the final height of a WBS patient, such as joint contractures

88

or scoliosis, which fits the assumption of Pankau et al. of a syndrome specific growth retardation (Morris et al. 1988).

Pankau et al. especially highlighted the importance of collecting growth data of WBS patients regularly. On one hand, they enable a possible individual prognosis about the expected growth of an affected individual. On the other hand, it is more likely to detect additional diseases affecting the development of a WBS child, such as celiac disease. Supervising physicians should be attentive to growth retardation which is more severe than in typical WBS cases. This failure to thrive hints for a possible additional cause of growth retardation. In cases of celiac disease, it is possible for affected individuals by maintaining a gliadin free diet to catch up in height and weight (Pankau et al. Das Williams-Beuren-Syndrom. P. 137, 144f.). Levy-Shraga et al. (2018) who analysed the data of a WBS cohort in Israel, further suggested to screen for growth hormone deficiency or hypothyroidism, if a more than tolerable growth retardation in WBS individuals occurs. In case of a deficiency, growth hormone or levothyroxine substitution would be required. As a frequent cause for growth retardation they named precocious puberty.

The clinical reports of case 2 do not provide any information about gastrointestinal problems besides vomiting and occasional diarrhoea which alone gives no hint pointing towards celiac disease. There was no information about diagnostics concerning celiac disease, growth hormone deficiency or hypothyroidism.

Case 3

Unfortunately, in this case only little clinical information could be collected, although it might have the greatest potential for a phenotype-genotype correlation of an extremely large deletion. Both approximate breakpoints lie significantly centromeric and telomeric to the previous breakpoints of the other cases. The deletion spans ~ 6.29 Mb, which is more than four times larger than the WBS-typical deletion. Compared to case 2, two of the additionally deleted coding genes are *CALN1* on the centromeric site of the q-arm and *MAGI2* on the telomeric side.

This male paediatric patient was diagnosed with Williams-Beuren-Syndrome at the age of just five months by FISH. This leads to the assumption that he showed specific, maybe alarming features very early in his life. By comparison, case 1 was diagnosed with WBS at the age of 13 months and case 2 at 12 months. It might have taken much longer time until the first clinical features appeared in the latter two cases.

One clinical feature of patient 3 were infantile spasms (IS). Infantile spasms are defined as serial spasms with symmetrical bending- and stretching-spasms that occur within the first two years of life (AWMF Guideline „Therapy of infantile spasms (West syndrome)". 2014). In half of the cases, epileptic seizures appear due to brain malformations, in the other half they occur idiopathic. Regardless of the origin of the seizures, infantile spasms are associated with a poor prognosis and lead to deficient development of the central nervous system (Marshall et al. 2008).

To date, there are five possible gene candidates for this condition which are all located on the affected site of chromosome 7: *MAGI2* (7q21.11), *CALN1* (7q11.22), *YWHAG* (7q11.23), *MDH2* (7q11.23) and *HIP1* (7q11.23).

MAGI2 stands for *MEMBRANE-ASSOCIATED GUANYLATE KINASE INVERTED-2 GENE*, comprises 1.44 Mb and is located on 7q21.11. It is located considerably more distal to the WBSCR. The protein products of *MAGI2* play a role at NMDA-receptors at excitatory as well as at inhibitory synapses in the brain (Deng et al. 2006). At least two isoforms of MAGI2 have been described (Marshall et al. 2008).

Marshall and colleagues published their findings about the context between infantile spasms and a deletion of *MAGI2* in 2008. They mainly referred to prior studies, which speculated a connection between a far more telomeric than usual breakpoint and the occurrence of infantile spasms. They analysed 28 cases with hemizygous 7q11.23-q21 deletions, out of which 16 suffered from IS or other seizure disorders. Of those, nine individuals presented IS and WBS, three had IS without WBS, two had WBS combined with another seizure disorder and finally two individuals with another seizure disorder without WBS.

They concluded that all but one of the 16 individuals with IS or a seizure disorder showed (partial) hemizygosity in *MAGI2*, which in all cases led to a hemizygous disruption and therefore decrease of both isoforms of MAGI2. The shortest deleted part of *MAGI2* and association with IS measured ~ 500 kb. On the other hand, in 11 of 12 patients from their study with deletions in the 7q region, who did *not* suffer from seizures, *MAGI2* remained intact. Those 11 patients had a contiguous hemizygous deletion either centromeric *or* telomeric of the *MAGI2* locus.

In addition, they discussed the possibility of a two-gene hypothesis and the possible requirement of a disruption of a second gene on 7q11.23-q21 to cause IS. They disproved this hypothesis

however by the fact that in some of their cases with IS or other seizure disorders the hemizygous deletion extended telomeric while in other cases centromeric to *MAGI2*. They concluded that an additional deleted gene accompanying *MAGI2* seemed to be various and therefore random.

The approximate distal breakpoint of case 3 is located ~ 0.73 Mb into *MAGI2*. The smallest region of overlap that was detected in the work of Marshall et al. (2008) measured about ~ 500 kb. Therefore, their results can be transferred to case 3.

The second candidate for infantile spasms is *CALN1* which stands for *CALNEURON1*. *CALN1* is located centromeric to the WBSCR on 7q11.22. Wu et al. identified *CALN1* in 2001 as a human brain-specific gene, especially in the cerebellum, hippocampus, striatum and cortex, which is thought to play a role in normal cognitive development, learning and memory signal transduction. In addition, Komoike et al. established a phenotype-genotype correlation in two atypical patients with extended WBS deletions in 2010. They referred to Wu and his colleagues' data that the expression of *CALN1* reaches its highest expression level at postnatal day 21 in mouse homologs. The postnatal expression pattern in mice might approximately fit the onset of infantile spasms in humans with their first manifestation from 3 to 6 months after birth. This led Komoike et al. to their conclusion that haploinsufficiency and thus deficiency in *CALN1* could be connected to the occurrence of IS.

Another promising candidate when focussing on infantile spasms is the gene *YWHAG*. Komoike et al. (2010) presented a disruption of *YWHAG* as a potential cause of IS and therefore neurodevelopmental disorders. *YWHAG* stands for *TYROSINE 3-MONOOXYGENASE/TRYPTOPHAN 5-MONOOXYGENASE ACTIVATION PROTEIN, GAMMA ISOFORM*. Komoike et al. referred to a previous study that described a possible function of *ywhag1* in zebrafish in cerebral and neural growth due to expression of the protein in some parts of the brain. Furthermore, Komoike and colleagues referred to a paper of Morrison et al. from 2009, in which *YWHAG* was presented as a member of the 14-3-3 protein family, which is involved in cellular processes including signal transduction, apoptosis and cell-cycle regulation and therefore cell growth. In conclusion, Komoike et al. considered haploinsufficiency of *YWHAG* to likely lead to apoptotic cell death in the central nervous system. They used amongst others *ywhag1* knockdown zebrafishes during their experiments, which then presented a reduced brain size.

The fourth candidate for causing epileptic traits is *MDH2, MALATE DEHYDROGENASE, MITOCHONDRIAL*, which was first described only in 2017. Ait-El-Mkadem et al. (2017) described three individuals with compound-heterozygous missense variants in the *MDH2* gene suffering from early-onset muscle hypotonia, psychomotor delay and refractory epilepsy. Compound-heterozygosity describes the state in which each allele of a gene carries a different mutation causing the loss of function of the gene (Murken et al. Taschenlehrbuch Humangenetik. P. 271). The reported *subject 1* presented with focal epilepsy, which developed into refractory myoclonic seizures from the age of five months. *Subject 2*, at two months presented refractory epileptic seizures with generalized tonic seizures and epileptic spasms. *Subject 3* showed refractory epilepsy as well and dystonia with unknown time of onset. All of them had non-specific brain MRI findings but elevated lactate levels in serum and cerebrospinal fluid. Ait-El-Mkadem et al. furnished proof that the *MDH2* missense variants indeed caused MDH2 deficiency and led to severe infantile neurological phenotypes. Although there is no curative therapy for MDH2 deficiency, the authors recommended a ketogenic diet to reduce frequency of epileptic seizures. This disorder, caused by *MDH2* compound-heterozygous missense variants, is now called *early infantile epileptic encephalopathy 51* (EIEE51, OMIM #617339). None of the patients had WBS. The WBS patients do not show the same phenotype as reported by Ait-El-Mkadem and colleagues. The remaining allele in case 3 of this thesis was not screened for any variants. Still, there seems to be a strong association between *MDH2* and infantile epilepsy which was observed in this patient.

The fifth, and to date last candidate in respect of neurodevelopmental disorders and/or infantile spasms is *HIP1, HUNTINGTIN INTERACTING PROTEIN 1*. Ramocki et al. published their results about *HIP1* haploinsufficiency as a potential cause for epilepsy, intellectual and neurobehavioral limitations only a half year after Komoike et al. (Ramocki et al. 2010, Komoike et al. 2010). Unfortunately, the results from both publications are contradictory towards each other. Ramocki et al. presented 13 unrelated individuals affected by epilepsy by varying degrees and harbouring a 7q11.23 hemizygous deletion adjacent to the WBSCR in telomeric direction spanning *HIP1*. Due to its involvement in AMPA receptor endocytosis in the central nervous system, they suggested that *HIP1* haploinsufficiency and therefore its altered function lead to an increased susceptibility of the human brain towards epileptic seizures. Komoike et al. (2010) who not only investigated *YWHAG*, but also *HIP1*, detected no increased susceptibility for seizures in the developing brain in their *hip1*$^{-/-}$ zebrafishes. Both authors however, agreed that *YWHAG* is a potential candidate for neurodevelopmental disorders.

4.3 Conclusion

4.3.1 Evaluation of the phenotype-genotype correlation

Finally, all potential phenotype-genotype correlations do not provide a sufficient answer to the question why case 3 is clinically more severely affected, especially concerning neurodevelopmental aspects, than the other patients (cases 1 and 2). It is noticeable, that the three male patients (cases 1 – 3) were attached to different clinics and paediatricians. Also, they were examined over different periods of time. But in all cases clinical data were available since the first potential manifestation of infantile spasms, which occurs between the age of three and twelve months. The documented clinical data in all cases begin from birth and often stretch several years of childhood. In case 1 developmental data are available from birth until 13 months of age, in case 2 from birth until 19 years and in case 3 from birth until 5 1/2 years. Two of the patients were seen by the same pediatric cardiologist. The interobserver differences bear a risk for deviations in the gathered results of clinical examination and patient's developmental course. Due to the rarity of WBS a prospective study of a large number of patients is difficult.

In 2009, Schubert summarized that a contiguous deletion of genes located telomeric to *ELN* seems to result in a clinically much more severe affected WBS phenotype in behavioural and cognitive abilities, such as mental retardation, visuospatial impairment or verbal skills.

Referring to *MAGI2* as potential gene candidate causing IS or other epileptic seizures, there is one report about a case with IS and a large contiguous 13 Mb deletion on chromosome 7 *without* affection of *MAGI2*. According to the authors this deletion encompassed a total number of 179 genes which might include several other causative genes or could cause epilepsy due to the large size of deletion (Roethlisberger et al. 2009). Marshall et al. (2008) presented 15 out of 16 cases of IS *with* a hemizygous disruption of *MAGI2* while 11 out of 12 other cases had no history of seizures and had a deletion sparing *MAGI2*. Roethlisberger and colleagues (2017) argued that in most of the cases from Marshall et al. (12 out of 16 cases with IS or a seizure history) the overlapping hemizygous deletions harbouring about 100 genes could all potentially cause IS or epilepsy if disrupted. However, this large number of genes included the WBSCR and pseudogenes as well. Finally, they agreed with Marshall et al. on the potential role of *MAGI2* in causing IS (Roethlisberger et al. 2009).
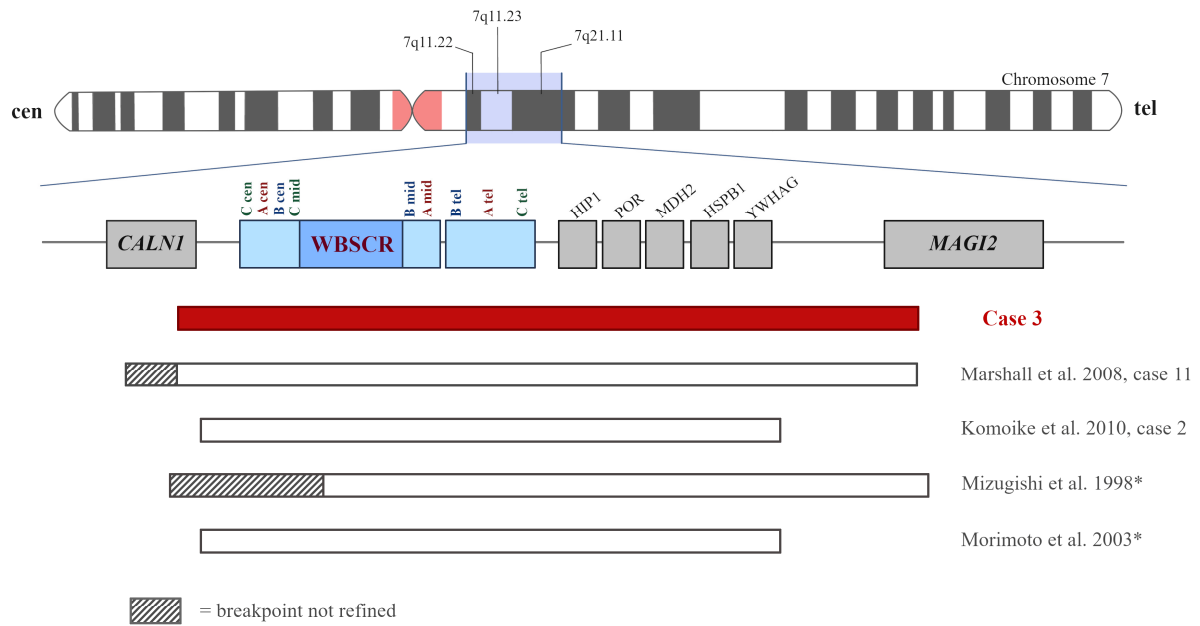
Figure 4.1: Comparison of case 3 of this thesis to other atypical WBS deletions in the literature associated with IS presenting a similar deletion. Asterisk: illustration of these two deletions were made after Komoike et al. (2010).

In contrast, the literature offers a total number of only ten cases of IS with *typical* WBS deletions (1.54 or 1.85 Mb) (Samanta 2017).

Considering all arguments for the previously discussed gene candidates, haploinsufficiency of *MAGI2* seems to be an as plausible candidate causing infantile spasms in case 3 as *CALN1*. The deletion of case 3 in this thesis comprises, besides *MAGI2* and *CALN1*, some additional gene candidates possibly associated with IS or epileptic seizures: *MDH2*, *YWHAG* and even the questionable candidate *HIP1*. An illustration of cases of patients with atypical WBS deletions and an association with IS that are comparable to case 3 can be found above (figure 4.1). All of them comprise *MDH2*, *YWHAG* and *HIP1* as potential candidate genes and either parts of *CALN1* or *MAGI2* or parts of both of them.

The available clinical data vary considerably between the cases investigated in this thesis and were not standardized. Therefore, a definitive determination, if the herein presented individuals are impaired in daily life as a result of their deletion size is not possible. For instance, facts about intellectual disabilities or neuroendocrine abnormalities were not available.

The genomic basis for the different neurological presentation of cases 1 – 3 remains unclear: A complete lack of neurological symptoms (case 1), an increased susceptibility for seizures (case 2) and manifestation of infantile spasms (case 3). Case 1 and 2 nearly harbour the same size of

contiguous hemizygous deletions. The deletion of case 2 spans ~ 400 kb beyond the deletion of case 1 without comprising any additional known potential candidates explaining the documented EEG findings. Comparable findings were not documented in case 1. Both cases share a hemizygous deletion of the same candidates with putative involvement in epileptic seizures: *HIP1*, *MDH2* and *YWHAG*.

This leads to the conclusion that infantile spasms as an additional symptom in case 3, compared to the other cases, can potentially appear as a result of haploinsufficiency of *CALN1* and/or *MAGI2*. Patients in general seem to suffer from a more severe manifestation of the syndrome, often suffering from epileptic seizures if their deletion is much larger than usual (Mizugishi et al. 1998, Wu et al.1999, Morimoto et al. 2003, Marshall et al. 2008). Most authors agree on a not yet fully understood effect of the haploinsufficient deletion in WBS on the special phenotype and its variability in WBS patients. At the same time, the intact flanking genes of the deletion are thought to have their own effect on the expression of certain proteins and on the phenotype of a patient. (1) It cannot be ruled out that intact flanking genes show altered expression levels, possibly due to positional effects of the deletion (Pober 2010). A positional effect occurs if a variant, in the case of WBS hemizygosity, affects control elements of one or more genes. The loss of these control elements could possibly lead to an increased or a reduced expression of certain gene products (Murken et al. Taschenlehrbuch Humangenetik, P. 83f). It is even considered that (2) polymorphisms in non-deleted gene copies of the WBSCR have or that (3) the deletion itself has an effect on neighbouring genes' protein expression or function (Pober 2010).

On the other hand, Marshall and colleagues (2008) stated with regards to IS and other epileptic seizures that the size and the location of a hemizygous deletion on the q-arm of chromosome 7 play a subordinate role so long as *MAGI2* is deleted. They presented several patients who showed a deletion encompassing *MAGI2* but extending *either* centromeric *or* telomeric of it and therefore lacking completely different genes. All of those patients suffered from IS or seizures, which assigned *MAGI2* alone a special role in being causative for such neurologic findings (Marshall et al. 2008).

In contrast to patients with typical WBS deletions, regular neurological examinations including EEGs seem to be an inexpensive, but informative diagnostic method for patients with atypical deletions comprising the above-mentioned gene candidates associated with epileptic seizures or IS. Early diagnostics and adequate therapy might prevent progressive neurodegeneration by recurrent seizures.

However, further investigations are required to narrow down potential phenotype-genotype associations and their impact on possible therapies and genetic counselling of the parents. This approach might provide prospects for the individual's future development. Regular examinations and documentation of clinical data by healthcare-experts in WBS can accelerate the knowledge in this well-known, but not yet fully understood syndrome.

4.3.2 Advantages of MLPA

By MLPA alone it is possible to get a relatively quick impression of the approximate size of the hemizygous deletion in the region that is causing Williams-Beuren-Syndrome. The commercial kit is readily available and performing MLPA does not take too much time.

MLPA gives additional information about deletions in the telomeric direction of the WBSCR (figure 3.2) but not in the centromeric direction. The most centromeric gene depicted by MLPA is *FKBP6*, which is the first gene of block C mid. MLPA can also reveal atypical short deletions (figure 3.3). Both are advantages towards the still wide-spread used FISH diagnostic, which depicts mostly the *ELN* and sometimes the *LIMK1* locus, which are located adjacent to each other within the WBSCR and therefore only depict a short segment of the expected deletion.

When MLPA gives a hint for an atypical deletion, further diagnostics like SNP array are recommended to get further insight into the actual size of the hemizygous deletion. When MLPA shows the typical deletion and the clinical presentation is within the normal range, there is no indication for further diagnostic means.

4.3.3 Disadvantages of MLPA

It is not possible to make any detailed conclusions about the exact size of a deletion with the help of MLPA alone. For example, in all three patients with an atypical large deletion, MLPA results were identical. Their deletions encompassed all of the exons provided by MLPA (figure 3.2). To obtain additional results about the actual size of the deletion, further diagnostic tests have to be performed, e. g. fragment or microarray analysis.

Fragment analysis also offered no hint towards the actual extent of the hemizygous deletions in the three atypical cases. Using this method, the results of all three cases seemed to be the same (chapter 2.7.7.2). They would have all pointed towards a hemizygous deletion that spans at least

1.85 Mb. Finally, SNP array analysis revealed three entirely different sizes of deletions in the cases 1 – 3 that all showed the same MLPA results (table 3.2).

In summary, MLPA serves as a diagnostic tool to distinguish *deleted*, *non-deleted* and *atypical deleted* patients. However, there are a lot more possibilities not detectable by this method. For example, the distance between *CLIP2* and *POR* spans ~1.7 Mb and is not depicted by MLPA. Therefore, a deletion between these two genes will be missed by MLPA alone. In conclusion, additional diagnostic options, such as microarray analysis might be useful, if MLPA results do not match the expected diagnostic results.

Because of the above-mentioned advantages, MLPA presents an evolution in the diagnostics of Williams-Beuren-Syndrome.

5 Summary

Williams-Beuren-Syndrome is a microdeletion syndrome on 7q11.23. Most of the patients present with a characteristic physical appearance, cardiovascular affections, endocrine problems including growth retardation and learning difficulties on one hand but great affection to music on the other hand. Their particular strength is a very friendly and hypersocial behaviour.

WBS emerges as a consequence of a contiguous hemizygous deletion of a gene region that in typical cases comprises ~ 1.54 Mb to ~ 1.85 Mb and spans 26 to 28 genes. Several cases of atypical deletions have been reported. Mostly, WBS occurs as a de-novo deletion but there are also cases of autosomal dominant inheritance. The Williams-Beuren-Syndrome Chromosome Region (WBSCR) is flanked by Low copy repeats (LCR) and therefore is predisposed for misalignment during meiosis. The best explored gene of the WBSCR is *ELASTIN* (*ELN*). Its haploinsufficiency is considered to be causative for cardiovascular abnormalities in this syndrome and hereditary supravalvular aortic stenosis, which is a disorder on its own.

This thesis aimed at verifying former FISH diagnoses in over 340 German WBS patients with the help of a newer method, Multiplex Ligation-dependent Probe Amplification (MLPA). MLPA is a semi-quantitative PCR-based technique to determine the relative copy number of a DNA site of interest.

This study of the largest WBS-cohort in Europe to date resulted in 218 cases, in which the former FISH diagnosis could be verified by MLPA. Four atypical deletions as a basis for potential phenotype-genotype correlations were detected: three long deletions and an exceptionally short one.

In addition, fragment analysis was performed to narrow down the approximate size of deletion (1.54 Mb vs. 1.85 Mb) and to detect, if the maternal or paternal allele were deleted. The results nearly fitted the previously published data: approximately 94% presented a small 1.54 Mb deletion. Results regarding the parental inheritance differed slightly from literature: in ~ 59 % (vs. 45 %) the deletion was of maternal and in ~ 41 % (vs. 55 %) of paternal origin. The origin of the deletion is not known to have an effect on the phenotype, whereas atypical deletions can have profound effects, especially regarding neurodevelopmental aspects, e. g. infantile spasms or other epileptic disorders.

By SNP array analysis, the approximate breakpoints were narrowed down. The shortest deletion spanned ~ 400 kb (case 4) and had to be considered a case of hereditary supravalvular aortic stenosis instead of WBS. The three other deletions comprised ~ 3.6 Mb (case 1), ~ 4 Mb (case 2) and ~ 6.3 Mb (case 3). The most remarkable clinical feature found in two cases was their shorter stature compared to other WBS patients. A potential (pseudo-)gene candidate causing this phenotype is *NSUN5P1*. Another patient suffered from infantile spasms. There were some potential candidates for the cause of IS: *MAGI2*, *CALN1*, *YWHAG*, *MDH2* and *HIP1*. Of these, *MAGI2* and *CALN1* are the most promising, but further research is necessary to enhance knowledge about the potentially deleted genes in atypical WBS patients.

FISH, which is widely used until today, seems inferior to MLPA, because it depicts hemizygosity mostly in only one gene (*ELN*), while MLPA depicts a larger gene region (~ 1.05 Mb) in one step. Commercial WBS MLPA kits are readily available. Array diagnostics should follow if MLPA reveals atypical results allowing detailed genetic counselling for the affected families.

6 German summary

Das Williams-Beuren-Syndrom ist ein Mikrodeletionssyndrom auf Chromosom 7q11.23. Es ist die Folge einer zusammenhängenden, hemizygoten Deletion, die im typischen Fall ~ 1.54 bis ~ 1.85 Mb misst und 26 bis 28 kodierende Gene umfasst. Es gibt zudem auch atypische Deletionen. Die meisten Patienten mit typischem WBS weisen ein charakteristisches Äußeres mit Kleinwuchs, sowie kardiovaskuläre und endokrine Veränderungen, eine Intelligenzminderung bei gleichzeitig ausgeprägter Musikalität und ein überaus freundliches und aufgeschlossenes Wesen auf.

In den meisten Fällen entsteht das Syndrom aufgrund einer de-novo Deletion. Der Erbgang ist autosomal dominant. Typischerweise ist die Williams-Beuren-Syndrom Chromosomen-Region (WBSCR) deletiert, welche von Low Copy Repeats (LCR) flankiert wird. Diese sind anfällig für eine fehlerhafte Paarung während der Meiose mit der Folge einer Deletion. Am besten ist das *ELASTIN* (*ELN*) Gen erforscht, welches ursächlich für die kardiovaskulären Veränderungen bei WBS Patienten, aber auch für die Entstehung der Hereditären Supravalvulären Aortenstenose (SVAS), einem eigenen Krankheitsbild, ist.

Im Rahmen dieser Doktorarbeit wurden mehr als 340 mittels FISH gestellte WBS-Diagnosen anhand einer neueren Methode überprüft, der Multiplex Ligation-dependent Probe Amplification (MLPA). Die MLPA ist eine semi-quantitative, PCR basierte Technik zur Erfassung von Kopienzahlvariationen innerhalb eines bestimmten Genabschnittes. Durch die MLPA wurden vier atypische Deletionen entdeckt, die als Grundlage für eine Phänotyp-Genotyp-Korrelation dienten.

Diese Untersuchungen des bislang größten WBS-Kollektivs in Europa, lieferten in 218 Fällen das Ergebnis einer hemizygoten Deletion im betroffenen Gen-Bereich. In vier Fällen offenbarten sich dabei atypische Deletionen: Drei längere und eine kurze.

Um die ungefähre Deletionsgröße (1.54 Mb vs. 1.85 Mb) und um den maternalen oder paternalen Ursprung der Deletion näher bestimmen zu können, wurde eine Fragment-Analyse durchgeführt. ~ 94 % wiesen eine 1.54 Mb Deletion auf, was den Zahlen in der Literatur entsprach. Die Zahlen bezüglich des Ursprungs der Deletion wichen etwas von den verfügbaren Vergleichszahlen ab: Maternalen Ursprungs waren 59% (vs. 45%) und paternalen Ursprungs 41% (vs. 55%) der Deletionen. Der Ursprung der Deletion wirkt sich nach heutigem Wissensstand nicht auf den Phänotypen aus. Im Gegensatz dazu, führen längere, atypische

Deletionen zu einer schwereren klinischen Beeinträchtigung, u. a. durch das Auftreten von Epilepsien.

Die Bruchpunkte in den vier atypischen Fällen wurden mittels SNP-Array-Analyse näher bestimmt. Die kürzeste Deletion umfasste ~ 400 kb (Fall 4) und konnte einer hereditären SVAS zugeordnet werden. Die drei anderen Deletionen umfassten ~ 3.6 Mb (Fall 1), ~ 4 Mb (Fall 2) and ~ 6.3 Mb (Fall 3).

Das auffälligste Merkmal der Patienten der Fälle 1 und 2 war ihre auch für WBS-Standards geringe Körpergröße. Ein potentieller (Pseudo-)Gen-Kandidat hierfür ist *NSUN5P1*.

Das größte Potential für eine Phänotyp-Genotyp-Korrelation bot Fall 3, da dieser Patient an einer BNS-Epilepsie (Infantile Spasmen) litt. Bezüglich Epilepsien gibt es in der Literatur ebenfalls einige potentielle Gen-Kandidaten: *MAGI2*, *CALN1*, *YWHAG*, *MDH2* und *HIP1*.

Die immer noch weit verbreitete FISH-Analyse scheint der MLPA unterlegen zu sein. Mittels FISH wird lediglich ein Gen abgebildet (*ELN*), während die MLPA insgesamt neun Gene in einer Region von ~ 1.05 Mb erfasst. Kommerzielle MLPA-Kits für WBS sind seit einigen Jahren verfügbar. Da sich mittels MPLA ein erster Hinweis auf eine atypische Deletion zeigen kann, empfiehlt sich in solchen Fällen eine weiterführende Diagnostik mittels Array-Analysen, um die tatsächliche Deletionsgröße bestimmen zu können.

Kenntnisse über die deletierten Gene und deren Bedeutung für den Phänotyp sind für die genetische Beratung der Patienten und deren Familie unerlässlich und sollten auch zukünftig Gegenstand intensiver Forschung sein.

7 Literature

1. Ait-El-Mkadem S. et al. Mutations in MDH2, encoding a Krebs cycle enzyme, cause early-onset severe encephalopathy. Am J Hum Genet. 2017 Jan 5; 100(1):151-159.

2. Applied biosystems by life technologies. DNA Fragment Analysis by Capillary Electrophoresis. Publication Number 447450. Revision B. Page 18.

3. Arbeitsgemeinschaft der Wissenschaftlichen Medizinischen Fachgesellschaften (AWMF) - Ständige Kommission Leitlinien. AWMF-Regelwerk S3 Leitlinie „Therapie der Blitz-Nick-Salaam Epilepsie (West-Syndrom)". Version 2.0, 1. Aktualisierung, 10/2014.

4. Bailey J. A. et al. An Alu transposition model for the origin and expansion of human segmental duplications. Am J Hum Genet. 2003 Oct; 73(4):823-34.

5. Bayés M. et al. Mutational mechanisms of Williams-Beuren Syndrome deletions. Am J Hum Genet. 2003 Jul; 73(1):131-51.

6. Bennett M. K. et al. A synaptic protein implicated in docking of synaptic vesicles at presynaptic active zones. Science. 1992 Jul 10; 257(5067):255-9.

7. Bouchrieb K. et al. Clinical features of arterial hypertension in children with Williams-Beuren syndrome. Nephrol Dial Transplant. 2010 Feb; 25(2):434-8.

8. Bozhenok L. et al. WSTF-ISWI chromatin remodeling complex targets heterochromatic replication foci. EMBO J. 2002 May. 21(9): 2231-2241.

9. Burn J. Williams Syndrome. Journal of Medical Genetics. 1986 Oct; 23(5):389-95.

10. Canales C. P et al. The role of GTF2IRD1 in the auditory pathology of Williams-Beuren syndrome. Eur J Hum Genet. 2015 Jun; 23(6):744-80.

11. Capossela S. et al. Growth defects and impaired cognitive-behavioral abilities in mice with knockout for Eif4h, a gene located in the mouse homolog of the Williams Beuren syndrome critical region. Am J Pathol. 2012 Mar; 180(3):1121-1135.

12. Chailangkarn T. et al. A human neurodevelopmental model for Williams syndrome. Nature. 2016 Aug 18; 536(7616):338-43.

13. Chailangkarn T. et al. The contribution of GTF2I haploinsufficiency to Williams Syndrome. Mol Cell Probes. 2018 Aug; 40:45-51.

14. Chantranupong L. et al. The CASTOR proteins are arginine sensors for the mTORC1 pathway. Cell. 2016 Mar 24; 165(1):153-164.

15. Chauhan S. et al. Evolution of the Cdk-activator Speedy/RINGO in vertebrates. Cell Mol Life Sci. 2012 Nov; 69(22):3835-50.

16. Chomczynski P. et Sacchi N. Single-step method of RNA isolation by acid guanidinium thiocyanate-phenol-chloroform extraction. Anal Biochem. 1987 Apr; 162(1):156-9.

17. Chomczynski P. et Sacchi N. The single-step method of RNA isolation by acid guanidinium thiocyanate-phenol-chloroform extraction: twenty-something years on. Nat Protoc. 2006; 1(2):581-5.

18. Collins R. T. et al. cardiovascular abnormalities, interventions, and long-term outcomes in infantile Williams Syndrome. The Journal of Pediatrics. 2010 Feb; 156(2):253-8.e1.

19. Curran M. E. et al. The elastin gene is disrupted by a translocation associated with supravalvular aortic stenosis. Cell. 1993 Apr 9; 73(1):159-68.

20. Cuscó I. et al. Copy number variation at the 7q11.23 segmental duplications is a susceptibility factor for the Williams-Beuren syndrome deletion. Genom Res. 2008 May; 18(5):683-94.

21. Daniel S. et al. Identification of the docked granule pool responsible for the first phase of glucose-stimulated insulin secretion. Diabetes. 1999 Sep; 48(9):1686-90.

22. Del Campo M. et al. Hemizygosity at the *NCF1* gene in patients with Williams-Beuren Syndrome decreases their risk of hypertension. The American Journal of Human Genetics. 2006 Apr; 78(4):533-42.

23. Del Pasqua A. et al. New findings concerning cardiovascular manifestations emerging from long-term follow-up of 150 patients with the Williams-Beuren-Beuren syndrome. Cardiology in the Young. 2009 Dec; 19(6):563-7.

24. Deng F. et al. Stargazin and other transmembrane AMPA receptor regulating proteins interact with synaptic scaffolding protein MAGI-2 in brain. J Neurosci. 2006 Jul; 26(30):7875-84.

25. Doll A. et Grzeschik K.-H. Characterization of two novel genes, WBSCR20 and WSCR22, deleted in Williams-Beuren syndrome. Cytogenet Cell Genet. 2001; 95(1-2):20-7.

26. Dutra R. L. et al. Copy number variation in Williams-Beuren Syndrome: Suitable diagnostic strategy for developing countries. BMC Res Notes. Jan 2012; 5:13.

27. Dutra R. L. et al. Detection of deletions at 7q11.23 in Williams-Beuren Syndrome by polymorphic markers. Clinics. 2011; 66(6):959-964.

28. Eisenberg R. et al. Familial supravalvular aortic stenosis. Am J Dis Child. 1964; 108(4):341-347.

29. Ewart A. K. et al. A human vascular disorder, supravalvular aortic stenosis, maps to chromosome 7. Proc Natl Acad Sci. 1993 April; 90(8):3226-3230. Cited as Ewart et al. 1993a.

30. Ewart A. K. et al. Hemizygosity at the elastin locus in a developmental disorder, Williams syndrome. Nat Genet. 1993 Sep; 5(1):11-6. Cited as Ewart et al. 1993b.

31. Ewart A. K. et al. Supravalvular aortic stenosis associated with a deletion disrupting the elastin gene. J Clin Invest. 1994; 93:1071-1077.

32. Ferrero G. B. et al. An atypical 7q11.23 deletion in a normal IQ Williams-Beuren syndrome patient. European Journal of Human Genetics. January 2010. Jan; 18(1):33-8.

33. Fricke T. A. et al. Surgical repair of supravalvular aortic stenosis in children with Williams Syndrome: A 30-Year Experience. The Annals of Thoracic Surgeons. 2015. Apr; 99(4):1335-41.

34. Fukami M. et Ogata T. Cytochrome P450 oxidoreductase deficiency: rare congenital disorder leading to skeletal malformations and steroidgenic defects. Pediatr Int. 2014 Dec; 56(6):805-808.

35. Funakoshi T. et al. Two distinct human POM121 genes: requirement for the formation of nuclear pore complexes. FEBS Lett. 2007 Oct 16; 581(25):4910-6.

36. Fusco C. et al. Smaller and larger deletions of the Williams Beuren syndrome region implicate genes involved in mid facial phenotype, epilepsy and autistic traits. Eur J Hum Genet. 2014. Jan; 22(1):64-70.

37. Gardino A. K. et Yaffe M. B. 14-3-3 proteins as signalling integration points for cell cycle control and apoptosis. Semin Cell Dev Biol. 2011 Sep; 22(7):688-95.

38. Gray V. et al. In-depth analysis of spatial cognition in Williams syndrome: a critical assessment of the role of the LIMK1 gene. Neuropsychologica. 2005; 44(5):679-685.

39. Hoeft F. et al. Mapping genetically controlled neural circuits of social behavior and visuo-motor integration by a preliminary examination of atypical deletions with Williams Syndrome. PLoS One. 2014. Aug 8; 9(8):e104088.

40. Hogervorst F. B. et al. Large genomic deletions and duplications in the *BRCA1* gene identified by a novel quantitative method. Cancer Res. 2003 Apr 1; 63(7):1449-53.

41. Hoogenraad C. C. et al. The murine CYCLN2 gene: genomic organization, chromosome localization, and comparison to the human gene that is located within the 7q11.23 Williams syndrome critical region. Genomics. 1998 Nov;53(3):348-58.

42. Hurles M. E. et Lupski J. R. Recombination Hotspots in nonallelic homologous recombination. In: Lupski J. R. et Stankiewicz P. (eds.). Genomic disorders. 2006. P. 341-355. Humana Press.

43. Iwaki S. et al. Ntal/Lab/Lat2. Int J Biochem Cell Biol. 2007; 39(5):868-73.

44. Jangani M. et. al. The methyltransferase WBSCR2/Merm1 enhances glucocorticoid receptor function and is regulated in lung inflammation and cancer. J Biol Chem. 2014 Mar 28; 289(13):8931-46.

45. Karp G. Cell and Molecular Biology: Concepts and Experiments. 6th edition. 2010. John Wiley & Sons, Inc.

46. Kerzendorfer C. et O`Driscoll M. Human DNA damage response and repair deficiency syndromes: linking genomic instability and cell cycle checkpoint proficiency. DNA repair. 2009 Sep; 8(9):1139-52.

47. Kitagawa H. et al. The chromatin-remodeling complex WINAC targets a nuclear receptor to promoters and is impaired in Williams syndrome. Cell. 2003 Jun 27; 113: 905-917. Retraction: Cell. 2012 Mar 30; 149:245.

48. Komoike Y. et al. Zebrafish gene knockdowns imply roles for human *YWHAG* in infantile spasms and cardiomegaly. Genesis. 2010 April; 48(4):233-43.

49. Kozel B. A. et al. Williams syndrome predisposes to vascular stiffness modified by anti-hypertensive use and copy number changes in *NCF1*. Hypertension. 2014 Jan; 63(1):74-9.

50. Lalli M. A. et al. Haploinsufficiency of *BAZ1B* contributes to Williams syndrome through transcriptional dysregulation of neurodevelopmental pathways. Hum Mol Genet. 2016 Apr 1; 25(7):1294-306.

51. Lam P. P. et al. Transgenic mouse overexpressing syntaxin-1A as a diabetes model. Diabetes. 2005 Sep; 54(9):2744-54.

52. Levy-Shraga Y. et al. Endocrine manifestations in children with Williams-Beuren syndrome. Acta Paediatr. 2018 Apr; 107(4):678-684.

53. Lin L. et al. Differing microdeletion sizes and breakpoints in chromosome 7q11.23 in Williams-Beuren Syndrome detected by chromosomal array analysis. Mol Syndromol. 2016 Feb; 6(6):268-275.

54. Lindgren D. et al. Genoytping techniques to address diversity in tumors. Advances in cancer research. Adv Cancer Res. 2011; 112:151-82.

55. Mariasina S. S. et al. NMR assignments of the WBSR27 protein related to Williams-Beuren syndrome. Biomol NMR Assign. 2018 Oct; 12(2):303-308.

56. Marshall C. R. et al. Infantile spasms is associated with deletion of the *MAGI2* gene on chromosome 7q11.23-q21.11. Am J Hum Genet. 2008 Jul; 83(1):106-11.

57. Martin L. A. et al. Consistent hypersocial behavior in mice carrying a deletion of Gtf2i but no evidence of hyposocial behavior with Gtf2i duplication: Implications for Williams-Beuren syndrome and autism spectrum disorder. Brain Behav. 2017 Dec 19; 8(1):e00895.

58. Matsumoto N. et al. Linking LIMK1 deficiency to hyperacusis and progressive hearing loss in individuals with Williams syndrome. 2011 Mar; 4(2):208-210.

59. Merla G. et al. Copy number variants at Williams-Beuren syndrome 7q11.23 region. Hum Genet. 2010 Jul; 128(1):3-26.

60. Merla G. et al. Identification of additional transcripts in the Williams-Beuren syndrome critical region. Hum Genet. 2002 May; 110(5):429-38.

61. Merla G. et al. Molecular Genetics of Williams-Beuren Syndrome. Encyclopedia of Life Sciences. John Wiley & Sons. 2012 Jan.

62. Mervis C. B. et al. The Williams Beuren Syndrome Cognitive Profile. Brain and Cognition. 2000 Dec; 44(3):604-28.

63. Metcalfe K. et al. Elastin: mutational spectrum in supravalvular aortic stenosis. Eur J Hum Genet. 2000 Dec;8(12):955-63.

64. Metcalfe K. et al. Autosomal dominant inheritance of Williams-Beuren syndrome in a father and son with haploinsufficiency for *FKBP6*. Clinical Dysmorphology. 2005 Apr; 14(2):61-5.

65. Metzler M. et al. Disruption of the endocytic protein HIP1 results in neurological deficits and decreased AMPA receptor trafficking. EMBO J. 2003 Jul 1; 22(13):3254-66.

66. Micale L. et al. Williams-Beuren syndrome *TRIM50* encodes an E3 ubiquitin ligase. Eur J Hum Genet. 2008 Sep; 16(9):1038-49.

67. Mitchell J. M. et al. Pom121 links two essential subcomplexes of the nuclear pore complex core to the membrane. J Cell Biol. 2010 Nov 1; 191(3):505-21.

68. Miyamato T. et al. Is a genetic defect in Fkbp6 a common cause of azoospermia in humans? Cell Mol Biol Lett. 2006; 11(4):557-69.

69. Mizugishi K. et al. Interstitial deletion of chromosome 7q in a patient with Williams syndrome and infantile spasms. J Hum Genet. 1998; 43(3):178-81.

70. Morimoto M. et al. Infantile spasms in a patient with Williams syndrome and craniosynostosis. Epilepsia. 2003 Nov; 44(1):1459-62.

71. Morita K. et al. Claudin multigene family encoding four-transmembrane domain protein components of tight junction strands. Cell Biol. 1999 Jan; 96(2):511-516.

72. Morris C. A. et al. Natural history of Williams Syndrome: Physical characteristics. J Pediatr. 1988 Aug; 113(2):318-26.

73. Morris C. A. et al. Williams syndrome: autosomal dominant inheritance. Am J Med Genet. 1993. Sep 15; 47(4):478-81.

74. Morris C. A. et al. *GTF2I* hemizygousity implicated in mental retardation in Williams syndrome: genotype-phenotype analysis of five families with deletions in the Williams syndrome region. Am J Med Genet A. 2003 Nov; 123A (1):45-59.

75. Morris C. A. The behavioural phenotype of Williams syndrome: A recognizable pattern of neurodevelopment. Am J Med Genet C Semin Med Genet. 2010 Nov 15; 154C(4):427-31.

76. Morrison D. K. The 14-3-3 proteins: integrators of diverse signaling cues that impact cell fate and cancer development. Trends Cell Biol. 2009 Jan; 19(1):16-23.

77. MRC Holland. MLPA General Protocol. Instructions for use. MLPA (Multiplex ligation-dependent probe amplification) general protocol for the detection and quantification of DNA sequences. MDP version-007; issued on 01 March 2019.

78. Mullis K. B. et al. Specific enzymatic amplification of DNA in vitro: The Polymerase chain reaction. Cold Spring Harb Symp Quant Biol. 1986; 51 Pt 1:163-73.

79. Mullis K. B. The unusual origins of the polymerase chain reaction. Scientific America. 1990 Apr; 262(4):56-61.

80. Murken J. D. et al. Taschenlehrbuch Humangenetik. 2011. 8th edition. Georg Thieme.

81. Noskov V. N. et al. The *RFC2* gene, encoding the third-largest subunit of the replication factor C complex, is required for an S-phase checkpoint in Saccharomyces cerevisiae. Mol Cell Bio. 1998 Aug; 18(8(:4914-23.

82. Ohazama A. et Sharpe P. T. TFII-I gene family during tooth development: candidate genes for tooth anomalies in Williams syndrome. Dev Dyn. 2007 Oct; 236(10):2884-8.

83. Osborne L. R. et al. A 1.5 million-base pair inversion polymorphism in families with Williams-Beuren syndrome. Nat Genet. 2001 Nov; 29(3):321-5.

84. Osório A. et al. Cerebral and cerebellar MRI volumes in Williams Syndrome. Res Dev Disabil. 2014. Apr; 35(4):922-8.

85. Palacios-Verdú M. G. et al. Metabolic abnormalities in Williams-Beuren syndrome. J Med Genet. 2015 Apr; 52(4):248-55.

86. Pankau R. et al. Incidence and spectrum of renal abnormalities in Williams-Beuren syndrome. Am J Med Genet. 1996 May 3; 63(1):301-4.

87. Pankau R. et al. Familial Williams-Beuren syndrome showing varying clinical expression. American Journal of Medical Genetics. 2001 Feb 1; 98(4):324-9.

88. Pankau R. et al. Das Williams-Beuren-Syndrom. Genetik-Medizin-Psychologie. 2014.

89. Partsch C. J. et al. Sigmoid diverticulitis in patients with Williams Beuren Syndrome. Relatively high prevalence and high complication rate in young adults with the syndrome. American Journal of Medical Genetics. 2005 Aug 15; 137(1):52-4.

90. Pérez-Jurado A. L. Williams-Beuren syndrome: a model of recurrent genomic mutation. Horm Res. 2003; 59 Suppl 1:106-13.

91. Pérez-Jurado L. A. et al. *TBL2*, a novel transducing family member in the WBS deletion: characterization of the complete sequence, genomic structure, transcriptional variants and the mouse ortholog. Cytogenet Cell Genet. 1999; 86(3-4):277-84.

92. Pober B. R. Williams-Beuren Syndrome. Review Article. NEJM. 2010 Jan 21; 362(3):239-52.

93. Pober B. R. et al. High prevalence of diabetes and pre-diabetes in adults with Williams-Syndrome. Am J Med Genet C Semin Med Genet. 2010 May 15; 154C(2):291-8.

94. Porter M. A. et al. A role for transcription factor *GTF2IRD2* in executive function in Williams-Beuren Syndrome. PloS One. 2012; 7(10):e47457.

95. Preus M. The Williams syndrome: objective definition and diagnosis. Clin Genet. 1984 May; 25(5):422-8.

96. Ramocki M. B. et al. Recurrent distal 7q11.23 deletion including *HIP1* and *YWHAG* identified in patients with intellectual disabilities, epilepsy, and neurobehavioural problems. Am J Hum Genet. 2010 Dec; 87(6):857-65.

97. Rassow J. et al. Duale Reihe Biochemie. 2012. 3rd edition. Georg Thieme.

98. Richter N. J. et al. Further biochemical and kinetic characterization of human eukaryotic initiation factor 4H. J Biol Chem. 1999 Dec; 274(50):35415-35424.

99. Roesler J, Curnutte JT, Rae J, et al. Recombination events between the p47-phox gene and its highly homologous pseudogenes are the main cause of autosomal recessive chronic granulomatous disease. Blood. 2000;95(6):2150-2156.

100. Röthlisberger B. et al. Deletion of 7q11.21-q11.23 and infantile spasms without deletion of *MAGI2*. Am J Med Genet A. 2010 Feb; 152A(2):434-7.

101. Roy A. L. et al. Cloning of an Inr- and E-box binding protein, TFII-I, that interacts physically and functionally with USF1. EMBO J. 1997 Dec 1; 16(23):7091-104.

102. Samanta D. Infantile spasms in Williams-Beuren syndrome with typical deletions of the 7q11.23 critical region and a review of the literature. Acta Neurol Belg. 2017 Mar; 117(1):359-362.

103. Sambrook J. et Russell D. W. Purification of nucleic acids by extraction with phenol:chloroform. CSH Protoc. 2006 Jun 1; 2006(1).

104. Sammour Z. M. et al. Congenital genitourinary abnormalities in children with Williams-Beuren syndrome. Journal of Pediatric Urology Company. 2014 Oct; 10(5):804-9.

105. Schouten J. P. et al. Relative quantification of 40 nucleic acid sequences by multiplex ligation-dependent probe amplification. Nucleic Acids Res. 2002 Jun 15; 30(12):e57.

106. Schubert C. The genomic basis of the Williams-Beuren syndrome. Cellular and Molecular Life Sciences. 2009 Apr; 66(7):1178-97.

107. Scott R. W. et Olson M. F. Lim kinases: function, regulation and association with human disease. J Mol Med. 2007 June; 85(6):525-528.

108. Serrano-Juarez C. A. et al. Cognitive, behavioral and adaptive profiles in Williams syndrome with and without loss of *GTF2IRD2*. J Int Neuropsychol Soc. 2018 Oct; 24(9):896-904.

109. Şimşek-Kiper P. O. et al. Celiac disease in Williams-Beuren syndrome. The Turkish Journal of Pediatrics. 2014 Mar-Apr; 56(2):154-9.

110. Smith A. D. et al. Inefficient search of large-scale space in Williams syndrome: further insights on the role of *LIMK1* deletion in deficits of spatial cognition. Perception. 2009; 38(5):694-701.

111. Stagi S. et al. Incidence of diverticular disease and complicated diverticular disease in young patients with Williams syndrome. Pediatr Surg Int. 2010 Sep; 26(9):943-4.

112. Stagi S. et al. Williams-Beuren Syndrome is a Genetic Disorder associated with impaired glucose tolerance and diabetes in childhood and adolescence: new insights from a longitudinal study. Hormone Research in Pediatrics. 2014; 82(1):38-43.

113. Stasia M. J. et al. Functional and genetic characterization of two extremely rare cases of Williams-Beuren syndrome associated with chronic granulomatous disease. European Journal of Human Genetics. 2013 Oct; 21(10):1079-84.

114. Stock A. D. et al. Heat shock protein 27 gene: chromosomal and molecular location and relationship to Williams syndrome. 2003 Jul; 120A(3):320-5.

115. Stuppia L. et al. Use of the MLPA assay in the molecular diagnosis of gene copy number alterations in human genetic diseases. Int J Mol Sci. 2012; 13(3):3245-76.

116. Takeyama K. et al. The BAL-binding protein BBAP and related Deltex family members exhibit ubiquitin-protein isopeptide ligase activity. J Biol Chem. 2003; 278:21930-21937.

117. Tebbenkamp A. T. N. et al. The 7q11.23 protein DNAJC30 interacts with ATP synthase and links mitochondria to brain development. Cell. 2018 Nov 1; 175(4):1088-1104.e23.

118. Thompson P. D. et al. GTF2IRD1 regulates transcription by binding an evolutionarily conserved DNA motif `GUCE`. FEBS Lett. 2007 Mar; 581(6):1233-42.

119. Todorovski Z. et al. LIMK1 regulates long-term memory and synaptic plasticity via the transcriptional factor CREB. Mol Cell Biol. 2015 Apr; 35(8):1316-1328.

120. Uehara T. et al. The tumour suppressor BCL7B functions in the Wnt signalling pathway. PLoS Genet. 2015 Jan 8; 11(1):e1004921.

121. Valero M. C. et al. Fine-scale comparative mapping of the human 7q11.23 region and the orthologous region on mouse chromosome 5G: the low-copy repeats that flank the Williams-Beuren Syndrome deletion arose at breakpoint sites of an evolutionary inversion(s). Genomics. 2000 Oct 1; 69(1):1-13.

122. Van Hagen J. M. et al. Comparing two diagnostic laboratory tests for Williams syndrome: fluorescent in situ hybridization versus multiplex ligation-dependent probe amplification. Genet Test. 2007 Fall; 11(3):321-7. Cited as Van Hagen et al. 2007a.

123. Van Hagen J. M. et al. Contribution of *CYLN2* and *GTF2IRD1* to neurological and cognitive symptoms in Williams syndrome. Neurobiol Dis. 2007 Apr; 26(1):112-24. Cited as Van Hagen et al. 2007b.

124. Vandeweyer G. et al. The contribution of *CLIP2* haploinsufficiency to the clinical manifestations of the Williams-Beuren syndrome. Am J Hum Genet. 2012 Jun; 90(6):1071-8.

125. Viana M. M., et al. Ocular Features in 16 Brazilian Patients with Williams-Beuren Syndrome. Ophthalmic Genet. 2015;36(3):234-8.

126. Wang Y.-K. et al. A novel human homologue of the drosophila frizzled wnt receptor gene binds wingless protein and is in the Williams syndrome deletion at 7q11.23. Hum Molec Genet. 1997 Mar; 6(3):465-72.

127. Welsch. U. et Deller T. Lehrbuch Histologie. 2006. 2rd Edition. Urban & Fischer in Elsevier.

128. Winter M. et al. The spectrum of ocular features in the Williams-Beuren Syndrome. Clin Genet. 1996. Jan; 49(1):28-31.

129. Woodruff-Borden J. et al. Longitudinal course of anxiety in children and adolescents with Williams Syndrome. Am J Med Genet C Semin Med Genet. 2010 May 15; 154C(2):277-90.

130. Wu Y. Q. et al. Identification of human brain-specific gene, *CALNEURON 1*, a new member of the calmodulin superfamily. Mol Genet Metab. 2001 April; 72(4):343-50.

131. Young E. J. et al. Reduced fear and aggression and altered serotonin metabolism in Gtf2ird1-targeted mice. Genes Brain Behav. 2008 Mar; 7(2):224-34.

132. Zarchi O. et al. Hyperactive auditory processing in Williams syndrome: evidence from auditory evoked potentials. Psychophysiology. 2015 Jun; 52(6):782-9.

Internet sources:

http://www.dna-diagnostik.hamburg

http://www.ensembl.org – Genome Browser

https://www.ncbi.nlm.nih.gov/genome/gdv/ - Genome Data Viewer

https://www.gfhev.de - Deutsche Gesellschaft für Humangenetik e. V.

https://www.klinikum.uni-heidelberg.de

https://www.medizinische-genetik.de

https://www.omim.org/ - Online Mendelian Inheritance in Man (OMIM)

http://www.radiopaedia.org

https://www.w-b-s.de/ - Bundesverband Williams-Beuren-Syndrom e.V.

http://www.williams-syndrome.org – Williams Syndrome association

8 Appendix

8.1 Clinical data

Case 1

Age	Height	Weight	Head circumference
Birth	**47 cm**[*3]	**2740 g**[*3]	36 cm[*5]
10.5 weeks	57 cm[*4]	**3680 g**[*3]	39 cm[*5]
5.5 months	**60 cm**[*3]	6200 g[*4]	ND
8.5 months	**66 cm**[*3]	8000 g[*6]	44 cm[*5]
13 months	ND	8800 g[*6]	ND
17 months	**74.5 cm**[*3]	9000 g[*5]	47 cm[*5]

Table 8.1: Developmental data of case 1.

Noticeable low measurements ([*1] - [*3]) were printed bold.

[*1] <u>below minus</u> 2 standard deviations for boys with WBS

[*2] <u>minus</u> 2 standard deviations for boys with WBS (-2 SD)

[*3] between average and <u>minus</u> 2 standard deviations for boys with WBS

[*4] average for boys with WBS

[*5] between average and <u>plus</u> 2 standard deviations for boys with WBS

[*6] <u>plus</u> 2 standard deviations for boys with WBS (+ 2 SD)

[*7] <u>above plus</u> 2 standard deviations for boys with WBS

ND = no data available. Reference height: https://williams-syndrome.org/growth-charts/growth-charts. 13.10.2019. 18:00.

Case 2

Age	Height	Weight	Head circumference
Birth	**48 cm**[*3]	**3190 g**[*3]	ND
12 months	**70 cm**[*3]	7400 g[*5]	46 cm[*5]
23 months	**78 cm**[*3]	9.4 kg[*4]	47 cm[*4]
2 4/12 years	**82.5 cm**[*3]	**10 kg**[*3]	ND
4 5/12 years	**89.5 cm**[*2]	13.5 kg[*4]	51 cm[*6]
5.5 years	**96 cm**[*2]	**13.5 kg**[*3]	52 cm[*7]
6.5 years	**101 cm**[*1]	**15 kg**[*3]	ND
7 5/12 years	**104 cm**[*1]	**16.8**[*3]	ND
8 5/12 years	**108 cm**[*1]	**17.9 kg**[*3]	ND

9 5/12 years	**111 cm**[*1]	**18.5 kg**[*2]	ND
14 5/12 years	**134 cm**[*1]	**32.5 kg**[*3]	ND
14.5 years	**137 cm**[*1]	**31.5 kg**[*3]	ND
15 8/12 years	**140 cm**[*1]	**33.2 kg**[*3]	ND
17 10/12 years	**144.6 cm**[*1]	**39.8 kg**[*3]	ND
19 years	**147.6 cm**[*1]	**39.4 kg**[*3]	ND

Table 8.2: Developmental data of case 2. Legend: see table 8.1.

Case 3

Age	Height	Weight	Head circumference
Birth	49 cm[*4]	**2655 g**[*2]	ND
3 4/12 years	**89 cm**[*3]	**11.2 kg**[*3]	ND
4 4/12 years	**92 cm**[*3]	**13 kg**[*3]	ND
5 6/12 years	**98.5 cm**[*3]	**12.2 kg**[*1]	ND

Table 8.3: Developmental data of case 3. Legend: see table 8.1.

Case 4

Age	Height	Weight	Head circumference
Birth	50 cm	3330 g	ND
10.5 months	70 cm	7.5 kg	ND
12 months	72.5 cm	8.1 kg	ND
1 1/12 years	74 cm	8.6 kg	ND

Table 8.4: Developmental data of case 4.

8.2 Devices and material

Device, material, procedure	Type	Manufacturer	Location
Caps	Domed Cap Strips	Sarstedt	Nümbrecht, Germany
Centrifuge	Hettich EBA 12R, Rotana 96R	Andreas Hettich GmbH & Co.KG	Tuttlingen, Germany
Distilled water	Aqua ad iniectabilia	B. Braun	Melsungen, Germany
DNA concentration measurement	Qubit® 2.0 Fluorometer	Thermo Fisher Scientific	Waltham, Massachusetts, United States
DNA concentration measurement	Qubit® dsDNA BR Assay Kit	Thermo Fisher Scientific	Oregon, USA
DNA concentration measurement tubes	Qubit® Assay tubes (500 µl)	Thermo Fisher Scientific	Waltham, Massachusetts, United States
DNA dilution	TE Buffer	Thermo Fisher Scientific	Waltham, Massachusetts, United States
DNA extraction	QIAamp® DNA Blood Mini Kit	Qiagen	Hilden, Germany
Ethanol	96 – 100%	Merck, Millipore	Massachusetts, United States
Fragment Analysis	Hi-Di Formamide	Applied Biosystems	Foster City, USA
Fragment Analysis	LIZ standard	Thermo Fisher Scientific	Waltham, Massachusetts, USA
Magnesium	$MgCl_2$	Thermo Fisher Scientific	Waltham, Massachusetts, USA
MLPA	Reagent kit	MRC Holland	Amsterdam, Netherlands
MLPA	SALSA MLPA probemix P029-B1	MRC Holland	Amsterdam, Netherlands
PCR	Oligonucleotides dNTP-Mix	Thermo Fisher Scientific	Waltham, Massachusetts, USA

PCR	GoTaq Green PCR Mastermix	Promega	Madison, USA
PCR	DreamTaq Green PCR Mastermix	Thermo Fisher Scientific	Waltham, Massachusetts, USA
PCR, Fragment Analysis	Sn and Asn primer	Metabion international AG	Planegg, Germany
PCR, Fragment Analysis	Taq polymerase recombinant	Invitrogen, Thermo Fisher Scientific	Waltham, Massachusetts, USA
PCR Plates	0,2ml Tube Plate 96 Well Multiply®	Sarstedt	Nümbrecht, Germany
Pipettes		Gilson	Ohio, United States
Pipette tips	Biosphere Filter tips 10µl, 100µl, 200µl, 1250µl type Eppendorf/Gilson	Sarstedt	Nümbrecht, Germany
Sequencer	ABI-Prism 3130 Genetic Analyzer	Applied Biosystems	California, United States
Thermal cycler	T-1 Thermoblock	Biometra	Göttingen, Germany
Thermal cycler	TProfessional Standard Gradient Thermocycler	Biometra	Göttingen, Germany
Tris-Acetat-EDTA-Buffer		Merck-Millipore	Burlington, Massachusetts, USA
Vortex		Heidolph	Schwabach, Germany

8.3 Tools and Software

Program	Manufacturer
Gene mapper 4.0	Thermo Fisher Scientific
GIMP 2.10.14 - GNU Image Manipulation Program	Open source
Microsoft Excel 2013	Microsoft
Microsoft Powerpoint 2013	Microsoft
Microsoft Word 2013, 2019	Microsoft
SeqPilot 4.1.2	JSI medical systems GmbH, Ettenheim, Germany

9 Acknowledgement - Danksagung

wusste nicht, dass es so bedingungslose Hilfsbereitschaft geben kann. Deine Liebe, deine Zuversicht und Kraft haben mich nie aufgeben lassen. Wenn ich mutlos den Kopf hingen ließ, hast du mich wachgerüttelt und angespornt, nicht aufzugeben. Du bist mein Vorbild und für das alles, was du bisher geleistet hast, empfinde ich den tiefsten Respekt. Als Team sind wir unschlagbar – in beruflicher wie in privater Hinsicht. Danke für unser gesundes, wunderbares, schönes Baby, unseren Sohn Frieder! Und an dich, kleiner Frieder, der Dank dafür, dass du in den ersten drei Monaten öfter mal brav geschlafen hast und ich weiter an meiner Doktorarbeit schreiben konnte!

10 Curriculum vitae

Der Lebenslauf wurde aus datenschutzrechtlichen Gründen entfernt.

11 Affidavit

Ich versichere ausdrücklich, dass ich die Arbeit selbständig und ohne fremde Hilfe verfasst, andere als die von mir angegebenen Quellen und Hilfsmittel nicht benutzt und die aus den benutzten Werken wörtlich oder inhaltlich entnommenen Stellen einzeln nach Ausgabe (Auflage und Jahr des Erscheinens), Band und Seite des benutzten Werkes kenntlich gemacht habe.

Ferner versichere ich, dass ich die Dissertation bisher nicht einem Fachvertreter an einer anderen Hochschule zur Überprüfung vorgelegt oder mich anderweitig um Zulassung zur Promotion beworben habe.

Ich erkläre mich einverstanden, dass meine Dissertation vom Dekanat der Medizinischen Fakultät mit einer gängigen Software zur Erkennung von Plagiaten überprüft werden kann.

Unterschrift: ....